2018

A continuum approach to modeling the vibrations within a block subjected to free rocking

Julia Raye Anderson-Lee
Iowa State University

A continuum approach to modeling the vibrations within a block subjected to free rocking

by

Julia Anderson-Lee

A dissertation submitted to the graduate faculty

in partial fulfillment of the requirements for the degree of

DOCTOR OF PHILOSOPHY

Co-majors: Applied Mathematics

Civil, Construction and Environmental Engineering

Program of Study Committee:

Scott Hansen, Co-major Professor

Sivalingam Sritharan, Co-major Professor

Leslie Hogben

Simon Laflamme

Paul Sacks

Iowa State University

Ames, Iowa

2018

DEDICATION

It takes a village to raise a child. I have, since long before I can remember, been the child of an amazing village. Starting with my parents, Lena, John and Margaret, to my huge networks of aunts. I am so grateful for their love and support. The village held me up, made me write and lauded me when I succeeded. I couldn't be more grateful. I arrived in Iowa August 10, 2010 intentioned on graduating Iowa State University with my doctoral degree in mathematics and civil engineering in 5 years. It took a bit longer but and while I thought I would have to finish this degree alone, I could not and would not have completed it with out the help of my family, friends and mentors.

I would like to dedicate this work to my mother, Lena Anderson, and grandparents John and Margaret Hargrove. There undying support and trust in my decision to move 21 hours away to a state where I knew no one and we had no family pushed me to complete my graduate school dreams. Countless phone calls about what I hated and conversations about how this is all part of a plan that is larger than whatever I was going to endure. My God parents Ronald and Soraya Coley for pushing me when I had no gas left in my tank. Thank you for seeing the finish line long before I could.

My friends who kept me sane throughout acclimating to the Midwest. We survived frigid winters, tornadoes, qualifying exams, the Iowa Caucus, and much much more. We broke a few bones and tore one ACL, but we made it out in one piece. To Arianne Ross, Travell Williams, Katrina Harden-Williams, Millicent Grant, Luvenia Hellams, Janelle Seward, Cameron Beatty, Lorraine Acker, Malika Butler, Trahvae Pearson, thank you. We've accomplished so much together and this is only the beginning.

I didn't think this was possible until two of my undergraduate professors and a mechanical engineer told me I had a strong mind and needed to explore where my creativity and my math

would take me. Thank you Dr. Nagambal Shah, Dr. Sylvia Bozeman and Dr. J. Adin Man. I'm so lucky to have been one of your last students to graduate. Thank you Dr. Leslie Hogben for being a true advocate. Of course my advisors, Dr. Sri Sritharan and Dr. Scott Hansen who held on and did not give up on me. This has been a monumental step in my scientific career and I'm so grateful for all of you.

TABLE OF CONTENTS

LIST OF TABLES

LIST OF FIGURES

ACKNOWLEDGEMENTS

This work presented in this thesis was funded by the National Science Foundation CMMI under Grant No. 1041650 and NSF Grant No. DMS-1312952, "Control of fluid-structure interaction and related topics."

ABSTRACT

Seismic events are unpredictable and in locations susceptible to these events, buildings and bridges must be designed to minimize societal impacts and structural damage. Accurately modeling structures subjected to seismic loads is important for improving the design techniques for structures in active seismic areas. Employing rocking motions in structural design can help minimize the effect of seismic loads on these structures by allowing critical structural elements to move with the earthquake motion. The rocking movement dissipates the energy imparted to the structure by the earthquake. This reduces the amount of structural deformation within the structure's members. Mathematical modeling techniques have the ability to capture the internal structural deformation of rocking structures. The models created in this research project yield an in-depth understanding of rocking structures by providing deeper insight into the characteristics of rocking dynamics.

The rocking system investigated in this research project is composed of a rectangular block rocking on a planar foundation. Traditional rocking models idealize this rocking block system by assuming the rocking block and foundation are infinitely rigid. Rocking models that consider the block and foundation infinitely rigid are referred to as *rigid rocking models*. In the rigid rocking model the energy dissipation characterized by rocking motion is concentrated at the interface between the block and foundation. In reality, structural systems are finitely rigid and there are many locations throughout the structure that can contribute to the total energy dissipation of the system. In particular, energy can be dissipated within the block or radiated through the foundation to the surrounding media, such as soil. Considering multiple locations for the energy dissipation complicates the mathematical representation of the rocking system. In the rigid rocking model, a single location that generalizes the energy dissipation is sufficient. The location of the energy dissipation is chosen according to the component of the system that is being investigated.

The focus of this study is the vibration energy within the block and the contribution of this vibration energy to the overall rocking motion. Rocking models that describe a rocking block system where the vibration energy is generated are generally referred to as *flexible rocking block models*. The rocking model in this study assumes the vibration energy in the block is the only contributor to the energy dissipation that occurs during rocking motion and that the only energy lost between impacts is the vibration energy developed within the block during each impact. The foundation is assumed to be perfectly rigid to simplify the impact dynamics and to further isolate the vibration energy in the block from other possible sources. The block vibration energy can be dissipated by being transferred to the foundation or to nonlinear phenomena such as internal friction, heat energy, and sound energy. Once this energy transfer occurs, the energy is assumed never to return to the block. This energy loss in the flexible rocking block model can account for as much as 3% of the equivalent amount of energy introduced into the rigid rocking block model, indicating the possibility that the vibration energy in the block contributes significantly to the energy loss of the rocking system. The model presented in this project is the result of finding the variational representation of the law of conservation of energy for the considered modes of deformation. This method is a modification of the derivation of the Mindlin-Timoshenko plate bending model detailed in Lagnese and Lions (15). The model created in this research project is equivalent to accepted rigid models in the absence of internal deformations and represents a higher degree of nonlinearity in rocking dynamics when vibrations are included.

The characteristics of the rocking block system that cause an increased amount of block vibration energy depend on the flexibility of the block and the initial displacement of the block. The mathematical model described herein substantiates the significance of the contribution of block vibration energy to rocking systems. The internal flexural, axial and shear deformations, in addition to the angular rocking displacement, are incorporated in the model. The minimum amount of block vibration energy in the rocking response is defined and based on the contribution of the block vibration energy, a rocking criterion is established. This criterion defines the initial displacement that will cause a block to rock on a rigid foundation, given the block's flexibility. The rocking criterion also defines the completion of the rocking response. These

assertions can help influence experimental design and further investigation into the nonlinear motions that occur during rocking motion.

CHAPTER 1. INTRODUCTION

The fields of seismic engineering and seismic design are advancing to satisfy the needs of growing cities. Cities are becoming more densely populated as people live and work closer together. Seismic events in these heavily, densely populated areas will more severely affect these larger populations. Between 1900 and 2014 there were 127 earthquakes, each causing 1000 or more deaths. Four of these occurred in the last 25 years in densely populated areas in Haiti, Sumatra, and Pakistan (5). These four earthquakes alone caused more than seven million deaths and 86 billion dollars in damage. In the United States, as many as 42 states may experience a seismic event that will subject bridges, buildings, and other structures to forces larger than what those structures were designed to accommodate (6). The goal of seismic engineering is to reduce the number of human and economic losses resulting from structural damage in seismic events. Advancing the methods of structural design (the practice of determining the load-bearing capacity of a structure) and structural retrofitting (the practice of determining and providing additional elements to support an existing structure) for more efficiently and economically built structures in seismic zones will significantly reduce these human and economic losses.

One such structural design and retrofit method used in seismic design is seismic isolation. The goal of this technique is to isolate a structure from ground shaking during an earthquake. Isolation can be incorporated in the design or retrofit of a structure. Common retrofit techniques use an external isolation mechanism. An example is the seismic retrofit of the Mackay School of Mines Building in Reno, Nevada. This retrofit design combines two forms of seismic isolators: rubber bearing pads and sliders (13). These two methods were used because of their economic savings and ability to preserve the detailed masonry of this early twentieth century building (see photo of original structure in Figure 1.1) (19). The location of the seismic isolation

Figure 1.1: Original Mackay School of Mines Building after completion circa 1900.

system was chosen to be at the interface between the structure and the foundation. This is the result of the assumption that the energy dissipation takes place at the interface between the structure and the foundation. This assumption, however popular, is misleading regarding the actual behavior of structures. Energy dissipation can take place throughout the structure and the location of the energy dissipation system depends on the desired structural response, as in the East Span of the San Francisco-Oakland Bay Bridge where seismic isolators are distributed throughout the structure (8).

Rocking systems are a class of seismic isolation systems that dissipate energy through oscillatory movement. Factory walls and ancient columns made of multiple blocks stacked on top of one another are examples of existing rocking systems. Slender structures, such as these ancient columns, have been considered unstable in seismic events (18). However; the survival of these columns in earthquakes led researchers to believe slender structures can in fact be stable in seismic events. This stability is attributed to the rocking of the stacked blocks with the shaking ground (9). These columns provide evidence of the possibility of using rocking motion

as a seismic isolation technique. In general, each component of a structure has the ability to participate in energy dissipation. The location where the structural energy dissipation is concentrated is based on a knowledgeable approach to modeling the system and an accurate mathematical representation of that model. Designing structures with the inherent ability to rock with the ground motion may provide a plausible method for reducing the risk of structures collapsing in large seismic events.

The rocking system with only a single block rocking on a foundation has been used to investigate rocking dynamics. The block displacement is assumed to occur in only two dimensions and hence, the block is treated as a rectangle. After a non-zero displacement at one of its top corners, the block impacts the foundation or ground interface and begins rocking. The repeated impacts with the foundation or ground interface introduce nonlinear dissipative effects that bring the block to rest. This rocking motion is a combination of an oscillating system, much like a pendulum, and an impact problem. The energy loss that causes the block to come to rest can be attributed to various mechanisms in the system: the energy transfer from the block to the foundation, the internal vibration energy in both the block and the foundation, the friction between the block and the foundation at the corners, the nonlinear deformation in the vicinity of the rocking interface and radial energy dissipation into the ground. Rocking models that assume the energy dissipation is completely concentrated at the interface of impact are moderately accurate for rigid systems; however, these models over predict the amount of energy lost at each impact. Some of these rocking models have been adapted to more closely reflect experimental tests by incorporating damping throughout the rocking response, rather than limiting the damping to occur only at impact, and modifying the location of the center of rotation of the rocking motion. These adaptations can be represented by including internal deformations in the rocking block models. Including these internal deformations will more accurately model the rocking system. The interest in nonlinear phenomena during the rocking response has expanded the scope of rocking models to include flexible and finitely rigid rocking systems.

This research investigates flexible rocking systems by focusing on the vibration energy developed within the block during rocking motion. The widely accepted rigid models, described

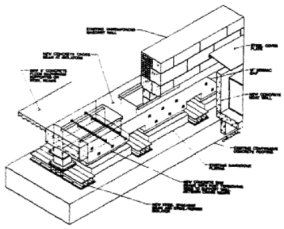

Figure 1.2: Typical isolator installed in the building.

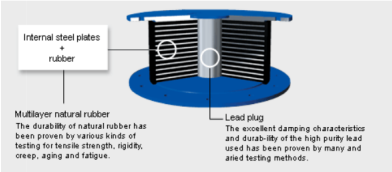

Figure 1.3: Rubber bearing isolator components.

in detail along with their mathematical representations in the following chapter, are unable to predict the vibration energy change in the rocking system because they do not consider the contribution of internal vibrations to the rocking response. In this thesis a new model is presented for a flexible block subjected to only gravitational forces that is rocked with varying initial drift (free rocking) on a rigid foundation.

1.1 Flexible rocking model (FRM)

The representation of a flexible block rocking on a rigid foundation, called the flexible rocking model (FRM), and its mathematical formulation, are presented in Chapter 3. The flexibility of the block is incorporated by assuming the block experiences internal deformations with the rigid rocking motion. The block develops flexural, axial and shear deformations that vary along its height. The FRM is a coupled system of three nonlinear partial differential equations and one nonlinear ordinary differential equation. Initial and boundary conditions are used to model the effect of the block impacting the foundation during rocking motion. The rocking motion is described in three phases with different initial and boundary conditions for each phase: *before impact*-the phase before the block strikes the foundation; *impact*-the phase when vibrations are generated in the block; and *after impact*—the phase when the block

rocks with a new center of rotation. The FRM is the comprehensive representation of the flexible rocking block motion. Additional forces and moments that represent other conditions for different rocking systems such as prestress, in controlled rocking, and flexible foundations can be included in the FRM in the boundary conditions and applied forces.

1.2 Simple flexible rocking model (SFRM)

The axial deformations in the flexible model developed in Chapter 3 are assumed to have the largest impact on the rocking response. In Chapter 4, the FRM is simplified by considering only these axial deformations in order to establish the affect of including vibrations on the rocking motion. This model is called the simple flexible rocking model (SFRM). The SFRM is a nonlinear coupled system of two differential equation. The implications of existence and uniqueness results for semilinear and quasilinear systems are discussed with respect to the SFRM. The boundary conditions in the FRM cannot strictly be applied in the SFRM because only the axial deformations are included in the model. To account for the missing FRM boundary conditions, the solution of the SFRM is found for each of the three phases of rocking motion by considering the solution at the end of the previous phase. The energy lost at each impact is defined by the amount of block vibration energy developed during each impact. The block vibration energy is explicitly defined and, under the assumption that the vibration energy is lost between impacts, a coefficient of restitution (COR) is obtained to create a complete rocking response for the SFRM.

1.3 Parametric study

In Chapter 5, the SFRM COR is used to create a rocking response. This SFRM rocking response and the SFRM COR are compared with the response and CORs of rigid models. The SFRM COR shows the block vibration energy has a more significant effect on the block rocking response than assumed by rigid rocking models. The relationship between the critical material flexibility and the amount of vibration energy developed in the block is defined as a function of the initial displacement of the block. The influence of the initial displacement, flexibility

and slenderness of the block on the block vibration energy and rocking motion are compared to similar results obtained for rigid models. The flexibility is directly related to the minimum initial drift that causes the block to experience rocking and is inversely proportional to the impact speed required to continue rocking. These relationships define the rocking condition that determines when the rocking response is initiated and when the rocking response ends.

1.4 Conclusion

This work expands the scope of rocking models to include the effect of internal motions on the energy dissipation of free rocking blocks. The following chapter is a literature review which briefly describes the current state of research regarding rocking models and impact problems that are relevant to this study. After the literature review are chapters 3, 4, and 5 as described previously, followed by a summary of results, suggestions for future research stemming from this work, and some conclusive remarks.

CHAPTER 2. REVIEW OF LITERATURE

Rocking structures have been explored in recent years as a structural design concept that enables structures constructed in seismic regions to be more resilient when subjected to earthquake loads (1), (27). The concept of rocking in seismic design is a new application of an old design concept. The representation of the rocking response of structures subjected to earthquake loading is often simplified by considering the response of controlled rocking rigid blocks (1), (27). The controlled rocking rigid block system is generated by applying forces that restrict the motion of the block to the free rocking rigid block system. This makes the free rocking block system an appropriate starting point for investigating the behavior of rocking blocks (9).

This chapter describes the origins of free rocking rigid block models, and the justification for adding models that represent the internal flexibility of the block to the current state of knowledge. Free rocking rigid block models established in the 1960s are the basis for most of the work in this area. The assumption that the block is completely rigid narrows the scope of the applications of the rigid block models and the rigid block assumption is not necessarily an appropriate representation for all rocking structures. Free rocking block models that encompass a larger scope of structural systems have been developed by including flexibility in the rocking block system. In the 1980s there was a significant effort to expand the scope of the applications of the free rocking rigid models, in which both rocking block and foundation are rigid, by considering a flexible interface between the rigid block and the foundation. Various mathematical methods and techniques to improve the stability and accuracy of the free rocking rigid models were also employed during this time. In the 2000s, studies about the internal and external deformations of the block and the influence of these deformations on the rocking motion were considered. This chapter begins with a complete overview of the free rocking rigid block model presented in 1963. Specifically, this chapter discusses the energy dissipation and

the limitations resulting from the rigid assumptions in rigid rocking models. Then, a discussion of mathematical models that improved aspects of the original free rocking rigid block model as well as the accompanying challenges of those mathematical models is presented. Finally, the mathematical tools used to create the free rocking flexible block model presented in Chapter 3 are introduced. The information in this chapter provides necessary context for understanding the free rocking flexible block model investigated in this research project.

2.1 History of rocking models

Earthquakes are an unpredictable natural phenomenon that have been studied by civil engineers in order to effectively design and build structures to withstand seismic events. In the late 19th century Milne (18) designed experiments to better understand the influence of earthquakes on buildings, bridges and other structures. The results of these experiments determined that the geometry of a free standing structure, and the foundation soil greatly influenced the likelihood of that structure overturning in a seismic event (18). In particular, softer soils dispersed the earthquake intensity while harder soils concentrated the earthquake more intensely in a smaller area. Additionally, stout structures were expected to experience less damage than slender structures because structures with more mass were expected to withstand larger seismic forces. According to Milne, accurate mathematical representations of free rocking structures should exhibit stability for non-slender structures on flexible soils.

Records from the May 22, 1960 Chilean earthquake contradicted these expectations (9). Concrete, non-slender water tanks were destroyed during this seismic event, while golf-ball-on-tee, slender water tanks remained standing. Structures subjected to large earthquakes in India, New Zealand and Greece exhibited the same effects as those in the Chilean earthquake (9). G.W. Housner developed a free rocking rigid block model to explain the structural stability of the slender water tanks as well as the instability of the large concrete tanks. This model provides the foundation for many of the research studies concerning rocking structures in the 1980s and today.

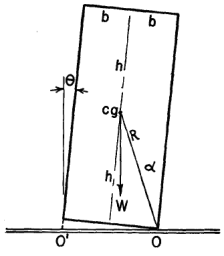

Figure 2.1: Schematic of the Housner block.

2.1.1 The simple rocking model

In 1963, Housner modeled the rocking motion of a tall slender rigid block as an inverted pendulum (9). The rigid block was given an initial angular displacement and released from rest. The block was subjected to free rocking, which means there are no applied restoration forces on the block. After this initial displacement, the rigid block rocked on the rigid foundation with respect to the assumed centers of rotation at its two bottom corners, O and O', as shown in Figure 2.1. The rocking motion is defined by the angle the bottom edge of the block makes with the foundation as a function of time, represented by θ. The coefficient of friction between the block and the foundation is assumed to be large enough to prevent the block from sliding or bouncing during the rocking motion. The rocking motion is characterized by the reduction of the angular displacement after each impact with the rigid foundation. The speed reduction throughout the rocking motion is a result of the system's kinetic energy loss. Under the assumption that both the block and foundation are infinitely rigid and incapable of developing internal vibrations, this energy loss is assumed to be concentrated at the interface between the block and the foundation. This rigid rocking block model developed by Housner is called the simple rocking model (SRM) and is the most general representation of free rocking block systems.

2.1.2 Energy Dissipation in Rocking Models

In response to the excitation of the block by an earthquake, a free rocking block rocks on top of its foundation, and then returns to its original position when the input energy from the earthquake in the rocking block system is completely dissipated. Each time the block impacts

the foundation, a portion of this energy is dissipated as a result of the input energy being transferred to another form of energy. This input energy can be transferred into vibrations within the block, vibrations in the foundation, energy loss at the interface, energy radiated through the foundation into the soil beneath it or any combination of an of these energies. Modeling the contributions of the vibration energy from the block, foundation, interface and soil to account for the energy loss can be cumbersome to analyze and represent accurately. The source of the energy loss that represents the conditions of the system is typically chosen to avoid this difficulty. In the case of the free rocking rigid block on a rigid foundation, Housner assumes that the energy loss occurs at the interface between the block and the foundation, as a result of their infinite rigidity. He assumes that, at each impact, a fraction of energy is removed from the system at the interface such that no vibrations or internal deformations occur in either the block or the foundation.

The ratio of the kinetic energy before and after a single impact determines the amount of energy retained by the system after impact. This ratio is called the coefficient of restitution (COR). The SRM defines the COR in terms of the geometry of the block. Therefore, the COR is constant over the entire rocking response and is equivalent for any rigid block with the same geometric dimensions. The assumptions of the SRM are appropriate for certain applications but should not be broadly applied to represent all free rocking structures because there are no completely rigid structures. Experimental studies in (11) and (27) show that for a block with a large modulus of elasticity (nearly rigid), a COR defined only by the geometric dimensions of the block overestimates the energy dissipated at each impact in the free rocking block system response (see Figure 2.2). The SRM has been an efficient starting point for investigations into free rocking rigid block motion but there are many areas where this model has been improved to provide a more general representation of free rocking block systems.

2.1.3 Changes and Extensions to Housner's Model

Buildings, bridges and other structures have a finite rigidity and are not completely rigid and the SRM Housner proposed is not an appropriate model for finitely rigid structures. Different researchers, such as Baratta et al. in (2), Chatzis et. al. in (3), Kalliontzis et. al. in (11),

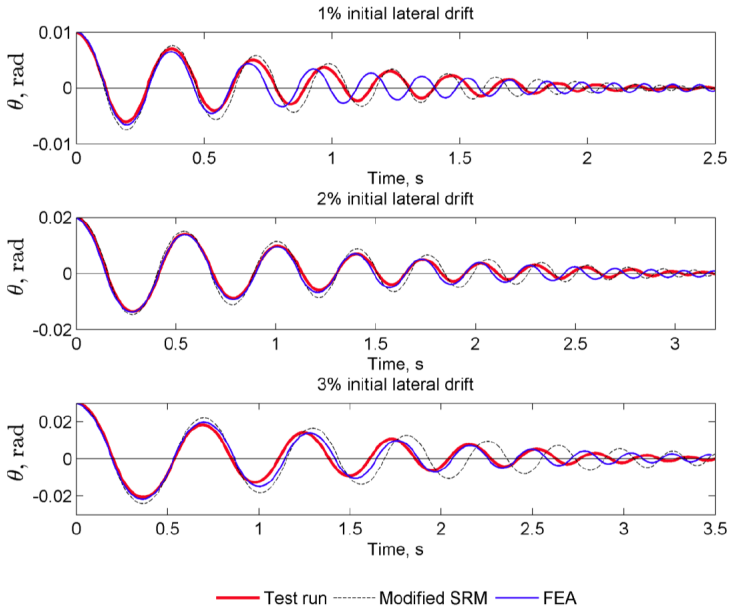

Figure 2.2: Comparison of SRM and Finite Element Analysis (FEA) with Test data response of rocking block in (11).

Lourenço et. al. in (22), and Vassiliou in (27), have made enhancements to the SRM to generalize the free rocking model of a rigid block. These enhancements include changed that incorporate the flexibility of the foundation, the damping at the interface between the block and the foundation, or the speed at impact and flexibility on the amount of energy dissipated during each impact. These changes capture how the motion and stability of the block are influenced when the assumptions that the block and foundation are rigid are relaxed.

Flexibility has been incorporated in the rocking block models in (3), (14) and (27) by adding springs at the interface of the block and the rocking surface to represent flexibility in the soil underneath the rigid foundation. Three popular configurations of these springs at the interface are: a single rotational spring (see Figure 2.8) (27); two linear springs at each corner O and O '(see Figure 2.4) (3); and a bed of nonlinear springs–which only exert a force on the block when compressed–known as the Winkler foundation (see Figure 2.5) (3). The rocking response of the block with an interface composed of springs and dampers is a more accurate representation of experimental block rocking responses than the theoretical rocking response created using rigid rocking block models (see Figure 2.2 and Figure 2.6). Vassiliou et al. propose a nonlinear

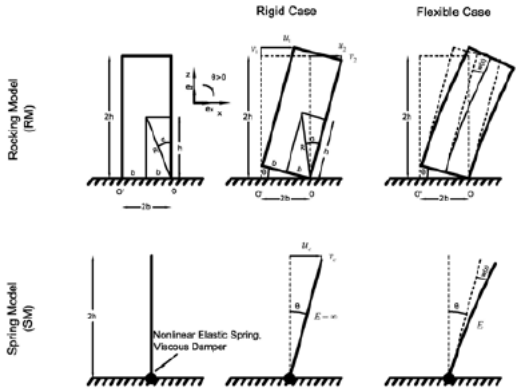

Figure 2.3: Original Rocking Model (SRM) and proposed Spring Model (SM)

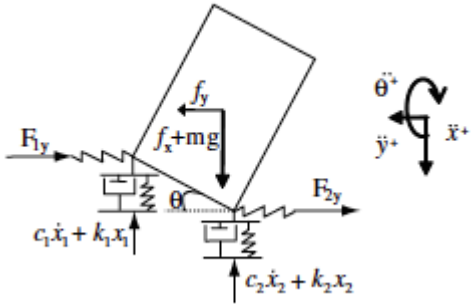

Figure 2.4: An illustration of the forces acting in the concentrated spring model (CSM)

single degree of freedom (SDOF) viscously damped flexible system and use FEM software to simulate the response of the flexible rocking system to earthquake motions. In this simulation, flexibility is included in both the block and the foundation, with the connection between the block and the foundation modeled by a nonlinear elastic spring with a viscous damper.

A key characteristic of the rocking block response is the stability of the block under seismic loads. The stability is described in terms of the likelihood that the block will overturn during the rocking response. The stability of the rocking block motion depends on small changes in the slenderness of the block, the size of the block, the initial displacement, and the flexibility in the system (see the effect of flexibility and damping in the responses pictured in Figure 2.6 and 2.7) (11) (27). Adding flexibility within the block or at the rocking interface to the system

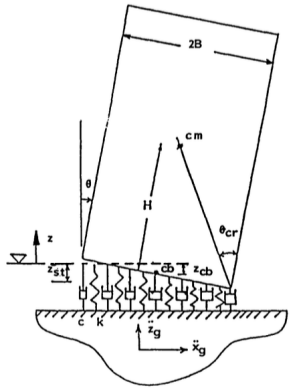

Figure 2.5: Rigid block rocking on Winkler Foundation in (14)

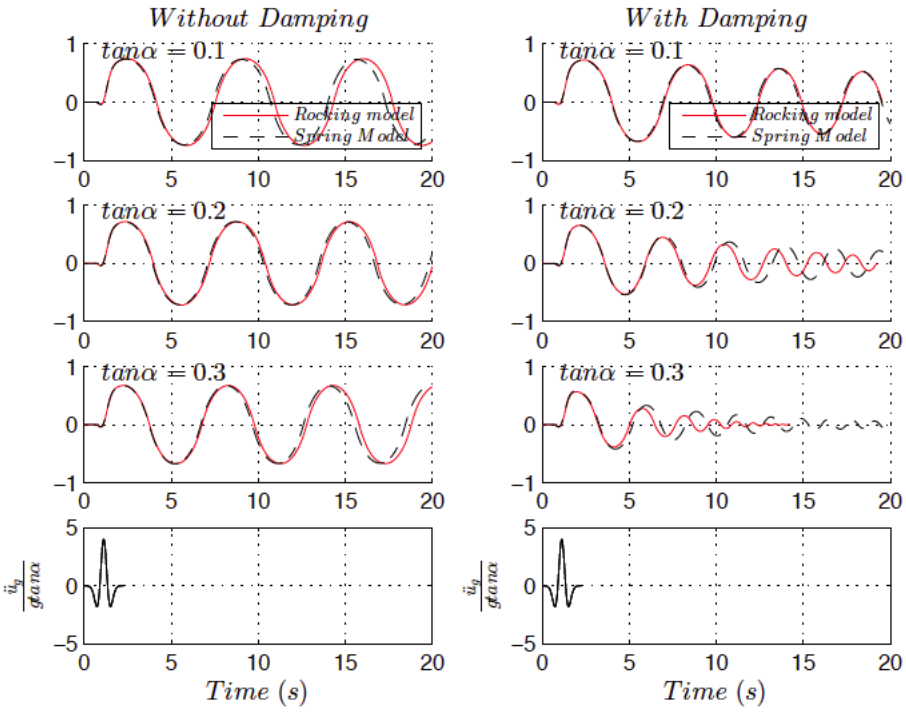

Figure 2.6: The time histories of the response of a rigid block with height 10m and slenderness ratio $\tan\alpha$ when excited by a symmetric Ricker Pulse excitation with $a_p = 4g\tan\alpha$ and $\omega_p = 2\pi$ rad/s. The response was computer for the Rocking Model(SRM) and the Spring Model (SM).

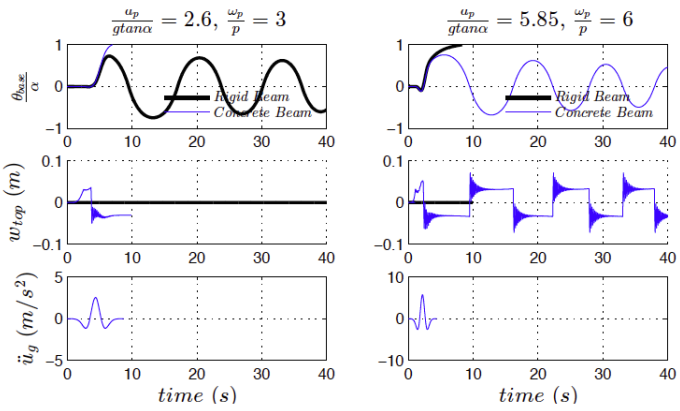

Figure 2.7: Comparison of the time histories of the response of a rigid and a concrete beam of slenderness and frequency parameter p, when subjected to a symmetric Ricker pulse with amplitude a_p and cyclic frequency ω_p. First row: normalized base rotation; Second row: top displacement due to bending; Third row: Ground acceleration.

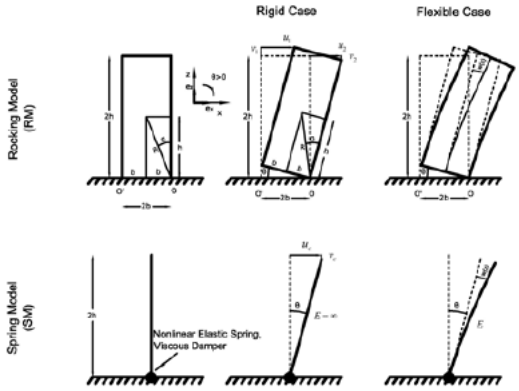

Figure 2.8: Original Rocking Model(RM) and proposed Spring Model(SM)

changes the influence of the slenderness, block size, and initial displacement on the rocking block response (1), (11), (14), (27), (22). Capturing the influence of flexibility at the interface and within the soil beneath the foundation has been covered extensively in the literature, for example in studies by Chatzis, Vassiliou and Prieto. The influence of block flexibility has not been discussed in an analytical way that defines the specific contribution of vibrations within the block to the free rocking block motion. The changes that were made to the SRM to broaden the scope of applications of the free rocking rigid model are used to guide the treatment of the free rocking flexible block model created in this thesis.

2.2 Mathematical modeling

A valid mathematical representation of the rocking block system is key to any design or analysis of a rocking structure. The focus of this section is on the mathematical representation of free rocking block systems. The mathematical model that represents the free rocking block must satisfy the assumptions that will govern the behavior of the rocking structure. These assumptions produce different rocking models and different rocking responses. The mathematical representation of the rigid rocking system is a simpler equation than the representation of any flexible rocking system because the rigid system is a simpler rocking system than any flexible rocking system. Relaxing the assumption that the block and foundation are infinitely rigid to the assumption that one or both are finitely rigid produces a more general representation of the rocking block system. Mathematical modeling techniques have produced representations for rigid blocks rocking on rigid foundations and rigid blocks rocking on flexible interfaces. Below is a summary of these mathematical representations of rocking block models for the free rocking rigid block systems with rigid and flexible rocking interfaces as well as techniques that are used to create the flexible block model.

2.2.1 Free Rocking Rigid models

The equation of motion for a free rocking rigid block was created by Housner in (9) by representing the rocking motion of the rigid block in the same way as the motion of an inverted pendulum, such as a metronome. The displacement θ, called the drift, is the angular displacement of the block measured between the block and the rocking interface. This displacement is defined as positive when the center of rotation is O, and negative when the center of rotation is O'(see Figure 2.1). The initial drift is the ratio of the lateral displacement of the top corner of the block to the total height of the block. When the block is released from this initial drift, the weight of the block acts as the restoring force of the block to return the block to rest. The component of the restoring force that contributes to the angular displacement of the block is only a fraction of the total weight, W, of the block. That fraction is determined by the angular displacement of the block. Conservation of angular momentum guarantees that for a block

with mass moment of inertia I_O and weight W (see Figure 2.1),

$$I_O \frac{d^2\theta}{dt^2} = sign(\theta) W R \sin(\alpha - |\theta|). \tag{2.1}$$

where $\ddot{I}_O$ is the angular momentum and $WR\sin(\alpha - |\theta|)$ is the restoring momentum from gravity. This is the simple rocking model (SRM) that represents the response of a rigid rocking block on a rigid foundation. The angle α represents the slenderness of the block and R is the distance from the center of gravity to either center of rotation. Under the assumption that θ is small, the sine term in eq. 2.2 is linearly approximated by the angle $\alpha - |\theta|$. The approximate SRM for small angular displacements, with $p^2 = \frac{WR}{I_0}$, is the piecewise ordinary differential equation (ODE)

$$\begin{cases} \ddot{\theta} - p^2\theta = -p^2\alpha, & \theta < 0 \\ \ddot{\theta} + p^2\theta = p^2\alpha, & \theta > 0 \\ \theta(0) = \theta_0,\ \dot{\theta}(0) = 0. \end{cases} \tag{2.2}$$

The rocking response in eq. 2.2 is a representation of continuous oscillatory motion, until the rocking behavior is added by incorporating energy dissipation throughout the entire response. In order to account for this energy dissipation Housner assumed that the energy lost during each impact is concentrated at the interface between the block and the foundation. This definition of energy loss neglects the development of any internal vibrations within the block, foundation, or soil. Under the assumption that energy dissipation occurs only at the interface, Housner expressed the energy loss at the interface with the coefficient of restitution (COR) defined as the ratio of the kinetic energy retained after an impact to the kinetic energy before that impact. The COR for the SRM is the constant geometric quantity

$$r_H = \left[1 - \frac{mR^2}{I_0}(1 - \cos 2\alpha)\right]^2. \tag{2.3}$$

Together, the SRM in eq. 2.2 and the COR in eq. 2.3 model the rocking response of a free rocking rigid block on a rigid foundation (9).

An entire free rocking response is created by connecting the piecewise solution of eq. 2.2 at the discontinuities where the center of rotation changes. Prieto et al. unify the piecewise SRM in (22) to create a continuous ODE with a continuous solution by taking advantage of

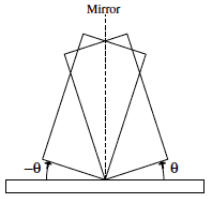

Figure 2.9: Dynamical symmetry associated with the sign of θ.

the symmetry inherent in the rocking system (see Figure 2.9). This produces a single ordinary differential equation analogous to the SRM

$$\begin{aligned} \frac{d}{d\tau}\left(\frac{\partial L_0}{\partial r'}\right) - \frac{\partial L_0}{\partial r} &= Q_r^d \\ \frac{d}{d\tau}\left(\frac{\partial L_0}{\partial \psi'}\right) - \frac{\partial L_0}{\partial \psi} &= 0 \end{aligned} \tag{2.4}$$

that is a function of the magnitude of θ, and the sign of θ, r and ψ respectively, where $L_0 = \frac{1}{2}\left(r'^2 + (r\psi')^2\right) - WR\cos(\alpha - r)$. The single ordinary differential equation in (22) includes impact in the Dirac-delta force, Q^d. Theoretically, the Dirac-delta force is an impulsive force that acts instantaneously and accomplishes the physical expectation that the energy in the continuous SRM is dissipated at the foundation interface between the rocking block and foundation. The COR in eq. 2.3 defines the amount of energy loss by defining the magnitude of the force Q^d. This method requires the use of numerical methods that cannot be strictly applied to an impulsive force to generate a rocking response. As the approximation of the Dirac-delta force approaches the Dirac-delta function, and the continuous solution becomes a better approximation of the rocking response than the response predicted by the piecewise SRM. The piecewise SRM and the numerical solutions of eq. 2.4 are shown in Figure 2.10with the numerical approximation $\delta_l(x)$ of the Dirac-delta function $\delta(x)$ for Q^d.

The instantaneous nature of impact forces gives rise to the formulation of the rocking system in terms of generalized functions known in mathematics as distributions. The instantaneous energy loss at the interface is captured by the introduction of a null distributiona distribution whose inner product, and the inner product of its derivatives, with any other distribution is zero. The null distributions model the dissipative nature of the system when the dissipation is concentrated at the interface by representing an instantaneous force that removes energy from the system. The null distribution approach employed by Baratta et al in (2) is a generalization

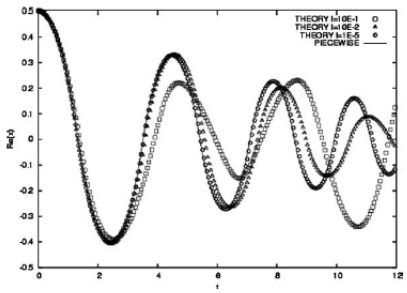

Figure 2.10: Comparison between Housner theory and complex formulation for different values of l under free rocking motion. $\mu = 0.925$ and $\alpha = tg^1(1/4)$ with initial conditions; ($\chi_1(0) = 0.5$, $\chi_2(0) = 0.0$, $\chi_3(0) = 0.0$, $\chi_4(0) = 0.0$).

of the Dirac-delta force approach in (22), which improves the stability of the problem by removing the dependence on the approximation of the Dirac-delta function. The study by Baratta proves different representations of the rigid rocking block system can yield similar rocking responses. The approach used for representing the energy dissipation greatly influences the different representations of the free rocking block system. Many different responses are possible depending on the assumed location of the energy loss in the rocking block system (2). The energy dissipation should be properly accounted for based on the properties of the system in order to create a response that represents the correct expected behavior of the rocking system. Accounting for this energy dissipation, in some cases, requires incorporating flexibility in the rocking block system.

2.2.2 Rocking models with flexible foundations

The mathematical formulations in the previous section are used to model the rigid rocking block system from (9). As previously noted, the rigid rocking block model with a rigid foundation assumes the energy lost at each impact is concentrated at the interface between the block and the foundation. In the case when the rigid body is supported by a flexible member, such as a rigid block supported on a flexible foundation or a rigid block and foundation supported on a flexible medium (e.g. soil), the treatment of the energy dissipation must reflect the flexibility introduced in the system. The rocking block systems with a rigid rocking block and a flexible interface (see Figures 2.8, 2.4 and 2.5), simulate conditions with flexible foundations or flexible

media beneath the foundation. These flexible systems have more complex mathematical representations than the rigid rocking block systems because of the added flexibility, particularly the complexity of properly accounting for the flexibility and its effect on the energy dissipation in the flexible system.

The energy dissipation in the flexible rocking system is captured with a COR, as in the rigid systems. The COR for the rocking block system with a rigid block and a flexible interface will depend on the characteristics of the flexible interface, in addition to the block geometry. This flexibility at the interface provides continuous damping throughout the duration of the rocking response. The COR for the rocking block system with a flexible interface quantifies the amount of energy lost after a single rocking period–the time it takes for the block to rock from its maximum displacement with one center of rotation, impact the foundation and rock to its maximum displacement balanced with the other center of rotation. The amount of energy lost over a single rocking period is concentrated at the rocking interface at the moment of impact as with the COR in eq. 2.3. Since the energy loss takes place at the same location in the rigid interface rocking system as the flexible interface rocking system, and the block remains rigid, eg. 2.2 is still used to determine the rocking block motion with the COR that accounts for the flexible interface.

The flexible interface is represented by different configurations of springs in (3) and (27). The energy lost at the interface after each impact is the result of the block causing the displacement of the spring(s) at the interface (3). In (27) the flexible interface is modeled by a single rotational spring with damping coefficient c. The COR of the system, ξ, is a function of the weight, size, slenderness, initial displacement and the flexibility of the interface (27). Figure 2.11 shows the COR decreasing as the damping, resulting from the flexible interface, is increasing. The decreasing COR indicates more energy is retained in the system as the damping at the interface increases. This experiment in (27) does not describe the form of the energy that is retained by the system is stored. A more comprehensive model could identify the form of this retained energy and the location within the rocking system the retained energy is concentrated, creating a more accurate representation of the rocking motion.

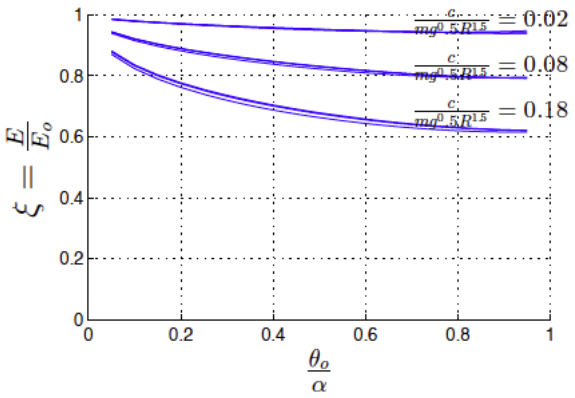

Figure 2.11: Damping ratio ξ plotted against the normalized initial angle of rotation θ_0/α for free vibrations of the spring model for different values of α and $\tilde{c}$.

In (3), which considers flexibility at the interface using springs and dampers, FEM software and other numerical solvers for the nonlinear mathematical representations create a rocking response for a rigid block on a flexible interface. A comparison of the rocking responses of the simple rocking model, the rigid block on the flexible interface represented with concentrated springs (see Figure 2.4), and the rigid block on the flexible interface represented with the Winkler interface (see Figure 2.5) is shown in 2.12 for two different soil conditions. This comparison highlights the limitations of the SRM. The SRM response does not reflect the change in foundation soil from Figures 2.12a and 2.12b because there is no parameter in the SRM to represent this change in foundation flexibility. The flexible interface models expand the scope of the applications of free rocking block systems beyond completely rigid systems.

In the last ten years, as a consequence of the curiosity in representing soils and other foundation media that are considered flexible, the consequences of block flexibility on the rocking block system have been studied. Block flexibility is added to the representation of the rocking block system in (27) using numerical solvers. These numerical solvers simulate the response of a beam with varying elastic moduli that represent various materials, such as concrete. The rigid model inaccurately represents the rocking response of a flexible block on a rigid foundation as shown in Figure 2.7 (27). Considering the flexibility of the rocking block is necessary in order to properly predict the rocking response of columns taller than 30 m (98 ft) (27)). The mathematical representation of block flexibility and the energy dissipation

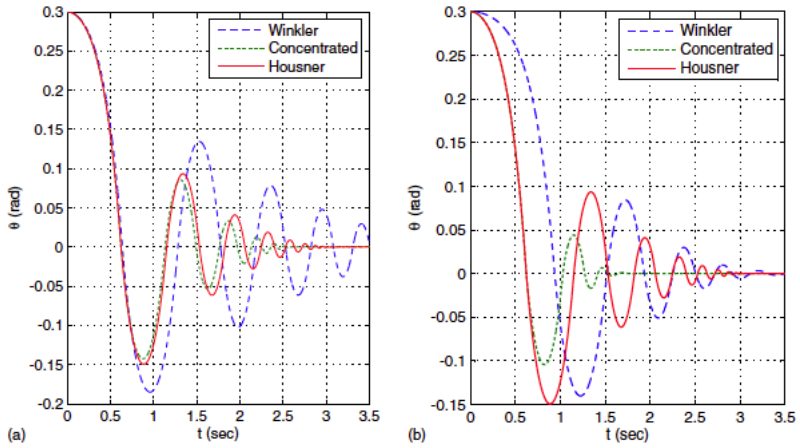

Figure 2.12: Comparison of the CSM and WM with Housner model for two different ground accelerations.

that results from the block flexibility in the free rocking model is required to create a more comprehensive model for a free rocking flexible block.

2.2.3 A new approach

The flexible rocking block model developed in this work investigates the interaction between the block vibrations that are created at impact and the rocking response of the flexible block. The block vibrations are internal deformations that result from axial loading caused by the impact of the flexible block with a rigid foundation. Similar internal displacements are the focus of Lagnese and Lyons in (15), which contains several models of thin plate deformations. The modeling techniques used in (15) capture the in-plane stretching and compressing within a plate that is loaded by some out-of-plane force. The Mindlin-Timoshenko plate model contains bending and shear plate deformations that represent the compressing, stretching and bending of the plate. This model is most appropriate for the internal block deformations that result from impact with the foundation. The flexibility of the block determines the extent of the stretching and compressing that represent the internal deformations. The total energy of the rocking block system, including the internal vibration energy, defines the internal deformations and the rocking motion. The flexible rocking block model includes the angular displacement θ, that defines the rocking motion as well as the flexural, axial and shear deformations that

constitute the stretching or compressing motions. This derivation of the flexible rocking block model, which is the focus of this research project, is described in depth in Chapter 3.

2.3 Impact problems

The rocking block motion is comprised of two types of dynamic motion: oscillatory motion of the block and impact with the foundation (2). The focus of the flexible rocking block model is characterizing the deformation of the block during impact, the duration of the impact, and the vibration energy developed during impact. This section is meant to provide the reader context regarding the scope and difficulty of impact problems, from a mathematical perspective.

Impact problems are used to model the state of two bodies before, during, and after they have impeded with one another. Impact problems are difficult to solve because of the instantaneous change in the system at impact and the sensitivity of impact models to small changes in the conditions governing the impact. The initial step in developing an accurate model for an impact problem is defining the conditions of the state of the impeding bodies at each of the three impact stages. The most crucial condition for impact problems is the energy transfer that occurs between the impact and after impact phases. There are different prevailing theories concerning the energy transfer between bodies during impact. Newtonian impacts measure the instantaneous energy transfer as energy lost in vibrations within the impinging objects and describes the energy retained in the objects with a COR. Poisson impacts divide the impact into phases and create a relation of the two impulses in each phase (24). The development of the flexible rocking model uses Newton's theory to compare the flexible rocking block system to the rigid systems discussed previously, and uses Poisson's theory to create a new description of the energy that relates the energy loss to the vibration energy developed within the block.

In order to discuss the impact problem within the rocking motion, the motion must be separated into three phrases. The before and after impact phases of the rocking block motion follow the dynamics used in the previous rocking models. The impact phase needs to be well defined in order to separate the rocking motion into these three phases. Impinging bodies are released from a state where there are no internal deformations or vibrations in either body. The internal vibrations are only developed in the bodies during impact. In the case when once body

has a larger mass and is stationary, for example a large block, and the other body, for example a thin rod, is moving toward the stationary body, the moving body develops more significant internal vibrations (17). The extensional, or axial, vibrations resulting from the impact between the one dimensional rod element and the large mass motivate the desire to create a rocking model that includes these types of deformations. This representation is adapted to the rocking system by considering the block to be the rod and the foundation as the large mass. The internal vibrations from the impact are represented by waves that travel through the rocking block after each impact with the foundation. The impact of the block with the foundation generates these waves in the block and in the foundation. The waves emanate from the impact interface between the two bodies. The impact is concluded when the stress on the bodies at this interface changes from a compressive stress to a tensile stress (17). This change in stress causes the two objects to separate. In the rod and large mass example, the duration of impact is the time it takes for a vibration wave to travel through the rod and back to the impact interface (17). This concept is also used to determine the duration of impact in the flexible rocking block system. The development of these vibration waves is the cause of the vibration energy developed within the block. After impact, this vibration energy can be dissipated or can return to the system as kinetic energy (11).

The existence of vibrations and the duration of impact may be generalized for the rocking block problem with the appropriate assumptions. After a rod impact the large mass, much like the case of a block impacting the foundation beneath it, the rod rebounds from the impact in the opposite direction with a lower velocity and the mass continues moving away from the rod (17). This is analogous to the block continuing in the opposite direction with reduced velocity. The reduced velocity is the result of the kinetic energy lost during impact and an increase in block vibration energy (28). Although the rod and mass never again collide, in the flexible rocking block model gravity acts as a restoration force and causes the block to impact the foundation repeatedly until the velocity at impact is too small to cause the block to uplift after impact (28). The conclusions from (17) and (28) define the conditions and behavior of the flexible rocking block during each impact with the rigid foundation during the rocking motion.

2.4 Conclusion

The vibrations developed within the flexible block during impact with the rigid foundation in the rocking block response is the focus of this thesis. Mathematical models that consider the various modes of internal deformations that result from impact are presented herein with specific attention to the proper boundary and initial conditions to represent the expected rocking block behavior. The energy in vibration within the block is carefully quantified using the energy equations that govern the model. Criteria for rocking, the amount of block vibration energy, and the limits of the rigid assumption are all determined with the explicit definition of the vibrations and the vibration energy within the block in the flexible rocking block system.

CHAPTER 3. FLEXIBLE ROCKING BLOCK MODEL

The application of flexible rocking models is currently limited to represent rigid structures with flexible foundation or rigid structures with rigid foundations on flexible soil. The addition of free rocking flexible models to the literature generalizes rocking models for a larger scope of structures. These flexible structures are generalized by blocks with finite modulus of elasticity rocking on a rigid foundation. The finite elastic modulus allows the block to experience deformations that are investigated in this chapter.

The rocking block motion is characterized by oscillatory motion that is disrupted by impacts with the foundation. The impact with the foundation compresses the block at the interface of the block and the foundation and creates interval deformations within the block. Contributors to the internal block deformation are the axial deformation along the height of the block, the flexural deformation along the width of the block, and the shear deformation. The flexibility of the block is represented by its ability to develop internal deformations after impact with the foundation. The axial, flexural and shear deformations within the flexible rocking block are similar to the shear and bending deformations within the plate bending models from (15). These internal deformations are considered in addition to the rigid displacement during the rocking response of the flexible block. This chapter defines the equation of motion for a flexible block rocking on a rigid foundation.

The internal and external displacements of the block during rocking motion are defined by the characterization of the energy within the rocking system. The initial drift of the block inputs kinetic energy into the block system. Each impact with the rigid foundation changes a portion of that kinetic energy to strain energy within the block. This strain energy creates internal stresses in the block that result in the internal deformations represented in the flexible rocking block model. The equations of motion of the flexible rocking block are determined by

conserving the rocking block system energy. Explicitly writing the energy of the block with the addition of the internal block deformations determines the rocking model of the flexible block.

3.1 Equation of motion

The rocking model of the rigid block system in (9) defines the rocking displacement of a two-dimensional block that results from an initial displacement at one of its top edges. The displacement at the top edge of the block causes the block to only contact the foundation on one of its bottom edges. The rigid block is released from this position with only one of its two bottom edges is in contact with the rigid foundation beneath, and the rocking motion described with the SRM begins. In the rigid rocking block model, the block strikes the foundation and the energy loss is assumed to be concentrated at the impact interface. This energy transfer causes the block to rock about the other bottom edge at a reduced speed.

In the rocking model with a flexible block and rigid foundation vibrations are assumed to develop within the block at the instant the block impacts the foundation. These vibrations continue moving through the block during impact until the stress in the block at the impact interface is large enough to cause the bottom face of the block to uplift. The block rocks about the opposite bottom edge with the block vibrations that were created during impact. The internal vibrations in the block are described as waves that result from the axial, flexural, and shear internal displacements. These internal block deformations are similar to the internal plate displacements modeled by Mindlin-Timoshenko in (15). The flexible rocking block is a special case of the Mindlin-Timoshenko plate with no bending in the direction of the thickness of the plate (no out-of-plane bending). The application of this plate theory is used to develop the flexible rocking block model.

The three-dimensional flexible block with finite modulus of elasticity (Young's modulus), E, used to develop the flexible rocking block model is shown in Figure 3.1. The block has volume density ρ, height $2h$, width $2b$, and thickness τ. Locations on the block are referenced with the block coordinate system designated by the coordinates (x_b, y_b, z_b) where x_b is in the direction of the width of the block, y_b is in the direction of the height of the block, and z_b is in the direction of the thickness of the block. The origin of the block reference frame (the $x_b - y_b - z_b$

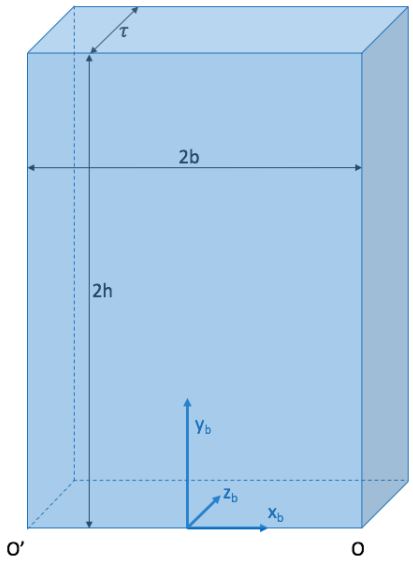

Figure 3.1: Schematic showing coordinate system for block.

axes system) is centered between the two bottom edges, O'and O (as in the SRM–see Figure 2.1), on the front face of the block.

The total internal displacements in the x_b, y_b, and z_b-directions, that result from impact with the foundation are U_{x_b}, U_{y_b}, and U_{z_b}, respectively. These three internal displacements form the triple that represents the total internal motion of the flexible block. The transformation from any original location on the block to its new position after applying the total internal displacements that result from impact are

$$(x, y, z) \mapsto (U_{x_b}(x, y, z; t), U_{y_b}(x, y, z; t), U_{z_b}(x, y, z; t)).$$

The flexible block is assumed to impact the foundation square on its bottom face so that the internal displacements are constant through the thickness of the block in the z_b direction. The block is therefore considered a two-dimensional block with displacements and forces that occur in the $x_b - y_b$ plane of the block. The total displacement functions U_i (where i denotes the direction of the displacement) represent a combination of the internal axial, flexural and shear deformations of the block. The axial deformation, u, is deformation in the direction of the height of the block. The flexural deformation, w, is deformation in the direction of the width. The shear deformation, ϕ, is the angular internal deformation that represents a combination

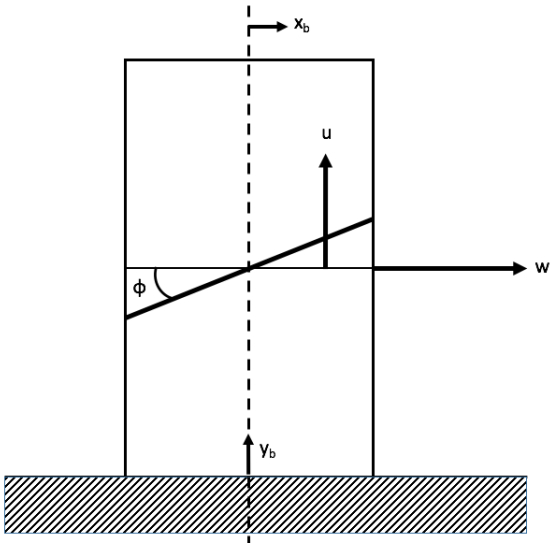

Figure 3.2: Schematic showing internal displacements of the block.

of movement in the x_b and y_b directions. The axial, u, flexural, w, and shear, ϕ, deformations are assumed to be constant along the width of the block and are functions of the height along the block, y, and time, t, only. These displacements, shown in Figure 3.2, define the equations for the total internal deformations of the block

$$U_{x_b} = w, \qquad U_{y_b} = u + x\phi \quad \text{and} \quad U_{z_b} \equiv 0. \tag{3.1}$$

The impact with the foundation during the rocking motion creates the internal deformations in the block. The rocking motion is defined using the rocking block coordinate system with $x-$ and $y-$ axes. This coordinate system is equivalent to the two-dimensional block coordinate system when the block is in contact with the foundation during impact. The rocking motion is represented by the angle between the y_b and y axes, θ, shown in Figure 3.3.

Any point on the block represented in the block coordinate system as $(x_{b_i}, y_{b_i}, z_{b_i})$, is represented during the rocking motion by applying the translation $(U_{x_b}, U_{y_b}, U_{z_b})$ and the rotation through θ. The rotation occurs in the rocking coordinate frame. The translated block coordinates are first transformed into coordinates in the the rocking coordinate frame, then rotated through the angle θ. The rotation in the rocking coordinate frame is defined by the matrix $R(\theta)$. The transformation from the block coordinate frame to the rocking coordinate frame

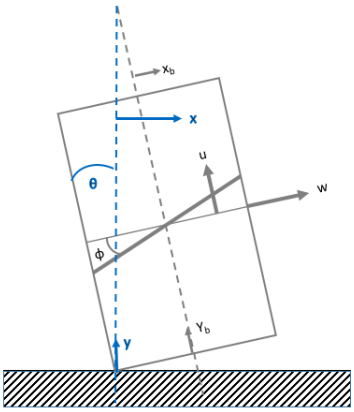

Figure 3.3: Schematic showing the internal displacements of the block with the rocking motion.

is a translation from the center of the block (the origin of the block coordinate frame) to the center of rotation of the rocking motion (the origin of the rocking coordinate frame).

The centers of rotation are the two bottom edges of the block O and O'; when O is the center of rotation θ is considered positive and the required translation from the block coordinate frame to the rocking coordinate frame is b along the positive x_b direction; when O'is the center of rotation θ is negative and the required translation from the bock coordinate frame to the rocking coordinate frame is b in the negative x_b direction. The rotation matrix $R(\theta)$ can be combined with the translation vector $(sign(\theta)b, 0, 0)$ to represent the rocking transform. The position of the point (x, y, z) during rocking motion is the point $(\tilde{x}, \tilde{y}, \tilde{z})$ that has been translated by $U_{x_b} + sign(\theta)b$, U_{y_b}, and U_{z_b} and rotated through an angle θ where

$$\begin{pmatrix} \tilde{x} \\ \tilde{y} \\ \tilde{z} \end{pmatrix} = R_\theta \begin{pmatrix} x + sign(\theta)b + w \\ y + u + x\phi \\ z \end{pmatrix} = \begin{bmatrix} \cos\theta & -\sin\theta & 0 \\ \sin\theta & \cos\theta & 0 \\ 0 & 0 & 1 \end{bmatrix} \begin{pmatrix} x + sign(\theta)b + w \\ y + u + x\phi \\ z \end{pmatrix}$$
$$= \begin{pmatrix} (x + sign(\theta)b + w)\cos\theta - (y + u + x\phi)\sin\theta \\ (x + sign(\theta)b + w)\sin\theta + (y + u + x\phi)\cos\theta \\ z \end{pmatrix} \quad (3.2)$$

The rotation through θ is the rigid rocking motion of the block and the internal deformations u, ϕ, and w are the vibrations or waves that travel through the flexible block. The transformed representation of locations on the block in terms of height and time are used below to write

explicit formulas for the kinetic, strain and work energy in the block. The general form for strain energy, kinetic energy and work energy used in the derivation of the flexible rocking block model were taken from (15).

3.1.1 Strain energy

The strain energy is the energy produced by the strain in the block that results from the impact with the foundation that occurs during rocking motion. This strain is measured according to the internal deformations within the block. The strain is the amount of deformation in one direction for each unit in that direction. The strain tensor is the movement in one direction for each unit of movement in another direction. For the two directions x and y is

$$\epsilon_{xy} = \frac{1}{2}\left(\frac{\partial U_x}{\partial y} + \frac{\partial U_y}{\partial x}\right) \tag{3.3}$$

as defined in (15). The internal deformations represented by the strain in the block occur as waves or vibrations, and the strain energy is the result of the stress induced by the internal movements over the volume of the block. The stress at a particular location on the block is the net displacement in one direction that results from the net force in another direction. The stress, σ, in the x direction due to the force in the y direction is

$$\sigma_{xy} = \frac{E}{1+\nu}\left(\epsilon_{xy} + \frac{\nu}{1-2\nu}\sum_k \epsilon_{kk}\delta_{xy}\right) \tag{3.4}$$

where the strain, ϵ, is defined by eq. 3.3. The definitions of the stress and strain tensors are the result of the tensor products of the displacements with the directions of movement.

The angular displacement during the rocking motion does not contribute to the internal deformations within the block. The strain in the block is the result of the total deformations U_{x_b} and U_{y_b}. The strain tensors that result from movement in the x_b and y_b directions from the total displacements in eq. 3.1 are

$$\begin{aligned}
\epsilon_{xx} &= \frac{\partial w}{\partial x_b} = 0 \\
\epsilon_{xy} &= \frac{1}{2}\left(\frac{\partial w}{\partial y_b} + \frac{\partial(u + x\phi)}{x_b}\right) = \frac{1}{2}\left(w_{y_b} + \phi\right) \\
\epsilon_{yy} &= \frac{\partial U_{y_b}}{\partial y_b} = u_y + x\phi_y.
\end{aligned}$$

The internal stresses in the block that result from internal strain in the x_b, y_b, and $x_b y_b$ directions as a result of those strains are

$$\sigma_{xx} = \frac{E\nu}{1-\nu^2}\epsilon_{yy}, \quad \sigma_{xy} = k\frac{E}{1+\nu}\epsilon_{xy}, \quad \text{and} \quad \sigma_{yy} = \frac{E}{1-\nu^2}\epsilon_{yy}, \tag{3.5}$$

where k is the shear constant. The strain energy, SE, that results from theses stresses and strains over the volume, V, of the block is the integral $SE = \frac{1}{2}\int_{\mathrm{V}} \sum_{i,j} \sigma_{ij}\epsilon_{ij}\, d\mathrm{V}$. The strain energy for the block in Figure 3.1 with the strain and stresses defined above is

$$SE = \frac{Eb\tau}{1-\nu^2}\int_0^{2h} (u_y)^2 + k\frac{(1-\nu)}{2}(w_y-\phi)^2 + \frac{b^2}{3}(\phi_y)^2\, dy. \tag{3.6}$$

This strain energy measures the effect of flexibility on the flexible rocking block system.

3.1.2 Kinetic energy

The kinetic energy of the flexible rocking block system is a measure of the energy produced by the block's movement. The kinetic energy is a function of the mass and speed of the block. The block speed is defined by any movement the block experiences. The blocks movement is assumed to be comprised of the internal deformations and the rigid rocking motion. The rigid rocking motion determines the rocking speed of the block. The speed of the internal deformations is the speed of the vibrations as they move through the block. The kinetic energy of the system is the integral of the product of the volume density of the block with the total speed of the block, $KE = \frac{\rho}{2}\int_{\mathrm{V}} ||(\dot{\tilde{x}}, \dot{\tilde{y}}, \dot{\tilde{z}})||^2\, d\mathrm{V}$, where $(\tilde{x}, \tilde{y}, \tilde{z})$ is defined in eq. 3.2. The kinetic energy for the block in Figure 3.3 is

$$KE = \rho b\tau \int_0^{2h} \left(\dot{\theta}(y+u) - \dot{w}\right)^2 + \left(\dot{\theta}(b+w) + \dot{u}\right)^2 + \frac{b^2}{3}\left(\left(\dot{\theta}+\dot{\phi}\right)^2 + \left(\dot{\theta}\phi\right)^2\right) dy. \tag{3.7}$$

3.1.3 Work energy

Work is the energy produced when an object is moved a certain distance by a particular force. The general formula for work energy from (15) in terms of generalized volumetric forces $(\tilde{f}_{x_b}, \tilde{f}_{y_b}, \tilde{f}_{z_b})$ and boundary forces $(\tilde{g}_{x_b}, \tilde{g}_{y_b}, \tilde{g}_{z_b})$ acting on the block in the (x_b, y_b, z_b) directions, respectively, is

$$WE = \int_V \tilde{f}_i U_i\, dV\, dx + \int_\Gamma \tilde{g}_i U_i\, d\Gamma.$$

where Γ is the boundary edge of the block and V is the total volume of the block. The rocking block in Figure 3.3 is only affected by the initial displacement and the force of gravity and therefore the only force that contributes to the work energy of the system is the force of gravity. Gravity is a volumetric force and only acts in the vertical directions of the block. The force of gravity or the weight of the block is the scalar product of the total mass of the block and the gravitational constant g. The work energy for the rocking block is

$$\begin{aligned} WE &= \rho g \int_{-b}^{b} \int_{\Omega} (x + b + w) \sin\theta + (y + u + x\phi) \cos\theta - y \, d\Omega \, dx \\ &= \rho \tau g \left[4b^2 h \sin\theta - 4bh^2 (1 - \cos\theta) + 2b \int_0^{2h} w \sin\theta + u \cos\theta \, dy \right] \end{aligned} \tag{3.8}$$

3.1.4 The flexible rocking block model

The development of the flexible rocking model is based on the energy present in the flexible rocking block system. Newton's second law is equivalent to Hamilton's principle (also known as the principle of virtual work) which states that a system evolves in such a way that the exchange of kinetic and potential energy is minimized. This minimization, defined in terms of the rigid rocking displacement and internal deformations, will yield a differential equation whose solution represents the motions of the flexible rocking block system.

The Lagrangian equation for the flexible rocking block system,

$$L = KE + WE - SE, \tag{3.9}$$

is the net energy in the flexible rocking block system, where KE is the kinetic energy due to the rocking motion, WE is the work energy due to gravity and SE is the strain energy from the internal deformations of the block, defined in terms of the unknown displacements θ, u, w, and ϕ. The angular displacement and internal deformations that characterize the flexible rocking block motion must conserve the energy of the system. Hence, the first variation of the functional $J = \int_0^t L \, ds$, with respect to admissible displacements, should vanish. The Euler-Lagrange equation is the optimization of the equation $J(X)$ in terms of small perturbations of the displacement vector X (i.e. $\left. \frac{\partial J(X + \epsilon Y)}{\partial \epsilon} \right|_{\epsilon} = 0$). The solution vector $X = (\theta, u, w, \phi)$ is the displacement vector which optimizes J and captures the motion of the rocking system. The

Euler Lagrange equation is the differential equation that represents the motion of the flexible rocking block.

Determining the Euler-Lagrange equation requires the calculus of variations. The energies in eqs. 3.6, 3.7 and 3.8 are combined to write $L(w,u,\phi,\theta,t)$ and $J(w,u,\phi,\theta,t)$ (see Appendix B for detailed calculations). The resulting system of partial differential equations that defines the equation of motion of the rocking block is

$$\begin{cases} \ddot{\theta}\left((y+u)^2+(b+w)^2+\frac{b^2}{3}(1+\phi^2)\right)+2\dot{\theta}\left((y+u)\dot{u}+(b+w)\dot{w}+\frac{b^2}{3}\phi\dot{\phi}\right) & \\ -(y+u)\ddot{w}+(b+w)\ddot{u}-\frac{b^2}{3}\ddot{\phi}+g\left((b+w)\cos\theta-(y+u)\sin\theta\right)=0, & t>0 \\ \ddot{w}-\ddot{\theta}(y+u)-2\dot{\theta}\dot{u}-(\dot{\theta})^2(b+w)-\frac{E}{2\rho(1-\mu^2)}k\frac{(1-\mu)}{2}\left(\frac{\partial^2 w}{\partial y^2}-\phi_y\right)+g\sin\theta=0 & (y,t)\in(0,2h)\times(0,\infty) \\ \ddot{u}+\ddot{\theta}(b+w)+2\dot{\theta}\dot{w}-(\dot{\theta})^2(y+u)-\frac{E}{2\rho(1-\mu^2)}\frac{\partial^2 u}{\partial^2 y}+g\cos\theta=0 & (y,t)\in(0,2h)\times(0,\infty) \\ \frac{b^2}{3}\left(\ddot{\phi}+\ddot{\theta}-(\dot{\theta})^2\phi\right)-\frac{E}{2\rho(1-\mu^2)}\left(k\frac{(1-\mu)}{2}(w_y-\phi)+\frac{b^2}{3}\frac{\partial^2\phi}{\partial y^2}\right)=0 & (y,t)\in(0,2h)\times(0,\infty). \end{cases} \tag{3.10}$$

This equation of motion determines the internal deformations, u, w, and ϕ and the rotation θ. The internal deformations act as vibration waves that move through the block and in eq. 3.10 the respective wave components are can be rewritten in terms of the wave equation operators

$$\Box_1 w := \ddot{w}-\frac{E}{2\rho(1-\mu)^2}\frac{k(1-\mu)}{2}w_{yy} \qquad \text{and} \qquad \Box_2 u := \ddot{u}-\frac{E}{2\rho(1-\mu^2)}u_{yy}. \tag{3.11}$$

These wave operators are substituted into eq. 3.10 to create the flexible rocking block model

$$\begin{cases} \ddot{\theta}\left(\dfrac{8bh^3}{3}+\dfrac{8b^3h}{3}+b\displaystyle\int_0^{2h} 2uy+u^2+2bw+w^2+\dfrac{b^2}{3}\phi^2\,dy\right) \\ \quad 2\dot{\theta}\displaystyle\int_0^{2h}(y+u)\dot{u}+(b+w)\dot{w}+\dfrac{b^2}{3}(\phi\dot{\phi})\,dy \\ g\left(2b^2h\cos\theta-2bh^2\sin\theta\right)+gb\left(\displaystyle\int_0^{2h} w\,dy\cos\theta-\int_0^{2h} u\,dy\sin\theta\right) \\ \quad -b\displaystyle\int_0^{2h}(y+u)\ddot{w}-(b+w)\ddot{u}+\dfrac{b^2}{3}\ddot{\phi}\,dy=0, \end{cases} \qquad t>0$$

$$\Box_1 w-\ddot{\theta}(y+u)-2\dot{\theta}\dot{u}-(\dot{\theta})^2(b+w)+\frac{E}{2\rho(1-\mu^2)}k\frac{(1-\mu)}{2}\phi_y+g\sin\theta=0, \quad (y,t)\in(0,2h)\times(0,\infty)$$

$$\Box_2 u+\ddot{\theta}(b+w)+2\dot{\theta}\dot{w}-(\dot{\theta})^2(y+u)+g\cos\theta=0, \qquad (y,t)\in(0,2h)\times(0,\infty)$$

$$\Box_2\phi-\left(-\ddot{\theta}+(\dot{\theta})^2\phi\right)-\frac{E}{2\rho(1-\mu^2)}\frac{3}{b^2}k\frac{(1-\mu)}{2}(w_y-\phi)=0, \qquad (y,t)\in(0,2h)\times(0,\infty). \tag{3.12}$$

The flexible rocking block model above in eq. 3.12 is a highly nonlinear system of coupled partial differential equations. The angular displacement θ is assumed to be small and only changes with time. The internal displacements u, w, and ϕ must at least be elements of the Sobolev space H^1 so that the derivatives in space and time are square integrable functions. This condition guarantees the bounded existence of the weakly defined second derivatives of these displacements that occur in eq. 3.12. The theory from (15) guarantees that the above equation, without the angular displacement, has a unique variational solution in H^1.

The flexible rocking model in eq. 3.12 represents the oscillatory motion of rocking with internal vibrations. This equation does not include the effect of the impact between the block and the foundation that initiates the internal vibrations and characterizes the rocking motion. The boundary and initial conditions for the rocking model add the effect of this impact to the block's oscillatory motion to create the complete rocking response.

3.2 Including impact

The impact that occurs between the flexible block and the foundation is represented using mathematical conditions of impact models that divide the impact into different phases of motion of the impinging bodies. These phases of motion represent the instantaneous changes in the

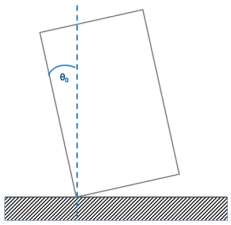

Figure 3.4: The angular displacement shown on the rocking block.

internal and external motion of the bodies involved in the impact. The changes in motion occurs three times in the rocking block system. The phases of the rocking block motion are named for when these changes occur in relation to the block's impact with the foundation. Impact with the foundation is included in the flexible rocking block model by defining the proper boundary conditions for each of three phases of impact motion and the conditions that define how to continue from one phase of impact motion to the next.

3.2.1 Before impact

Before rocking begins, the block has an initial angular displacement measured between the bottom face of the block and the foundation with center of rotation arbitrarily chosen about the bottom left edge, O'in Figure 3.1 (rocking could equivalently start with the block balanced on the bottom right edge so that the center of rotation is O). The initial angle the block makes with the foundation is called the initial drift, θ_0, and is represented as the ratio of the lateral displacement of the top edge to the total height of the block. The motion is initiated by releasing the block from this position (see Figure 3.4) with an initial speed of θ_1. The edge O'is pinned to the foundation and there is no displacement other than the rotation about this edge. All other surfaces of the block are not in contact with any other interfaces or forces and are stress free. The natural boundary conditions that arise from the calculus of variations (see Appendix A) conclude that all internal strains are absent before impact.

The conditions of the block in this phase reflect the state of the block before any impacts have occurred. The flexible block is treated as a rigid block during this phase of motion since

there are no internal deformations present. The boundary conditions that result from the description of the system before the first impact are

$$\begin{cases} (\theta, \dot{\theta})\Big|_{t=0} = (\theta_0, \theta_1) & \in (\mathbb{R} \times \mathbb{R}) \\ (w, \dot{w})|_{t=0} = (0,0) & \in (H^1[0,2h] \times L^2[0,2h]) \\ (u, \dot{u})|_{t=0} = (0,0) & \in (H^1[0,2h] \times L^2[0,2h]) \\ (\phi, \dot{\phi})\Big|_{t=0} = (0,0) & \in (H^1[0,2h] \times L^2[0,2h]) \\ \\ w(0,t) = 0, \quad u(0,t) - b\phi(0,t) = 0 & \text{at } x = -b \quad \text{(pinned edge)} \\ \\ \dfrac{Eb^3}{3(1-\nu^2)}\phi_y - \dfrac{Eb^2}{1-\nu^2}u_y\Big|_{y=0} = 0 & \text{at } x = b \quad \text{(stress-free edge)} \\ \\ w_y(2h,t) = 0, \quad \phi_y(2h,t) = 0, \quad u_y(2h,t) = 0 & \text{along the top edge of the block.} \end{cases} \tag{3.13}$$

3.2.2 Impact

As soon as the bottom face of the block is completely in contact with the foundation surface, the impact phase begins. Once impact is initiated the previous boundary conditions are no longer valid. The impact interface below the block is assumed to be completely horizontal such that $\theta = 0$ when the bottom face of the block is in contact with the foundation surface. The entire bottom face of the block is in contact with the foundation throughout the impact and is restricted from any displacements. The speed with which the block impacts the foundation causes an impulse that creates deformations in the flexible block. The initial speed of these deformations, w_1, u_1, and ϕ_1, is equivalent to their respective component of the inertia created by the angular impact speed θ_1.

These deformations travel through the block as waves. The waves have an initial velocity equal to the speed of the block at impact. The waves travel through the block until they reach the top of the block. Once the vibration waves reach the top of the block, they reflect back through the block until they reach the base of the block that is in contact with the foundation.

The waves return to the base of the block and cause the stress along the bottom face of the block to change from a compressive stress to a tensile stress. The change in stress causes the block to separate from the foundation and defines the end of the impact phase. The duration of the first phase of impact is determined by the speed of impact of the block, the height of the block and the material of the block. There are still no external forces acting on the block and all edges,other than the bottom edge, remain stress free. The conditions that govern the impact phase are described below:

$$
\begin{cases}
(\theta, \dot{\theta})\Big|_{t=t_0} = (\hat{\theta}_0, \theta_1) & \in (\mathbb{R} \times \mathbb{R}) \\
(w, \dot{w})|_{t=t_0} = (0, w^1) & \in (H^1[0, 2h] \times L^2[0, 2h]) \\
(u, \dot{u})|_{t=t_0} = (0, u^1) & \in (H^1[0, 2h] \times L^2[0, 2h]) \\
(\phi, \dot{\phi})\Big|_{t=t_0} = (0, \phi_1) & \in (H^1[0, 2h] \times L^2[0, 2h]) \\
\\
w(0,t) = 0, \quad u(0,t) - b\phi(0,t) = 0 & \text{(pinned both edge)} \\
\\
w_y(2h,t) = 0, \quad \phi_y(2h,t) = 0, \quad u_y(2h,t) = 0 & \text{along the top edge of the block.}
\end{cases}
\tag{3.14}
$$

3.2.3 After impact

The rocking motion is continued by pinning the bottom right edge to the foundation and releasing the bottom left edge. This forces the block to rotate about the new center of rotation O. During impact, the surface of the block in contact with the foundation is loaded and suddenly released. The stress at the contact surface changes sign just before the bottom surface lifts off of the foundation surface, indicating the conclusion of impact. The duration of impact is short compared with the other phases of motion (17). Some of the kinetic energy in the rocking block system is changed to internal vibration energy within the block during the impact phase of the rocking block motion. The block will continue to rock about point O with a lower angular speed and the residual vibrations that were generated during impact. All the faces of the block are again stress free, while the center of rotation edge is pinned to the foundation. The conditions

in this phase are similar to those before impact with the added contribution of the speed and magnitude of the internal block vibrations. These conditions are shown in eq. 3.15:

$$
\begin{cases}
(\theta,\dot{\theta})\Big|_{t=0} = (-\hat{\theta}_0,\theta_2) & \in (\mathbb{R}\times\mathbb{R}) \\
(w,\dot{w})|_{t=0} = (w^0,-w^1) & \in (H^1[0,2h]\times L^2[0,2h]) \\
(u,\dot{u})|_{t=0} = (u^0,-u^1) & \in (H^1[0,2h]\times L^2[0,2h]) \\
(\phi,\dot{\phi})\Big|_{t=0} = (\phi_0,-\phi_1) & \in (H^1[0,2h]\times L^2[0,2h]) \\
\\
w(0,t)=0, \quad u(0,t)+b\phi(0,t)=0 & \text{at } x=b \\
\\
\dfrac{Eb^3}{3(1-\nu^2)}\phi_y + \dfrac{Eb^2}{1-\nu^2}u_y\Big|_{y=0} = 0 & \text{at } x=-b \\
\\
w_y(2h,t)=0, \quad \phi_y(2h,t)=0, \quad u_y(2h,t)=0 & \text{for } -b\le x\le b
\end{cases}
\tag{3.15}
$$

3.3 Conclusions

The internal block vibrations captured by the flexible rocking block model are the result of the energy transferred to internal block energy during impact. This internal energy is retained within the block by the internal block vibrations. The energy retained by the block can dissipate the energy input by the initial drift or can continue to contribute to the rocking motion. The FRM captures this energy retention to model the rocking motion of the block and the effect of this internal vibration energy on the block rocking response.

The flexible rocking model (FRM) is composed of eqs. 3.12 - 3.15. These equations represent the complete displacement of the flexible rocking block through one impact. After the first impact, the before impact conditions are no longer valid before successive impacts because they do not include the effects of the vibrations that are developed during impact on the rocking block motion. The FRM can be extended to represent an entire rocking response by successively linking the impact and after impact boundary and initial conditions with eq. 3.12 after the first impact with the foundation. The development of numerical solutions to eq. 3.12

is possible for boundary conditions other than those specified in eq. 3.13 - 3.15. The unknown contact region makes defining the stress at the contact surface of the block impossible. In order to apply numerical methods to this flexible rocking problem, the contact region between the block and the foundation requires a continuous definition over the entire rocking response. Numerical solutions are not possible in the flexible rocking block rocking problem because there is no suitable definition of the contact region or the deformation along the contact region.

The flexible rocking model represents the axial, flexural and shear deformations that result from the rocking block motion. The impact that causes these deformations imposes an axial load on the rocking block. The flexural and shear deformations result when the block does not impact the foundation with the bottom surface completely flat. The axial deformation is therefore assumed to be the most significant contributor to the strain energy in the block. The significance of the block vibrations is discussed in the next chapter with the focus on the significance of the axial vibrations in the block. The FRM is presented here to provide a basis for the simplification made in the next chapter. The rest of this thesis concentrates on the simplified model and the contributions of the axial vibrations that the simplified flexible rocking model represents.

CHAPTER 4. SIMPLIFIED FLEXIBLE ROCKING BLOCK MODEL

The flexible rocking block model (FRM) in the previous chapter describes the internal block deformations and the external rotational displacement that characterizes the rocking motion of the block. The FRM provides a new mathematical representation of the rocking block motion by generalizing the simple rocking block model, which only represents rigid blocks, to represent flexible blocks by incorporating the internal block deformations present in a flexible block. The FRM defines the internal block energy, which is useful in the load analysis of structures in seismic areas.

The impact of the block with the foundation applies an axial force on the block that causes the internal deformations. The internal deformations in the same direction of this axial force are assumed to be larger than the internal deformations that occur in other directions. The axial deformations are presumed to be the largest contributor to the block vibration energy. The goal of this research study is to quantify the axial vibration energy within the flexible block and determine the significance of this internal block energy to the rocking motion of the block. This in-depth study of the block's axial deformations and their effect on the rocking motion of the block determines that the vibration energy can have a more substantial affect than initially considered by the SRM and other rigid block models. The simple flexible rocking model (SFRM) is a simplification of the FRM presented in Chapter 3 that considers only the axial deformation of the block and the angular rocking motion. The rocking block that only experiences axial deformation and rotation displacement from rocking is called the simple flexible rocking block. Considering only one mode of internal deformation simplifies the FRM in such a way that explicit solutions for the motion can be determined in terms of the flexibility of the block and the initial drift angle. As a result, a detailed analysis of the block during the impact phase of the rocking motion is considered in this thesis. In this chapter the SFRM is

described in terms of the three phases of impact, the internal axial deformation during impact and the internal block energy are defined as functions of the block flexibility.

4.1 Equation of motion

The SFRM models the rocking response of a flexible block that only develops axial deformations rocking on a rigid foundation after an initial angular displacement. The block conditions before the rocking motion is initiated, the block geometry shown in Figure 3.1, and the notation shown in Figure 3.2 and Figure 3.3 that were used in the development of the FRM in Chapter 3, are used again for developing the SFRM. The simple flexible block is assumed to experience only the external angular displacement, $\theta(t)$, and the internal axial deformation, $u(y,t)$. The axial deformation varies along the height of the block but remains constant along the width of the block. The two axes that represent the width and the height of the block are the x_b and y_b axes respectively (see Figure 3.3). The total displacements in the x_b, y_b, and z_b directions are $U_{x_b} \equiv 0$, $U_{y_b} = u$, and $U_{z_b} \equiv 0$, respectively. This definition of the total displacements simplifies eq. 3.2 for the transformed block location, $(\tilde{x}, \tilde{y}, \tilde{z})$, with rotation matrix R_θ to

$$\begin{pmatrix} \tilde{x} \\ \tilde{y} \\ \tilde{z} \end{pmatrix} = R_\theta \begin{pmatrix} x + b + U_x \\ y + U_y \\ z \end{pmatrix} - \begin{pmatrix} b \\ 0 \\ 0 \end{pmatrix} = \begin{pmatrix} (x+b)\cos\theta - (y+u)\sin\theta - b \\ (x+b)\sin\theta + (y+u)\cos\theta \\ z \end{pmatrix}. \tag{4.1}$$

The block is unchanged in the z_b direction and, as in the FRM, any change in the x_b or y_b directions are constant through the thickness of the block. The expressions for the energy in the SFRM are simplified representations of the energy in the FRM in terms of the block displacements. Without the flexural and shear deformations, the kinetic, strain, and work energy in the SFRM from eqs. 3.6, 3.7 and 3.8 are

$$SE = \frac{Eb\tau}{1-\nu^2} \int_0^{2h} (u_y)^2 \, dy \tag{4.2}$$

$$KE = \rho b\tau \int_0^{2h} \left(\dot{\theta}(y+u)\right)^2 + \left(\dot{\theta}b + \dot{u}\right)^2 + \frac{b^2}{3}\left(\dot{\theta}\right)^2 dy \tag{4.3}$$

$$\text{and } WE = \rho\tau g \left[4b^2 h \sin\theta + 4bh^2\cos\theta + 2b\int_0^{2h} u\cos\theta \, dy\right]. \tag{4.4}$$

and the Euler-Lagrange equation that arises from conserving the energy of the simplified flexible rocking system, as before in Section 3.1.4 (see Appendix B for the detailed calculation), is the coupled system of differential equations

$$\begin{cases} \theta: & \ddot{\theta}\left(\frac{8bh^3}{3}+\frac{8b^3h}{3}\right)+g\left(2b^2h\cos\theta-2bh^2\sin\theta\right) \\ & +\int_0^{2h}\ddot{\theta}b\left(2uy+u^2\right)+2\dot{\theta}(y+u)\dot{u}+b^2\ddot{u}-gbu\sin\theta\,dy=0 & (0,t) \\ u: & \Box u+\ddot{\theta}b-(\dot{\theta})^2(y+u)+g\cos\theta=0 & (0,2h)\times(0,t) \end{cases} \tag{4.5}$$

where the wave equation operator, $\Box$, is defined

$$\Box u := \ddot{u}-\frac{E}{2\rho(1-\nu^2)}u_{yy}. \tag{4.6}$$

Equations 4.1 - 4.6, can also be derived by neglecting the flexural and shear deformations, w and ϕ respectively, and their derivatives in eqs. 3.7 - 3.15.

Remark 4.1.1. *The system of differential equations in eq. 4.5 is equivalent to Housner's SRM in (9) when the internal displacement, u, is absent. Impact has not occurred yet and there is no force on the system that creates internal displacements. Hence $u\equiv 0$ and eq. 4.5 simplifies to the SRM with $I_O=\frac{4}{3}MR^2=\left(\frac{16bh^3}{3}+\frac{16b^3h}{3}\right)$ in the following way:*

$$\left(\frac{16bh^3}{3}+\frac{16b^3h}{3}\right)\ddot{\theta}=-g\left(4b^2h\cos\theta-4bh^2\sin\theta\right) \tag{4.7}$$

$$I_0\ddot{\theta}=-WR\sin\left(\alpha-\theta\right). \tag{4.8}$$

In fact, as with the FRM, before the first impact takes place the rocking response of the simplified flexible block is modeled using the SRM.

The rocking response of the simple flexible rocking block is divided into the three phases of impact defined in Chapter 3: *before impact*, *impact* and *after impact*. The characteristics of the block before impact are the same as the flexible rocking block; however, the conditions and assumptions that govern the rocking response during the impact and after impact phases depart slightly from the FRM. The conditions that cause impact, the axial waves that vibrate through the block, and the internal strain energy within the block after impact are explicitly defined as a result.

4.2 Phase 1: Before impact

Before impact, the block is released from the initial drift θ_0 and rotates about its bottom edge (which bottom edge is arbitrary because of the system's symmetry) until the bottom face of the block contacts the foundation. There are no internal deformations during this phase of the rocking motion, and the rigid rocking block model in (9) is sufficient to represent the motion of the block. The characteristics of the system at the conclusion of this phase determine the characteristics for the other impact phases.

4.2.1 Time of impact, t_1 and Impact Speed

The length of time it takes for the block to strike the foundation is called the time of impact or impact time,t_1, and the speed of the block when it strikes the foundation is $\dot{\theta}(t_1) = \dot{\theta}_1$. At the time of impact when the block makes contact with the foundation there is no angular displacement and the corresponding speed of the block is at its maximum value. The duration of time between the release of the block and impact with the foundation is found by solving eq. 2.2 with $\theta(t_1) = 0$ or solving $\ddot{\theta}(t_1) = 0$. In (9), Housner solves the differential equation for t_1 such that

$$t_1 =: t_{0_H} = \frac{1}{p}\cosh^{-1}\left(\frac{1}{1-\theta_0/\alpha}\right) \quad \text{where} \quad p^2 = \frac{WR}{I_0} \quad \text{and} \quad \tan\alpha = \frac{b}{h}. \tag{4.9}$$

The time it takes for the block to hit the foundation, rock to the maximum displacement about the opposite edge, strike the foundation again and rock back on the original edge to the new maximum displacement is a single rocking period. These four phases are assumed to take an equal amount of time called a quarter period (9). Housner refers to the impact time t_1 as the quarter period. This quarter period is used to determine the impact time for the SFRM. The same quarter period for the SFRM can be defined by conserving the initial energy of the system to the energy at the moment the block impacts the foundation. The initial energy of the system before the block is released, E_i, is due to the initial conditions imposed on the block. This energy is the work energy of gravity that allows the block to uplift. The energy components in this position from eq. 4.2 - 4.4 are

$$SE_i = KE_i = 0 \quad \text{and} \quad WE_i = 4\rho\tau g\left[b^2 h\sin\theta_0 + bh^2\cos\theta_0\right]. \tag{4.10}$$

Directly before impact occurs, the energy is defined by the angular speed at impact and the gravitational force on the block, without any angular displacement. At the time of impact the internal displacements have not yet taken place and hence the energy components of the system are

$$SE_0 = 0, \quad KE_0 = \rho\tau\dot{\theta}_1^2\left(\frac{8bh^3}{3} + \frac{8b^3h}{3}\right) \quad \text{and} \quad WE_0 = 4\rho\tau bh^2 g = W. \tag{4.11}$$

There are assumed to be no interactions with the block that change the amount of energy between release and impact, the initial energy is equivalent to the energy just before the first impact, E_0. The angular speed at the moment when the block strikes the foundation, the impact speed, that conserves the energy of the system is defined by

$$\dot{\theta}_1^2 = \frac{2WR}{I_0}\left(\cos(\alpha - \theta_0) - \cos\alpha\right). \tag{4.12}$$

Remark 4.2.1. *An alternative approach for solving for the impact speed uses the SRM instead of the system energy expressions from eq. 4.2 - 4.4. Both sides of eq. 2.2 are multiplied by $\dot{\theta}$ and integrated over the length of the before impact phase. On the right hand side of the equation, there is an integration from the initial position θ_0 to the impact position $\theta(t_1) = 0$, and on the left side of the equation, there is an integration over the initial speed, $\dot{\theta} \equiv 0$ to the impact speed $\dot{\theta}_1$. These two operations yield eq. 4.12. This approach is also applicable to rocking block systems that only have an initial displacement. In the case of a block with an initial speed, $\dot{\theta}_0$, the square of the impact speed, $\dot{\theta}_1^2$, is increased by $\dot{\theta}_0^2$ in eq. 4.12.*

The speed at impact is imperative for the analysis of the axial deformations that occur as a result of the impact. This speed determines the magnitude of the internal deformations and whether or not the block will rock about the other edge, continuing the rocking response. These deformations are explored in depth in the next section regarding the impact phase of the simplified flexible rocking block response.

4.3 Phase 2: Impact

The conditions at the conclusion of the before impact phase define the conditions that determine the behavior of the block during the impact phase. The impact speed, impact time,

and initial energy just before impact determine the deformations created during impact. Before impact, only the edge of the block that the block is rotating about, the center of rotation, is assumed to be in continuous contact with the foundation. This continuous contact, defined by restricting the displacement of the center of rotation edge, is equivalent to a pinned boundary condition on that edge. During impact, the boundary is assumed to remain in contact with the foundation until the impact is over. This forced pin condition at the impact face of the block defines the desired rocking motion. The rocking dynamics are added to the SFRM, as in the FRM, by imposing different boundary conditions on the edges and faces of the block during each of the three phases of the rocking motion. The pin condition in the FRM is defined as a function of the shear and flexural deformations of the block. These deformations allow each center of rotation to have a different displacement. The SFRM conditions require the axial deformation to be the same along the depth and width of the block. Defining the pinned conditions for the bottom edges of the block (O and O'in Figure 3.1) requires a new coordinate system in order to maintain the simplified structure of the SFRM.

4.3.1 Change of Variables to Include Rocking

A new variable is needed to define the boundary conditions that represent the change in the center of rotation that occurs during impact. The total vertical displacement of any point on the block, v, is the difference between the height of the point along the block when the block is not rocking, and the height of the point along the block during rocking motion, from eq. 3.2

$$v = \tilde{y} - y = (x + b)\sin\theta + u\cos\theta - y. \tag{4.13}$$

Every point along the bottom surface of the block has the same zero axial deformation since at least one edge is always pinned to the impact surface (during impact the entire surface is pinned to the impact surface). The total vertical displacement varies along the surface when the block is rotating (see Figure 4.1). This variation of the vertical displacement during rocking along the bottom surface is assumed to be a linear function of the location along the width of the block. The total height at the center of the bottom face is zero during impact and the vertical displacement at the center of the bottom face of the block is assumed to be zero throughout

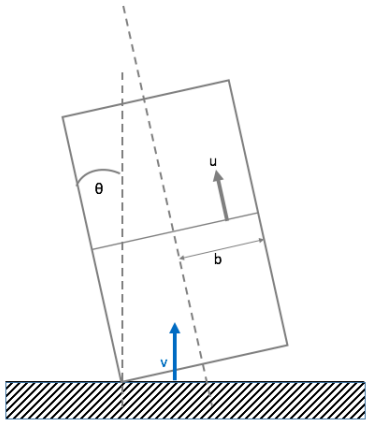

Figure 4.1: The simple flexible rocking block undergoing rocking motion θ with total displacement v.

the impact phase. The angular displacement is less than 20 % of the block height which is small enough to approximate $\sin\theta$ by θ and $\cos\theta$ by 1. The new variable $v := u + b\theta$ represents the approximate total vertical displacement of any point on the block in the block coordinate system. The strain, kinetic, and work energy of the block during impact in terms of the angular displacement and the approximate total vertical displacement are

$$SE = \frac{Eb\tau}{1-\nu^2}\int_0^{2h} (v_y)^2 \, dy \tag{4.14}$$

$$\begin{aligned} KE &\approx \rho b\tau \int_0^{2h} \left(\dot{\theta} y\right)^2 + (\dot{v})^2 + \frac{b^2}{3}\dot{\theta}^2 \, dy \\ &= \rho b\tau \left[\dot{\theta}^2 \left(\frac{8h^3}{3} + \frac{2b^2 h}{3}\right) + \int_0^{2h} (\dot{v})^2 \, dy\right] \end{aligned} \tag{4.15}$$

$$\text{and } WE = \rho\tau g \left(4b^2 h \sin\theta + (4bh^2 - 4b^2 h\theta)\cos\theta + 2b\int_0^{2h} v\cos\theta \, dy\right). \tag{4.16}$$

The vibrations have an initial speed equal to the angular speed of the block at impact. At the moment the bottom surface of the block comes in contact with the impact interface, the edge O is restricted from any displacement. During impact, the center of rotation changes from edge O to edge O' (Figure 3.1). The impact phase boundary conditions define the speed that preserves the angular momentum of the system when the center of rotation changes from one edge to the other at the beginning of the impact phase (see Figure 2.1). These boundary conditions are written in terms of v below to represent the axial deformation and the rotation that occurs

during impact. The axial deformation before impact is zero and hence the change in the total displacement with respect to time is $\dot{v} = -\dot{\theta}_1 b$. The opposite edge is pinned immediately after impact and the change in the total displacement with respect to time is $\dot{v} = \dot{\theta}_1 b + \dot{u}$ where $\dot{u} = \dot{u}_0 \neq 0$. The block momentum at the beginning of the impact is equal to the momentum just before impact is concluded, hence

$$-\dot{\theta}_1 b = \dot{\theta}_1 b + \dot{u}_0, \tag{4.17}$$

and therefore the initial speed of the axial deformations is $\dot{u}_0 = -2\dot{\theta}_1 b$.

The SFRM during impact is a valid representation of the rocking block deformation when the motion is described in terms of the total vertical displacement. During impact, the angular displacement, as previously noted, is zero because the bottom surface of the block is in contact with the foundation. The total vertical displacement, $v = u + \theta_1 b$, and $\theta \equiv 0$ in eq. 4.5 defines the equation of motion during the impact phase as the nonhomogeneous wave equation

$$\begin{cases} \ddot{v} - c^2 v_{yy} = -g & \text{in } (0, 2h) \times (t_1, t_2) \\ v = 0,\ v_t = -\mu & \text{in } (0, 2h) \times \{t = t_1\}, \\ v(0) = 0,\ v_y(2h) = 0 & \text{in } (t_1, t_2) \end{cases} \tag{4.18}$$

where $c^2 = \frac{E}{\rho(1-\nu^2)}$ and $\mu = \dot{\theta}_1 b$. The bottom surface that is in contact with the foundation must remain in contact during impact, hence the Dirichlet boundary condition, $u(0,t) = 0$, is applied along this surface. Along the top surface of the block there are no applied forces so the Neumann boundary condition $u_y(2h,t) = 0$ is applied to the SFRM system.

Remark 4.3.1. *In the case when there are no axial deformations (i.e $u \equiv 0$), $v = b\theta$ and the first equation in eq. 4.5 becomes*

$$\begin{aligned} 0 &= \ddot{\theta}\left(\frac{16bh^3}{3} + \frac{4b^3h}{3}\right) - \left(4bh^2 - 4b^2h\theta + 2b\int_0^{2h} b\theta\, dy\right) g\sin\theta \\ &= \ddot{\theta}\left(\frac{16bh^3}{3} + \frac{4b^3h}{3}\right) - \left(4bh^2 - 4b^2h\theta + 4b^2h\theta\right) g\sin\theta \\ &= \ddot{\theta}\left(\frac{16bh^3}{3} + \frac{4b^3h}{3}\right) - 4bh^2 g\sin\theta. \end{aligned} \tag{4.19}$$

Similarly, the second equation in eq. 4.5 becomes

$$0 = \ddot{\theta} b - g\cos\theta. \tag{4.20}$$

Multiplying eq. 4.20 by $4b^2h$ and then adding to eq. 4.19 gives

$$
\begin{aligned}
0 &= \ddot{\theta}\left(\frac{16bh^3}{3} + \frac{4b^3h}{3}\right) - 4bh^2 g\sin\theta + 4b^3h\ddot{\theta} + 4b^2hg\cos\theta \\
0 &= \left(\frac{16bh^3}{3} + \frac{16b^3h}{3}\right)\ddot{\theta} + g\left(4b^2h\cos\theta - 4bh^2\sin\theta\right) \\
0 &= I_0\ddot{\theta} + WR\sin\left(\alpha - \theta\right)
\end{aligned}
$$

and again the SRM in eq. 2.1 is recovered.

The one-dimensional wave is equation has well-defined explicit solutions on finite intervals with both Neumann and Dirichlet boundary conditions. The representation using the total vertical displacement of the block has piecewise continuous solutions that are defined in regions that are based on the height and time after the impact phase started. Below is the explicit definition of these solutions to eq. 4.18 and the axial deformation that results from the flexible block impacting the foundation.

4.3.2 Axial vibration waves

D'Alembert's formula defines the solution of the one-dimensional wave equation defined over the entire space of real numbers. Since eq. 4.18, that defines the total vertical displacement of the block, is only defined over the height of the block, a reflection technique defines an equivalent wave equation that is defined for all real numbers. This technique extends the application of D'Alembert's formula to equations defined over finite intervals. The most natural extension of the wave equation defined over a finite region is a periodic extension of eq. 4.18.

The vibrations defined in eq. 4.18 are defined over the one-dimensional space $\Omega = [0, 2h]$, where $2h$ is the height of the block. The solution to the wave equation derived by D'Alembert assumes the wave equation is defined for all real numbers (7). D'Alembert's formula is the simplest solution of the wave equation and in order to use the solution formula, eq. 4.18 is extended from Ω to all real numbers. The wave equation in eq. 4.18 is extended by creating a periodic function over the entire real line, such that when that periodic function is considered on Ω it is equivalent to wave eq. 4.18. Extending eq. 4.18 over the entire real line requires the PDE, the boundary and the initial conditions to be appropriately extended.

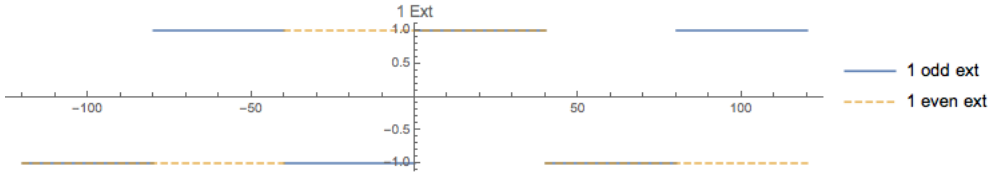

Figure 4.2: Graph of 1_e^{ext} and $(1)_o^{ext}$ with Dirichlet condition at (0,0) and Neumann conditions at (2L,0) with L = 1.

The boundary and initial conditions are constants defined for the PDE at specific locations in the space Ω. The definition of the initial displacement of any boundary point of Ω is called a Dirichlet boundary condition. The initial displacements should be the same for points on either side of the boundary and hence Dirichlet boundary conditions are extended to the entire real line by defining the initial displacement as an odd periodic function. This is considered an odd reflection of the Dirichlet boundary condition.

The first derivative of the displacement with respect to the displacement variable (y in this case), defined at the boundaries of Ω are called Neumann boundary conditions. These boundary conditions should switch direction at the boundary and hence Neumann boundary conditions are extended to define an even periodic function. The even and odd extensions of the constant function 1, $(1)_e^{ext}$ and $(1)_o^{ext}$ respectively, are shown in Figure 4.2.

The initial conditions and the nonhomogeneous right hand side, the input data, of eq. 4.18 are also extended. The extension creates odd $4h-$periodic initial and input data functions. The extended wave equation is

$$\begin{cases} \ddot{v} - c^2 v_{yy} = (-g)_o^{ext} & \text{in } \mathbb{R} \times (0, \infty) \\ v = 0,\ v_t = \mu_o^{ext} & \text{in } \mathbb{R} \times \{t = 0\}, \\ v(0) = 0,\ v_y(2h) = 0 & \text{in } (0, \infty). \end{cases} \tag{4.21}$$

The solution of the extended wave eq. 4.21 using D'Alembert's formula is

$$v(y,t) = \frac{1}{2c} \int_{y-ct}^{y+ct} \mu^e \, dx + \frac{1}{2c} \int_0^t \int_{y-c(t-s)}^{y+c(t-s)} (-g)^e \, dx \, ds. \tag{4.22}$$

D'Alembert 's solution defines two waves emanating from a particular point (y,t): one traveling forward in time and the other traveling backward in time. Linear equations of y and

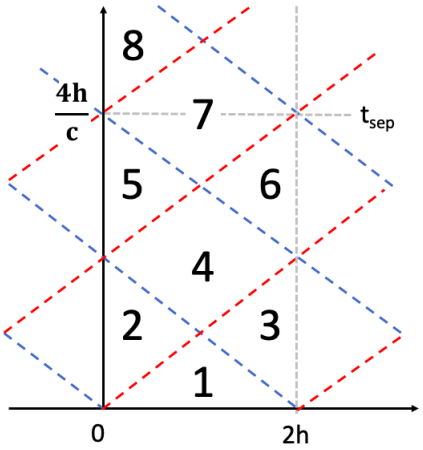

Figure 4.3: Regions of solutions

t that connect points with constant solutions are called characteristics. The characteristics of the solution of the wave equation break up the space and time plane into regions where the solution changes. D'Alembert's formula provides a different solution of eq. 4.21 for each region in Figure 4.3. The slope of the characteristics is the period of the extended wave equation divided by the wave speed, c.

Explicitly writing $v(y,t)$ using eq. 4.22 requires integrating the oddly extended constant function in Figure 4.2 in the first seven of the regions shown in Figure 4.3 (For details about integrating the piecewise function over the different regions is detailed in Appendix F). The solution of eq. 4.21 from eq. 4.22 is defined below for Regions 1-8:

$$v = \begin{cases} \text{Region 1}: & -\frac{gt^2}{2} - \mu t \\ \text{Region 2}: & -\frac{g\left(2y\left(t-\frac{y}{c}\right)+\frac{y^2}{c}\right)}{2c} - \frac{\mu y}{c} \\ \text{Region 3}: & -\frac{gt^2}{2} - \mu t \\ \text{Region 4}: & -\frac{g\left(2y\left(t-\frac{y}{c}\right)+\frac{y^2}{c}\right)}{2c} - \frac{\mu y}{c} \\ \text{Region 5}: & -\frac{g\left(2y\left(t-\frac{y}{c}\right)+\frac{y^2}{c}\right)}{2c} - \frac{\mu y}{c} \\ \text{Region 6}: & -\frac{g\left(-\frac{16h^2}{c}+2y\left(\frac{4h-y}{c}-\frac{y}{c}\right)-ct^2+\frac{2y^2}{c}+8ht\right)}{2c} - \frac{\mu(8h-2ct)}{2c} \\ \text{Region 7}: & -\frac{g\left(-\frac{16h^2}{c}+2y\left(\frac{4h-y}{c}-\frac{y}{c}\right)-ct^2+\frac{2y^2}{c}+8ht\right)}{2c} - \frac{\mu(8h-2ct)}{2c} \\ \text{Region 8}: & \frac{\mu y}{c} - \frac{g\left((8h-2y)\left(t-\frac{4h+y}{c}\right)+2y\left(\frac{4h-y}{c}-\frac{y}{c}\right)+\frac{y^2}{c}\right)}{2c}. \end{cases} \tag{4.23}$$

Eq. 4.23 defines the total vertical displacement within the block during impact. This solution is only valid while the block is in contact with the foundation. Once the block begins rotating about the opposite edge, the impact is over. The next section defines the system parameters that govern the conclusion of impact.

4.3.3 Time of separation

The axial deformation at the conclusion of impact determines the block vibrations that continue throughout the next phase of rocking motion. The magnitude of these vibrations and the stress induced in the block by these vibrations determine the amount of vibration energy retained by the block after impact. The amount of energy retained by the block after impact depends on the duration of the impact. The duration of impact is the time it takes the axial vibrations to travel through the block to its maximum height and back to the impact surface. The time of separation, denoted t_{sep}, is equivalent to the duration of impact. The time it takes for the waves to travel through this distance, equal to twice the height of the block $4h$ at wave speed c, determined by the modulus of elasticity in eq. 4.18, is

$$t_{\text{sep}} = \frac{4h}{c}. \tag{4.24}$$

The time of separation occurs at the intersection of regions 5,7 and 8 in Figure 4.3.

The axial vibrations within the block are initiated by the compression of the block at the impact interface. The block separates from the foundation when this compression stress instantaneously changes to tensile stress along the bottom surface. The total vertical distance in region k, defined by eq. 4.23, is denoted by ${}^{k}v$. At the bottom surface of the block that is in contact with the foundation, $y = 0$ and the stress in Regions 5, 7 and 8 is

$$\begin{aligned} {}^{5}v_y(0,t) &= -\left(\tfrac{\mu}{c} + \tfrac{gt}{c}\right) < 0, t \in \left(\tfrac{2h}{c}, \tfrac{4h}{c}\right), \\ {}^{7}v_y(0,t) &= -\tfrac{4gh}{c^2}, \text{ and} \\ {}^{8}v_y(0,t) &= \left(\tfrac{\mu}{c} + \tfrac{gt}{c}\right) - \tfrac{4gh}{c^2} > 0, t \in \left(\tfrac{4h}{c}, \tfrac{6h}{c}\right). \end{aligned} \tag{4.25}$$

The instantaneous stress change occurs at t_{sep} from eq. 4.24 if and only if the stress right before the time of separation is a compressive stress and the stress immediately after is a tensile stress

(17). The stress immediately before the time of separation is defined by ${}^5v_y$ and is negative when the impact speed μ satisfies

$$\mu > \frac{4gh}{c}. \tag{4.26}$$

The time of separation is defined by eq. 4.24, when the impact speed satisfies eq. 4.26. In the SFRM this condition must be satisfied to define the impact phase throughout the rocking response. Therefore, if eq. 4.26 is violated, the time of separation is greater than t_{sep} and rocking is assumed not occur.

The bouncing condition for a damped rod dropped vertically on a rigid surface is written in terms of the impact speed μ, and the critical speed of the rod with length L is $\mu_c = \frac{2gL}{c}$ in Hansen and Wang (28). The rod will bounce when the impact speed is greater than the free fall speed. The vibrations in the impacting rods travel along the length of the rod. In this damped rod example in (28) the rocking block example in this research project, both objects experience axial deformations. The rocking condition for the SFRM is equivalent to the bouncing condition from the impacting rod. Hence, eq. 4.26 defines the required magnitude of the impact speed for the block to rock. This equation is referred to hereafter as the rocking condition for the SFRM. Any impact speed satisfying the rocking condition will cause the block to rock after that impact. The change in the sign of the stress between ${}^5v_y(0, t_{\text{sep}})$ and ${}^8v_y(0, t_{\text{sep}})$ confirms the assumption used to define the time of separation in the SFRM as $t_{\text{sep}} = \frac{4h}{c}$.

The time of separation occurs in Region 7 in Figure 4.3. The total vertical displacement is defined by the corresponding expression in eq. 4.23. Given the duration of the first phase of rocking motion, t_1, the block separates from the ground and begins rocking about the opposite corner O' at time $t_2 = t_1 + t_{\text{sep}}$. At t_2 the axial deformations initiated during impact continue propagating through the block with every boundary face subjected to free boundary conditions since the bottom face of the block is no longer in contact with the foundation. Although the block is no longer in contact with the foundation, the axial deformations continue to propagate through the block. The energy associated with these internal vibrations is the result of the transfer of kinetic energy to block vibration energy at impact. This energy transfer reduces the amount of kinetic energy in the system. In the SFRM the block vibration energy resulting from impact is assumed to be the only contributor to the reduction in the kinetic energy that

determines the rotation of the block as it continues to rock. This kinetic energy is considered the rigid kinetic energy. The remaining rigid kinetic energy and the state of the block and the internal deformations are used to define the final phase of impact. These conditions at the conclusion of the impact phase define the initial conditions for the after impact phase of the rocking motion.

4.4 Phase 3: After impact

The angular displacement of the block after rocking about the edge O and impacting the foundation is negative when the center of rotation changes to the edge O' after impact (see Figure 3.1). The speed and magnitude of the axial deformation at the time of separation determines the amount of vibration energy within the block. This block vibration energy reduces the amount of kinetic energy left in the block as it continues to rotate. The residual kinetic energy determines the magnitude of the rocking motion of the block after impact. There are at least three theoretical types of motion the block will undergo after the impact phase of the rocking motion is over: the block can rock about the same center of rotation, edge O; the block can remain in contact with the foundation; and the block could continue the rocking motion with the new center of rotation at the other bottom edge, O'. The boundary and initial conditions of the SFRM determine which motions are possible after impact. The boundary and initial conditions after impact are defined to continue the expected rocking motion by restricting the block from rocking about the same center of rotation. The block is restricted from rocking about edge O by the boundary condition that pins the edge O' and releases edge O. If the block remains in contact with the foundation, the rocking motion of the block stops after the impact phase. In this case, the rigid kinetic energy is too small for the block to continue rocking. This occurs when the drift is extremely small and creates an impact speed that does not satisfy eq. 4.26. When the drift is large enough to create an impact speed that satisfies eq. 4.26, the block continues its rotation and begins the third and final phase of the rocking motion. The after impact phase is over when the block is balanced on the edge O' at the block's maximum angular displacement without overturning. The boundary conditions after impact are identical to those before impact. The initial conditions after impact include

the magnitude and speed of the axial deformation at the moment the block separates from the foundation. The axial deformation within the block determines whether the rocking response of the block will continue or if the block will simply rest on the foundation.

4.5 Rocking Phenomenon

The rocking block motion is the result of gravity trying to stabilize the block after an initial angular displacement of the top corner of the block. The behavior of the rocking motion depends on the initial drift, the material of the rocking block, the material of the foundation, and the type of soil beneath the foundation. The block may rock about its two bottom edges or the block may slide or bounce because of the friction or lack of friction between the block and the foundation ((22), (23), (27)). Rocking without sliding or bouncing defines standard rocking motion. During standard rocking the centers of rotation alternate between the two bottom edges of the block without bouncing, sliding or any other displacement or deformation at the edges. Standard rocking is characterized by impact speeds that satisfy the rocking condition in eq. 4.26. Non-standard rocking defines the motion of the block when the rocking condition is violated and is characterized by small rigid displacements.

The complete rocking response is composed of standard rocking motion and non-standard rocking motion. Standard rocking occurs until the vibration energy created during impact grows large enough to increase the duration of impact to a value larger than t_{sep}. The vibration energy at this particular impact reduces the rigid kinetic energy in the block and the speed after impact is not large enough to cause the block to continue the rocking about the alternative center of rotation. The reduction of the kinetic energy eventually brings the block to rest. The impact speed required to cause rocking in the SFRM is small during non-standard rocking. The end of the rocking response in the SFRM is defined as the time when the rocking response becomes non-standard. The rocking response becomes non-standard when the bounce condition is violated and the non-standard rocking motion begins.

4.5.1 Energy Mechanisms After Impact

After impact the vibrations in the block and the rigid rocking motion continue simultaneously. The energy in the block that is unaffected by the vibrations is called *rigid energy*. The rigid energy retained by the block after impact is a fraction of the rigid energy in the block before impact. Under the assumption that all the kinetic energy is represented by the motion of the block, this fraction of remaining rigid kinetic energy, written as a percentage, is called the coefficient of restitution (COR) of the impact of the rocking block with the rigid foundation. The COR of impeding objects is determined by the vibration energy in the system that is developed as a result of the speed at impact, the size, and the flexibility of the objects.

Once the rigid energy is transferred to block vibration energy, the vibration energy remains as internal energy in the block. The vibrations that develop in the block travel twice the height of the block in $4h/c$ seconds. The number of times the axial waves propagate through the block is the duration of the phase after impact divided by the time duration for the waves to travel through the height of the block and back to the bottom surface. The number of times the waves travel through the block is large when the time from the end of one impact to the beginning of the next impact is large. This provides internal energy dissipation in the system. The time between impacts is assumed to be large enough to dissipate the block vibration energy before the next impact.

The energy in the system before impact, E_B, is purely rigid energy and the energy after impact, E_A, is the sum of the rigid and the vibration energy. The COR represents the fraction of the kinetic energy retained by the block after each impact during the rocking motion. This fraction is the ratio of kinetic energy after impact to the kinetic energy before impact and simplifies to the ratio of the squares of the corresponding speeds. In the SFRM, the block vibration energy is assumed to be the only source of energy loss in the rocking block system.

4.5.1.1 Rigid Energy

The total energy is the sum of the strain, kinetic and work energy from eqs. 4.2 - 4.4. Hence, the total energy after impact is

$$E_{\text{After}}(\dot{\theta}) = \rho b\tau \left[\dot{\theta}^2 \left(\frac{8h^3}{3} + \frac{2b^2h}{3}\right) + 4h^2g + b\int_0^{2h} \dot{v} + 2gv + 2\left(cv_y\right)^2 \, dy\right]. \tag{4.27}$$

The axial vibrations are captured by the total vertical displacement, v, defined by eq. 4.23 at the conclusion of the impact phase of rocking. The kinetic energy of the block is reduced by the energy transfer that occurs during impact. Kinetic energy is transferred to vibration energy reducing the speed of the block. This energy transfer reduces the amount of kinetic energy and therefore reduces the speed of the block after impact. The speed after impact depends on the amount of vibration energy created within the block. The vibration energy depends on the magnitude of the axial deformations that occur during impact and the block material and geometric properties. The speed after impact is defined by conserving the energy after impact with the energy before impact, such that $E_{\text{rigid before}} = E_{\text{rigid after}} + E_{\text{vibration}}$. This equality defines a quadratic equation for the speed after impact when the amount of strain energy within the block is known. The ratio of the square of the rigid speed after impact to the square of the rigid speed before impact defines the COR for the SFRM. This COR_{SFRM} represents the amount of rigid kinetic energy retained in the flexible rocking block after impact. The rigid kinetic energy retained by the flexible block can be compared with the rigid kinetic energy retained by the rigid block in the SRM. Comparing the energy retained in the system simplifies creating a rocking response and defines a comparison metric for the flexible and rigid rocking block systems that is discussed in more detail in Chapter 5.

4.5.1.2 Block Vibration Energy

The strain energy in the rocking block system determines the characteristics of the rocking response, such as the angular displacement and the duration of the rocking response. In the rocking block system the total vibration energy has two components: the portion of energy transferred to the block, E^b_{vib}, and the portion of energy transferred to the foundation, E^f_{vib}. The energy transferred to the foundation is regarded as the most important contributor to

the dissipation of energy in the rocking system in (1), (3), (9), (11), (27). Representing the vibration energy has centered around the properties of the impact interface between the block and the foundation. The effect of the impact interface characteristics (stiffness, size, etc.) is not included in the SFRM. The development of the SFRM in this chapter assumes the foundation and impact surface are perfectly rigid and therefore the only vibration energy developed in the system exists within the block. The goal of this research is to capture the vibration energy within the block and hence, the SFRM represents the internal deformation of the block created by the rocking motion absent any effects from the foundation. Under the rigid foundation assumption, E^f_{vib} is zero. In this case, the change in kinetic energy that occurs during impact is equivalent to the amount of vibration energy developed within the block during impact. The block vibration energy is the change in the strain and work energy that results from the axial deformation of the block, therefore

$$E^b_{\text{vib}} = 2\rho b\tau \int_0^{2h} gv + (cv_y)^2 \, dy. \tag{4.28}$$

The amount of kinetic energy after impact is the amount of kinetic energy before impact minus the block vibration energy that is developed during impact $KE_A = KE_B - E^b_{\text{vib}}$. The COR_{SFRM}, which removes only E^b_{vib} from the rigid block energy, is defined as the ratio of the amount of kinetic energy that remains in the system after impact to the amount of kinetic energy before the impact. The corresponding COR that depends on the block vibration energy E^b_{vib} is

$$COR_{SFRM} = 1 - \frac{E^b_{\text{vib}}}{KE_B} = 1 - r_b \tag{4.29}$$

where KE_B is defined in eq. 4.3, and r_b is the ratio of block vibration energy to the kinetic energy before impact.

The SRM assumes the kinetic energy loss in the rocking block system is attributed to the kinetic energy loss at the impact interface and as a result of the rigid rocking block assumption, the vibration energy within the block is negligible. The SFRM, by contrast, assumes the kinetic energy loss is the result of the block vibrations and no vibrations are developed at the interface or within the foundation. These two models concentrate any flexibility in the system either at the foundation or within the block. Determining which representation of system flexibility

is appropriate depends on the material of the block and foundation in the rocking system to be modeled. Some rocking systems may require exclusively using one of these two models to represent the system's flexibility or a representation that combines the two different modeling philosophies.

4.6 Comments about well-posedness of SFRM

The simple flexible rocking system is represented by the coupled nonlinear partial differential equation (PDE) 4.5. The simple flexible rocking block, with the geometry defined in Figure 3.1, the explicit solution is defined in eq. 4.23. A rigorous proof is required to guarantee the general solution of eq. 4.5. The existence and uniqueness of solutions for such a PDE should be guaranteed before attempting to find any solutions and a definition of where solutions are defined is also important to characterize this mathematical problem. These qualities define the equation's regularity and are discussed in the sections below for eq. 4.5. While no precise definition for the regularity of solutions of eq. 4.5 has been previously defined, these solutions are guaranteed by preexisting theories for similar PDE systems.

The SFRM is composed of a partial differential equation coupled with an ordinary differential equation. This system is defined as a quasilinear differential equation because it has the form $\partial_t u + L(u)u = f(u)$ where L is an operator that depends on u and its derivatives up to but not including the highest order of the differential equation. By rewriting the system of differential equations in vector form, such that

$$A(\mathbf{u}, y)\dot{\mathbf{u}} = L(\mathbf{u}, y) + f(\mathbf{u}, y) \tag{4.30}$$

where

$$A(\mathbf{u}, y) = \begin{pmatrix} 1 & 0 & 0 & 0 \\ 0 & \int_0^{2h} \left((y+u)^2 + \frac{b^2}{3}\right) dy & 0 & 0 \\ 0 & 0 & 1 & 0 \\ 0 & b & 0 & 1 \end{pmatrix}, \tag{4.31}$$

$$\mathbf{L}(\mathbf{u},y)=\begin{pmatrix}0 & 1 & 0 & 0\\ 0 & 0 & \int_0^{2h}\tilde{E}\left((y+u)^2+\frac{b^2}{3}\right)D^2\,dy & 0\\ 0 & 0 & 0 & 1\\ 0 & 0 & \tilde{E}D^2 & 0\end{pmatrix} \tag{4.32}$$

and

$$f(\mathbf{u},y)=\begin{pmatrix}0\\ \int_0^{2h}(\dot{\theta})(y+u)\left[\dot{\theta}\left((y+u)^2+\frac{4b^2}{3}\right)+2b\dot{u}\right]\\ -g\left[\left((y+u)^2+\frac{b^2}{3}\right)\cos\theta+b(y+u)\sin\theta\right]\,dy\\ 0\\ (\dot{\theta})^2(y+u)-g\cos\theta.\end{pmatrix} \tag{4.33}$$

with $\mathbf{u}=\left(\theta,\,\dot{\theta},\,u,\,\dot{u}\right)$ and $\tilde{E}=\frac{E}{2\rho(1-\mu^2)}$ the SFRM is shown to be quasilinear. The theory that governs ordinary differential equations guarantees local existence and uniqueness of solution of the small time interval of each phase of impact. The solution of eq. 4.30 is $\mathbf{u}\in D(\mathbf{L})\subset V$, subject to the initial condition $\mathbf{u}(0,y)=\mathbf{u}_0(y)=\left(\theta_0,\dot{\theta}_0,u_0(y),\dot{u}_0(y)\right)\in V$ where

$$V=\mathbb{R}\times\mathbb{R}\times H^1_{\Gamma_0}(\Omega)\times L^2(\Omega),$$
$$D(\mathbf{L})=\mathbb{R}\times\mathbb{R}\times H^2_{\Gamma_0}(\Omega)\times H^1_{\Gamma_0}(\Omega),$$
$$\Gamma_0=\{\phi\in H^1(\Omega)\,|\,\phi(0,t)=0\}$$
$$\Gamma=\{\phi\in H^2(\Omega)\,|\,\phi(0,t)=0,\phi_y(2h,t)=0\}$$
$$\text{and }\Omega=(0,2h).$$

The matrix $\mathbf{L}$ from eq. 4.32 depends on the parameter u, which characterizes the nonlinearity of the PDE in eq. 4.5. When L is independent of u, eq. 4.30 is a semilinear PDE. Below are global existence and uniqueness theories of semilinear equations for the SFRM when u^2 is negligible..

4.6.1 The Semilinear PDE

Semilinear PDEs have the form $\partial_t u+Lu=f(u)$ where L is a linear differential operator independent of u. A unique solution that depends Lipschitz continuously on the initial data $u_0\in V$ is guaranteed by (20) when $\mathbf{L}$ is a densely defined operator on the function space V

and F is also defined on V. The impact phase of the SFRM from eq. 4.18 in terms of the total vertical displacement v is a semilinear equation and has the vector representation

$$\tilde{A}(y)\dot{\mathbf{v}} = \tilde{\mathbf{L}}\mathbf{v} + \tilde{f}(\mathbf{v}, y) \tag{4.34}$$

with $\mathbf{v} = \left(\theta,\, \dot{\theta},\, v,\, \dot{v}\right)$,

$$\tilde{A}(y) = \begin{pmatrix} 1 & 0 & 0 & 0 \\ 0 & \frac{8h^3}{3} + \frac{2b^2h}{3} & 0 & 0 \\ 0 & 0 & 1 & 0 \\ 0 & 0 & 0 & 1 \end{pmatrix}, \tag{4.35}$$

$$\tilde{L} = \begin{pmatrix} 0 & 1 & 0 & 0 \\ 0 & 0 & g & 0 \\ 0 & 0 & 0 & 1 \\ 0 & 0 & \tilde{E}D^2 & 0 \end{pmatrix}, \text{ and} \tag{4.36}$$

$$\tilde{f}(\tilde{\mathbf{v}}, y) = \begin{pmatrix} 0 \\ 2g(h-b)h\sin\theta \\ 0 \\ -g\cos\theta \end{pmatrix}. \tag{4.37}$$

The nonlinear function $\tilde{f}$ is Lipschitz continuous with Lipschitz constant $C = \max\left(2g(h-b)h, g\right)$. These well-posedness results are guaranteed for the SFRM since the nonlinear function $f(\mathbf{u}, y)$ is Lipschitz continuous in V (20). A similar argument applied to the quasilinear system, eq. 3.12, lends similar local well-posedness results with eq. 4.5; however the proof of this claim is beyond the scope of this work.

Remark 4.6.1. *In the vector representation of the SFRM, eq. 4.30, consider* $||\mathbf{u}|| \leq 1$ *where* $\mathbf{u} \in D(L) \subset V$ *, then* A *and* L *are bounded. The Lipschitz constant* $C = \max(C_1, C_2)$ *for* f*, which depends on the total energy in the system, where*

$$C_1 = 4\max\left[\left(c_3 + \frac{8b^2h}{3}\right)E_0 + gc_2 + 2bE_0^2 + 2gbh, 4bhE_0\left(2h^2 + 2hc_0\right),\right.$$
$$\left(2h^2 + 2hc_0\right)\left(\left(\frac{8h^3}{3} + \frac{2b^2h}{3} + 2h\left|c_0\right|\right)E_0 + 2bE_0\right),$$
$$\left.g\left[\left(\frac{8h^3}{3} + \frac{2b^2h}{3} + 2h\left|c_0\right|\right) + b\left(2h^2 + 2hc_0\right)\right]\right] \tag{4.38}$$

$$C_2 = \max\left(E_0^2, 4h^2E_0^2(h + c_0)^2, g^2\right). \tag{4.39}$$

(See Appendix C for the detailed calculations).

4.7 Conclusion

Broadening the scope of the rigid models to include the representation of the block vibration energy provides the ability to model rocking block systems composed of flexible materials. This representation considers the total amount of internal block energy in the rocking block system, which increases until the block comes to rest. Determining the effect of incorporating the flexibility on the entire response is the primary focus of this research project. The conditions used to approximate the rocking response in the first three phases of rocking motion can not be strictly applied to the entire rocking response because the block vibrations change the initial and boundary conditions for each of the subsequent phases. Creating an entire rocking response with the SFRM was briefly discussed in this chapter and is covered in detail for a specific block in the next chapter. The implications of the block vibration energy on the rocking response and the factors that influence the motion are also discussed in terms of the flexibility of the block.

CHAPTER 5. ROCKING RESPONSE WITH THE SFRM

The SFRM is a piecewise model that requires the consideration of the block conditions before and after each phase of rocking motion in order to appropriately represent the rocking response. The conditions that govern the rocking motion for the flexible block are the initial drift and impact speed. The initial drift is the initial displacement at the start of the rocking response and the impact speed at each impact determines if the block will have enough rigid kinetic energy after the impact to continue the rocking motion. These two conditions define the rocking criteria in the SFRM and determine the number of impacts that occur before the block stops rocking. The rocking criteria, the conditions that initiate rocking, and the number of impacts are all functions of the block flexibility. These rocking motion characteristics are used to define the rocking response captured with the SFRM. The definition of an entire rocking response with the SFRM is discussed in this chapter.

5.1 SFRM Rocking Response

The SFRM rocking response of a flexible block is created by sequentially linking the three phases of rocking motion by their boundary and initial conditions. The after impact phase of rocking motion of one impact, the after impact phase described in Section 4.4, must be linked to the before impact phase of rocking motion of the next impact described in Section 4.2, in order to create a continuous rocking response with the SFRM. This creates a continuous cycle of the three impact phases that define an entire rocking response using the SFRM. This continuous cycle is shown in Figure 5.8. The energy transfer from rigid kinetic energy to block vibration energy during the impact phase reduces the angular speed of the block after impact with the foundation (see Figure 5.6). The rocking motion continues with this reduced speed and a new

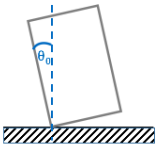

Figure 5.2 Initial position of the rocking block.

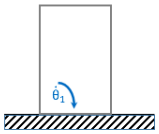

Figure 5.3 The instant the block strikes the foundation just before the *impact phase* begins.

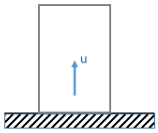

Figure 5.4 The beginning of the *impact phase* of rocking motion.

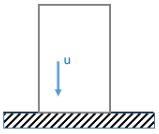

Figure 5.5 Just before the *impact phase* of rocking motion is over.

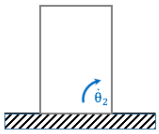

Figure 5.6 Immediately after the *impact phase* of rocking motion.

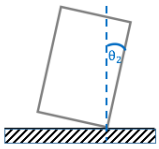

Figure 5.7 The maximum displacement of the block after a single impact.

Figure 5.8: Schematic of the rocking response sequence for the SFRM.

center of rotation (see Figure 5.7). It is possible for vibrations to contribute to the rocking response and cause motions that are out of phase with the angular rocking displacement; however, the SFRM assumes that vibration energy within the block can not be transferred to rigid kinetic energy during the rocking response (Section 2.1.3 discussed the possibility of vibration energy returning to the rocking block system as rigid kinetic energy and influencing the angular rocking motion).

After impact, the block vibrations travel through the entire height of the block at a speed that is proportional to the block's stiffness. The vibration energy is dissipated within the block as the vibrations travel through the block. The length of the after impact phase of the rocking block motion is much greater than the length of time it takes the vibrations to travel twice through the block. During this time, the vibrations travel through the block at least $\frac{t_1}{t_{\text{sep}}}$ times after impact, where t_1 is the quarter period defined in eq. 4.9 and t_{sep} is the duration of impact defined in eq. 4.24. The number of times the vibrations propagate through the block allows the vibrations to be dissipated by internal mechanisms present in the block, such as the molecular phenomenon that causes energy dissipation through heat transfer. Assuming this block vibration energy is dissipated, the flexible block acts as a rigid block after impact and the

speed of the block at the next impact is equivalent to the speed of the block after the previous impact. The maximum angular displacement, or the drift, after impact is defined by solving eq.4.12 for the drift value θ_0, given the speed after impact $\dot{\theta}_1$. The drift after the k^{th} impact, with the after impact speed $\dot{\theta}_k$, is

$$\theta_{k+1} = \alpha - \arccos\left(\frac{I_0}{2WR}\dot{\theta}_k^2 + \cos\alpha\right). \tag{5.1}$$

This drift after the k^{th} impact determines the impact speed, the block vibration energy, the speed after impact and the maximum drift after the $(k+1)^{th}$ impact. The initial conditions of the block before the next impact are the same as the conditions of the block at the conclusion of the previous impact.

After each impact, the new impact speed is calculated and the rocking condition from eq. 4.26, $\mu \geq \mu_c$, is tested to determine if the block will continue rocking after the next impact with the COR_{SFRM} in eq. 4.29. This principle is also used in the rigid block models in Chapter 2 to predict the speed after impact (3), (9), (22), (27). The COR_{SFRM} is a function of the ratio of the speed after the impact to the speed before the block impacts the foundation. The characteristics of the flexible block system are defined using the COR_{SFRM} in the next section.

5.1.1 SFRM Coefficient of Restitution (COR)

The COR quantifies the percentage of rigid kinetic energy retained by the rocking system after impact with the foundation. The COR_{SFRM} is the ratio of the rigid kinetic energy after impact to the rigid kinetic energy before impact. The rigid kinetic energy after each impact is a function of the impact speed of the block, which is defined by the drift angle during that impact. The impact speed throughout the rocking motion captures the loss of rigid kinetic energy as a result of the energy transfer to block vibration energy during the rocking response. The COR_{SFRM} in eq. 4.29 defines the reduction factor of the block speed after the block impacts the rigid foundation. The COR_{SFRM} is a function of the total vertical displacement and changes for each successive impact. The change in the COR_{SFRM} for each impact is small and, hence, the COR_{SFRM} is assumed to be constant throughout the rocking response. The

speed after impact defined as a function of COR_{SFRM} is

$$\dot{\theta}_{\text{after}} = \sqrt{COR_{SFRM}}\dot{\theta}_{\text{before}}. \tag{5.2}$$

The rocking condition that determines the end of the rocking response written in terms of COR_{SFRM} is

$$\sqrt{COR_{SFRM}}\dot{\theta}_{\text{before}}b = \mu \geq \mu_c. \tag{5.3}$$

Each time the block impacts the foundation, the speed before impact is reduced by the root of COR_{SFRM}. The angular speed at the first impact is $\dot{\theta}_1$ and after k impacts, the angular speed after impact is

$$\dot{\theta}_k = (\sqrt{COR_{SFRM}})\dot{\theta}_{k-1} = (\sqrt{COR_{SFRM}})^2\dot{\theta}_{k-2} = (\sqrt{COR_{SFRM}})^{k-1}\dot{\theta}_1. \tag{5.4}$$

The impacts will continue until the speed before impact violates the rocking condition in eq. 5.3. The total number of impacts during the standard rocking response is defined by the number of impact that reduce the speed $\dot{\theta}_1 b$ below μ_c such that $\dot{\theta}_k b < \mu_c$. The standard rocking response is over after

$$n = 1 + 2\frac{\ln(\mu_c/\mu_1)}{\ln(COR_{SFRM})} \tag{5.5}$$

impacts where $\mu_1 = \dot{\theta}_1 b$ is the impact speed at the first impact. The duration of the rocking response is the time it takes to complete each of the three impact phases for all n impacts. The entire response evolves in $t_n = 2nt_1$, where t_1 is the quarter period defined by eq. 4.9.

The entire rocking response of the flexible block on a rigid foundation modeled by the SFRM is summarized in the following steps: the block is tilted to an initial drift θ_0, balanced on edge O and released (Figure 5.2); at time t_1 the block strikes the foundation with speed $\dot{\theta}_1$ from eq. 4.12 (Figure 5.3); if the rocking condition is satisfied the block rocks about the opposite edge, O', with angular speed $\dot{\theta}_2 = (\sqrt{COR_{SFRM}})\dot{\theta}_1$, from eq. 5.4 (Figure 5.6); the block rocks to the maximum angular displacement, and new initial drift for the next impact, θ_2 defined by eq. 5.1 (Figure 5.7). This process is repeated until the rocking condition is violated, i.e. $\mu_n < \mu_c$ where n is the final impact defined by eq. 5.5, to create a complete rocking response of the flexible rocking block.

As discussed in Section 4.5, the total response is composed of a standard rocking response, followed by a non-standard rocking response. The SFRM captures the standard rocking portion of the rocking response. This standard rocking response is assumed to end when the rocking condition, specified by the impact speed, is violated. When the impact speed, μ, is less than the critical speed of the block, μ_c from eq. 4.26, the center of rotation of the block will not change and the bottom surface of the block will remain in contact with the foundation. The block will, therefore, stop rocking in the standard sense when the rocking condition is violated (nonlinear bounces and rocking may occur–this kind of motion defines the non-standard rocking response response).

5.1.2 Flexibility in the SFRM

The standard rocking response incorporates the assumption that the vibration energy within the block is lost after each impact during the after impact phase of the rocking motion. The effect of the block vibrations must be considered because the vibrations are assumed to dominate this portion of the total rocking response. Concrete is a material that is considered relatively rigid and, therefore, the block vibrations have been assumed to have negligible effect on the rocking response of concrete blocks. The models used to derive the rocking response of rigid blocks in Section 2.2 were derived based on concrete blocks. The numerical studies and experiments that were used to validate these studies also used concrete blocks. The rest of this chapter will focus on creating a standard rocking response for the concrete block in (11) using the SFRM and investigating the key parameters that influence the rocking response when flexibility is considered.

The contribution of the block vibration energy to the rocking response is expected to be less significant for the concrete block from (11) than blocks composed of other materials. The comparison of rigid models with the SFRM will provide insight about the predicted behavior of the rocking block using the SFRM. Below, the SFRM block rocking response is compared with the observed experimental block rocking response from (11) and the block rocking response predicted by the SRM. This comparison shows the viability of the SFRM as a model for rocking block behavior. The block characteristics that drive the differences between the SFRM, and the

experimental and rigid block rocking responses are discussed in terms of how their contribute to the block vibration energy and the corresponding loss of the rigid kinetic energy associated with the rigid movement of the block.

5.2 Experimental Study

In (11), Kalliontzis recorded the rocking response of a concrete block rocking on a concrete foundation to compare the theoretical rocking response modeled by the SRM, presented in (9), with the experimental rocking response. There were six separate experimental responses recorded, each of which had different initial conditions. The experimental responses began by releasing the concrete block from rest with the specified initial drift (initial drift values 1%, 2%, and 3% were each used twice). Recall from Section 3.2.1, the initial drift is the angle the block makes with the foundation and is defined as the ratio of the lateral displacement to the height of the block. In this section, these experimental rocking responses and the corresponding theoretical SRM responses are compared with the rocking response produced by the SFRM for the same block. This comparison determines the contribution of block vibration energy to the rocking response of a concrete block.

5.2.1 Evidence of Internal displacement

The experimental rocking response of the concrete block in (11) was measured with an optical measurement system composed of eight LED sensors that measure the three-dimensional block displacement (see Figure 3.1 to reference the x-, y- and z-axes). These sensors were placed on the block at heights 0”, 0.8”, 39.4”, and 63.0” along each side of the block, as shown in Figure 5.9. The experimental rocking responses of the concrete block for all six tests are shown in Figure 5.10 (see Appendix G for more details about generating the rocking responses from the experimental data).

The SRM from (9), presented in Section 2.1, assumes that there is no internal block displacement throughout the rocking block response. The block modeled in (11) is assumed to be a rigid block satisfying the conditions of the SRM. Under the SRM assumptions, any internal motions of the block are assumed to have a negligible effect on the rocking response. Therefore,

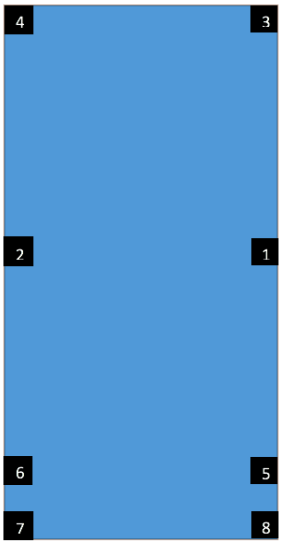

Figure 5.9: Configuration of sensors used in experiments in (11).

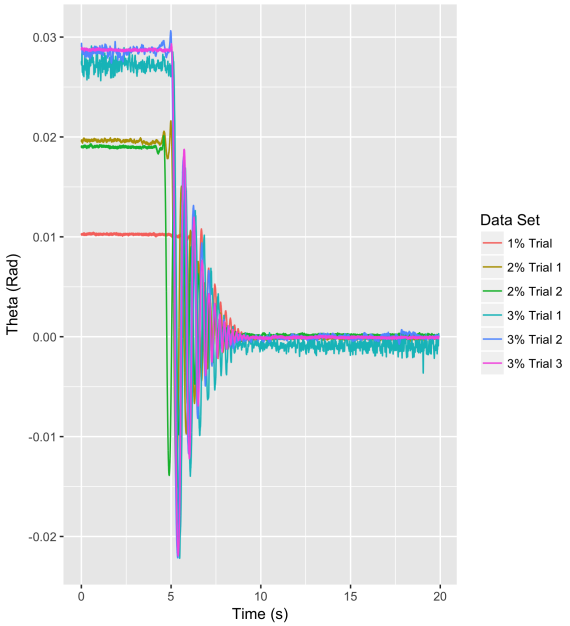

Figure 5.10: The rocking response in terms of θ for each of the six tests using sensors 8 and 5 from Figure 5.9.

each of the eight sensors on the block should measure the same rocking response. In addition, since there are no axial deformations or other internal deformations, the distance between any two points on the rigid block should remain constant throughout the rocking motion. The distance along the height of the block between two points, for example two sensors, should also remain constant throughout the rocking response. A significant change in this distance indicates the existence of internal deformations.

5.2.2 Relative Displacement

The optical measurement system in (11) records the position of the LED sensors at a frequency of 496 Hz (i.e. every second the optical measurement system takes 496 pictures, or measurements). The time between each measurement is 2016 microseconds. This time difference between each measurement defines the time step at which the rocking block response is being captured by the optical measurement system. There were a total of 9880 measurements recorded during each of the experimental rocking block responses and the duration of each of the rocking responses was just under 20 seconds. The last measurement recorded by the optical system was assumed to define the resting position of the block. At this resting position, it was assumed that there are no internal deformations within the block and that the angular displacement is zero. The resting position is used as the reference position to define the absolute fixed distance between any two points on the block, for example between two LED sensors. This fixed distance is constant throughout the rocking response created using the SRM. The change in the distance along the height of the block (along the y_b axis in Figure 3.3) between two sensors and the fixed distance at the reference position defines the relative displacement between the two sensors. Any non-zero relative displacement between two sensors represents the vertical internal deformation of the block.

The relative displacement between Sensor 3 and Sensor 1 is shown in Figure 5.11 with the experimental rocking response for the concrete block in (11) with a 1% initial drift. The relative displacement between these two sensors is not constant for any of the six experimental responses (similar graphs that depict only the relative displacement for the other sensors are shown in Appendix G). The relative displacement from the experimental rocking response in (11) shows

oscillatory motion throughout the rocking response. The time of separation during the impact phase defines the period of the internal block vibrations. The relative displacement can not be recovered from the experimental data because the period is smaller than the recording frequency of the optical measurement system. At the beginning of the rocking response however, the magnitude of the relative displacement oscillates close to zero. This indicates the two sensors are close to their reference positions. Throughout the response the block is stretching and compressing (mainly stretching) from it's resting zero position. During the rocking response the relative displacement undergoes larger oscillations near 0.0015 in. before the response ends with a relative displacement near 0.0020 in.

The oscillations in the signal prompted further investigation into the origins of the oscillations, however; no dominant peaks in the frequency domain of the relative displacement were found. This could be the result of the small magnitude of the vertical vibrations and the low resolution of the optical measurement system. It is possible that peaks would be seen in rocking block experiments with increased flexibility (i.e. low modulus of elasticity). The filtered relative displacement, shown in Figure 5.12, excludes response frequencies lower than 2Hz and higher than 60Hz. The filtered relative displacement confirms the existence of the internal block vibrations between the two sensor locations on the block. The existence of the internal block vibrations promotes modeling the block in (11) as a flexible block using the SFRM. Using the flexible model will consider the effect of these small internal vibrations on the rocking block response.

5.2.3 SFRM Rocking Response

The properties of the block in (11), summarized in Table 5.1, are used to define the parameters of the SFRM rocking block response for this concrete block. These parameters are the rocking criteria from eq. 4.26, the speed after impact from eq. 5.2, and the COR_{SFRM} from eq. 4.29, as shown in Table 5.2 and 5.3 for the block in (11). The critical impact velocity that initiates rocking for the block is $\mu_c = \frac{4gh}{c} = 0.565$ in/s and the minimum initial drift that will cause rocking at this impact speed, defined in eq. 5.9, is $\theta_0 = 0.2\%$. The block will stop

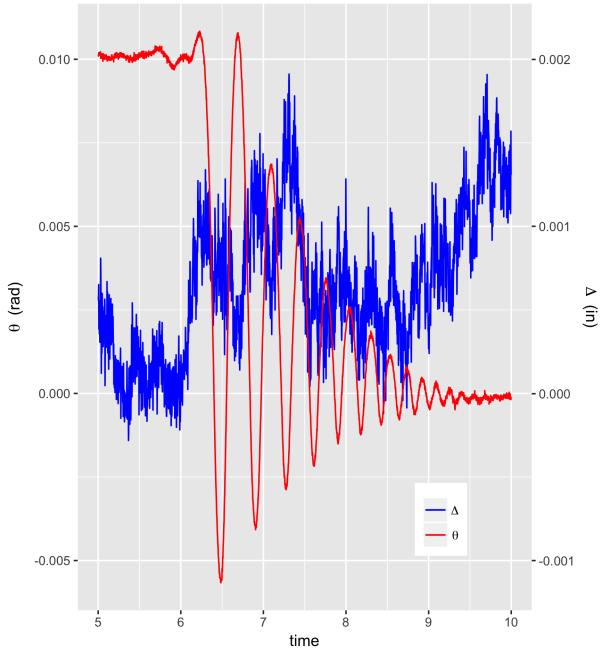

Figure 5.11: The relative displacement, Δ, between Sensors 3 and 1 developed during the rocking response θ from (11) with $\theta_0 = 1\%$.

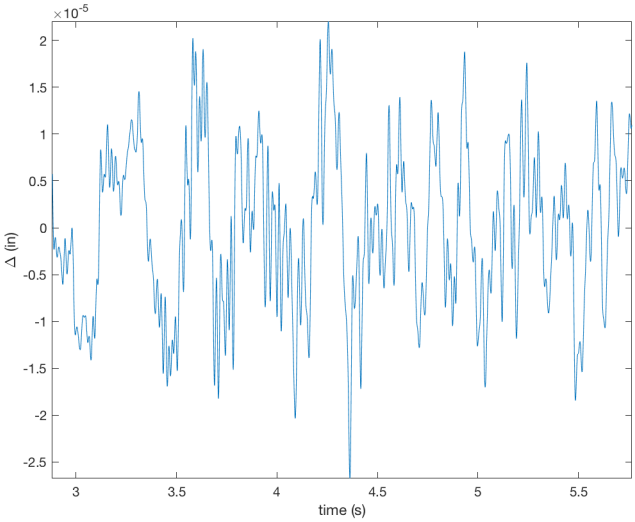

Figure 5.12: The relative displacement filtered for frequencies about 2.0Hz and below 69.0 Hz between Sensors 3 and 1 during the rocking response with $\theta_0 = 1\%$.

Table 5.1: Geometric properties for the block in (11). (Poisson's ration, $\nu = 0.20$)

Parameter	English Units	SI Units
base length, b	7 in	178 mm
height of the block, h	33 in	838 mm
$R = \sqrt{b^2 + h^2}$	33.7343 in	856.8501 mm
weight, W	1220 lbs	5426.83 N
volume density, ρ	2.4407×10^{-7} k s^2/in^4	2.6084×10^{-9} kg/mm^3
$I = \frac{4WR^2}{3g}$	4.7908 k in s^2	541282 N mm s^2
Young's Modulus, E	3825 ksi	26372 MPa
Impact Duration, t_{sep}	0.00146107 s	—
Critical speed, μ_c	0.564556 in/s	14.3397 mm/s

Table 5.2: Rocking properties for the block in (11). (Poisson's ration, $\nu = 0.20$)

Parameter	English Units	SI Units
Impact Duration, t_{sep}	0.00146107 s	—
Critical speed, μ_c	0.564556 in/s	14.3397 mm/s

rocking when the drift value is less than this minimum drift value or, equivalently, when the impact speed is less than μ_c.

The steps outlined in Section 5.1 are followed to create a rocking response using the parameters from Tables 5.1, 5.2 and 5.3. After the block is titled through some initial drift, the impact speed (eq. 4.12), the COR_{SFRM} (eq. 4.29), the speed after impact (eq. 5.2), and the rocking condition (eq. 5.3) and the maximum displacement after impact (eq. 5.1) define the SFRM rocking response. Figure 5.13 shows the peak displacements of the SFRM, the peak displacements of the SRM and the experimental rocking response after a 1% initial drift (see Appendix G for the comparisons of the peak displacements for other initial drift values). The SFRM, with the assumptions for creating a response, captures the displacement peaks and

Table 5.3: Parameters that govern the SFRM rocking response for the block with properties from (11).

$\theta_0\%$	$\dot{\theta}_1$	μ_1	COR_{SFRM}
1	0.186577	1.30604	0.960393
2	0.260649	1.82454	0.963434
3	0.315242	2.20669	0.964445

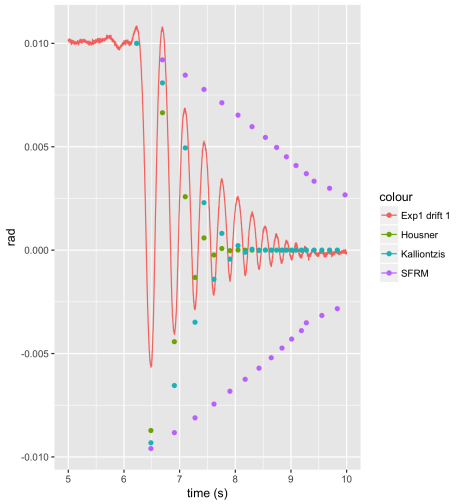

Figure 5.13: Response of the flexible system compared with Housner COR and Kalliontzis COR with the test data from (11) for $\theta_0 = 1\%$.

the decaying motion that characterizes the rocking behavior. The COR_{SFRM} used to reduce the speed at impact and the subsequent peak displacement, only removes the block vibration energy from the system. The amount of energy dissipated after each impact during the experimental rocking block response is greater than the energy dissipated by the SFRM rocking block response. The block vibration energy is a smaller percentage of the rigid kinetic energy than the energy that is lost during impact in the experimental rocking response. The energy in the SFRM rocking block response is dissipated at a slower rate than the experimental rocking block response. The SRM rocking response, on the other hand, assumes that all the energy loss occurs at the interface. This assumption overestimates the energy dissipation of the block in the SRM rocking block response. The SFRM appropriately measures the vibration energy and in conjunction with a model that captures the rigid kinetic energy loss at the impact interface can provide an appropriate representation of the rocking block response.

The purpose of the SFRM is to demonstrate the existence of block vibrations and the significance of the energy loss associated with those block vibrations. The amount of vibration energy that is lost at each impact depends on the modulus of elasticity. The amount of vibration energy increases with the block flexibility and decreases with modulus of elasticity. The ability of the SFRM to predict the experimental block rocking response depends on the flexibility of

the block because of the sensitivity of the SFRM to the elastic modulus. The rocking response of blocks composed of more flexible materials represented with the SFRM experience a faster rocking response decay rate than the concrete block SFRM rocking response shown in Figure 5.13. The block vibration energy clearly contributes to the rocking response although this energy is not solely responsible for dissipating all the input energy in the system. A block with a large modulus of elasticity and less flexibility may see contributions to the energy dissipation in the rocking response through mechanisms other than block vibrations, such as the loss of energy at the rocking interface as assumed in the SRM. A block with smaller modulus of elasticity and increased flexibility should consider the block vibration energy in deciding how to model the rocking block response. A model that encompasses both block vibration energy, energy loss at the rocking interface and foundation vibration energy would more closely represent the experimental rocking block response. The effect of flexibility on the rocking block response, as well as the other key characteristics of the SRM rocking block response, are discussed in the next section.

5.3 Parametric Study of the SFRM

The three characteristics that significantly change the rocking response of the block are flexibility, slenderness, and initial drift. The block flexibility defines the block vibrations that determine the amount of rigid kinetic energy loss throughout the SFRM rocking response into vibration energy within the block. The SRM uses only the block geometry to define the rigid kinetic energy lost at each impact throughout the rocking block response. The slenderness of the block is a characterization of the block geometry and is used in rigid models to define the stability of the block in terms of the block's probability of overturning (**?**). The rigid kinetic energy loss at each impact reduces the speed after impact and therefore the drift after impact. The flexible rocking block response will have smaller maximum drift values than a rigid rocking block response. Given the block properties listed in Table 5.1, this section discusses the effect of the flexibility, slenderness, and initial drift on the rocking response modeled with the SFRM.

The SFRM accounts for block flexibility and the SRM does not. When the SFRM assumes the block is rigid, the differential equation governing the SFRM is equivalent to the differential

equation in the SRM. The COR_{SFRM}, however, is still based on the possibility of vibration energy being developed within the block.

5.3.1 Block flexibility

The flexibility in the block is defined in the SFRM in terms of the modulus of elasticity of the material that composes the block. The modulus of elasticity is a measure of the amount of stress required to cause deformation in an object composed of a specific material and defines the flexibility of the block. A flexible block has a smaller modulus of elasticity and is susceptible to more pronounced internal vibrations than a rigid block with a large modulus of elasticity. The block flexibility determines the amount of block vibration energy generated at each impact and the rigid kinetic energy retained by the block as the rocking response progresses. The duration and magnitude of the rocking block response are strongly impacted by the amount of vibration energy developed throughout the rocking response. The effect of the block vibration energy on the SFRM rocking response is discussed in this section.

5.3.1.1 Rocking motion

The SFRM considers the block flexibility by quantifying the block vibration energy. This vibration energy determines key characteristics of the rocking block response: the rocking condition and the COR_{SFRM}. Both characteristics of the rocking response are functions of the block flexibility. The block flexibility, as mentioned above and in Chapter 3, is defined by the modulus of elasticity of the material of the block. The modulus of elasticity is inversely proportional to the block flexibility. Blocks with a large modulus of elasticity are considered rigid blocks. The rocking condition is a comparison of the speed just before impact to the critical speed to determine if the block will rock.

The rocking condition written in terms of the modulus of elasticity with the impact speed constant defines the minimum modulus for a block material that will experience rocking at that impact speed. The rocking condition in eq. 5.3 can be written in terms of the block modulus of elasticity, E. The minimum modulus of elasticity of a block that will experience rocking and

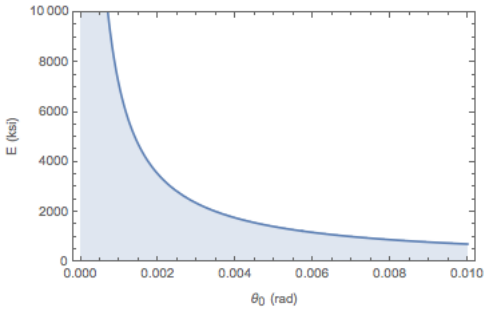

Figure 5.14: The initial drift required to induce rocking in a block by the modulus of elasticity of the block.

internal vertical deformation is

$$E_{\min} = 2\rho(1-\nu^2)\left(\frac{4gbh}{\dot{\theta}}\right)^2 \tag{5.6}$$

where $\dot{\theta}$ is the impact speed of the block after the block is released from the initial drift θ_0 and begins the rocking motion. This equation for the minimum material modulus of elasticity can equivalently be written in terms of the initial drift using eq. 4.12. The minimum rocking modulus of elasticity is shown in Figure 5.14 as a function of the initial drift. The shaded region defines the moduli where a block with geometry defined in Table 5.1 will rock (e.g. At the initial drift 0.0018 radians, any block with modulus of elasticity 3825 ksi or greater will rock). Higher initial drift values, and higher impact speeds, are required to cause rocking in more flexible blocks and lower initial drift values cause rocking in more rigid blocks.

The other key characteristic of the SFRM rocking block motion is the COR_{SFRM}. The SFRM assumes that the speed just before one impact is equivalent to the speed after the previous impact. The speed after the previous impact depends on the axial vibrations within the block. The block vibration energy resulting from these axial vibrations, determines the amount of rigid kinetic energy lost in the system during each impact. The COR_{SFRM} in eq. 4.29 is a function of the block flexibility and the block geometry. The COR_{SRM} from eq. 2.3

$$COR_{SRM} = \left[1 - \frac{mR^2}{I_0}(1-\cos 2\alpha)\right]^2 \tag{5.7}$$

only accounts for the geometry of the block. The experimental response in (11) showed that the edges of the block, used as the centers of rotation for the rocking motion in the SRM and

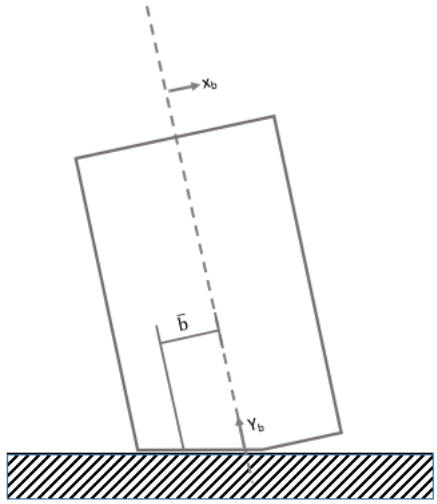

Figure 5.15: The deformed corner seen in experiments in (12) that led to the COR_{MSRM} r_K.

SFRM, deform. Kalliontzis et al. define a modified COR_{SRM}, COR_{MSRM}, that accounts for the shift of the center of rotation toward the center of the block and away from either of the two bottom edges of the block O or O'. The actual centers of rotation were experimentally defined at a distance $\bar{b}$ along the width of the block from the center-line of the block, as shown in Figure 5.15. The COR_{MSRM} that accounts for the deformation of the bottom edges of the block is

$$COD_{MSRM} = \left[\frac{4 - 3(\sin^2\alpha)(1+k^2)}{4 - 3(\sin^2\alpha)(1-k^2)}\right]^2 \tag{5.8}$$

where $k = \bar{b}/b$ ($k = 0.72$ for the block in (11)).

The COR_{SRM} defines a 12.5% decrease in the rigid kinetic energy of the block after each impact while the COR_{MSRM} defines a 3.82 % decrease in the rigid kinetic energy. The percentage of rigid kinetic energy transferred into block vibration energy defined by the SFRM COR_{SFRM} depends on the initial energy input into the system by the initial drift of the block, the block flexibility and the block geometry. The percentage of rigid energy before impact that is transferred into vibration energy after impact is shown in Figure 5.16 for three initial drift values. The minimum COR_{SFRM} for any initial drift defines at least a 3.337% decrease in the rigid kinetic energy before impact. This is the minimum block vibration energy generated during impact as a percentage of the input energy in any rocking block response modeled with

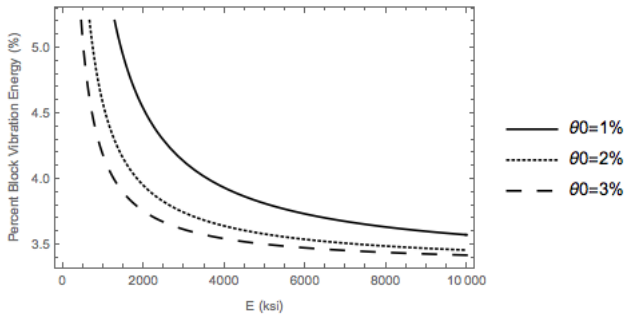

Figure 5.16: The percentage of the initial energy that is transferred to block vibration energy in the SFRM rocking block response.

the SFRM. As the initial drift increases the amount of input energy and block vibration energy increases; however, the percentage of input energy that is transferred to block vibration energy decreases.

The COR_{SFRM} only accounts for vibration energy lost within the block and neglects other possible locations where the energy dissipation could accumulate, such as at the rocking interface or within the foundation as vibration energy. These other sources of energy dissipation have been proven to have a significant influence on the rocking response of rigid blocks in (9), (3), (22), and (27). The modulus of elasticity of a block with properties in Table 5.1 that transfers at least 4%, 5%, 7% and 10 % of the rigid kinetic energy before each impact into vibration energy during impact are shown in Table 5.4 for different initial drifts. These moduli indicate materials of the rocking block where the block vibration energy has a significant effect on the rocking motion of a block rocking on a rigid foundation. Materials that will cause the rocking block to develop a significant amount of vibration energy are shown in Figure 5.17. The SFRM approach is only appropriate for flexible materials where the contribution of the block vibration energy to the energy dissipation at impact is greater than 5% of the rigid kinetic energy, such as in blocks composed of rubbers, polymers, woods and other materials with modulus of elasticity less than 1400 ksi.

The block vibration energy is calculated at each impact. the duration of the impact phase is a function of the speed of the vibrations traveling through the block. The duration of the impact phase of rocking from eq. 4.24 is proportional to the flexibility of the block. The duration of impact increases when the flexibility increases. Block flexibility will also have an effect on the

Table 5.4: Parameters that govern the SFRM rocking response for the block with properties from (11).

θ_0%	3.337%	4%	5%	7%	10%
1	772522390.88	3598.05	1434.31	651.15	357.97
2	395836738.85	1843.62	734.93	333.65	183.42
3	270608432.81	1260.37	502.43	228.09	125.39
4	208264313.98	970.00	386.68	175.54	96.50
5	171091470.34	796.86	317.66	144.21	79.28

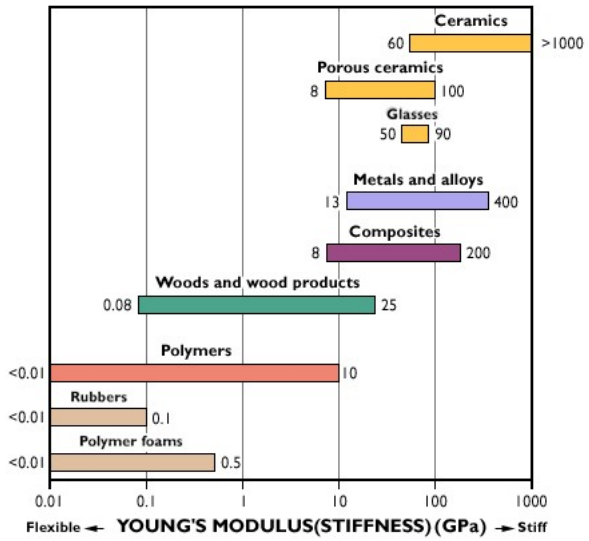

Figure 5.17: Ranges of moduli of elasticity for different materials 1 GPa = 145.0377 ksi (Image sourced from (29)).

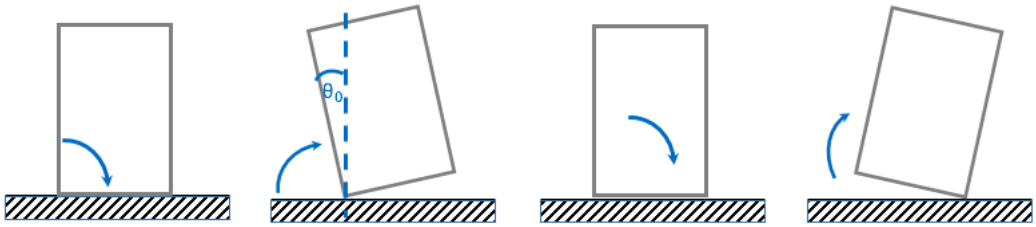

Figure 5.18: Stable rocking diagram where block only rocks on a single face.

number of impacts with foundation and the overall duration of the rocking response. Flexible blocks impact the foundation a fewer number of times throughout the rocking block response than rigid blocks. The amount vibration energy in the block after each impact increases as the block flexibility increases. Increasing flexibility reduces the number of impacts and creates more block vibration energy with a longer duration of impact. This decreases the duration of the rocking response of a flexible block compared with the duration of the rocking response of a rigid block.

5.3.2 Stability Indicated by Slenderness

The stability of rigid rocking structures is defined in terms of the structures rocking stability in (9) and (18). Stability is the likelihood that the rocking block will rock on the foundation with the same surface of the block impacting the foundation. By contrast, overturning is the rocking behaviors of a different surface of the block impacting the foundation. These two characteristics are shown in Figures 5.18 and 5.19. The slenderness has been used to characterize the stability of the rocking behavior of rigid blocks (9). The assumption that larger stout blocks were more stable than tall slender structures prompted Housner to characterize the stability of slender structures in (9). The slenderness of a structure is the ratio of the width of the structure to the height of the structure: stout structures have slenderness ratios close to one while slender structures have small slenderness ratios. Housner proved that slender structures were more stable than previously shown in (18) and that the initial drift that causes a particular rigid rocking block to overturn is equal to the slenderness ratio of that block. The block

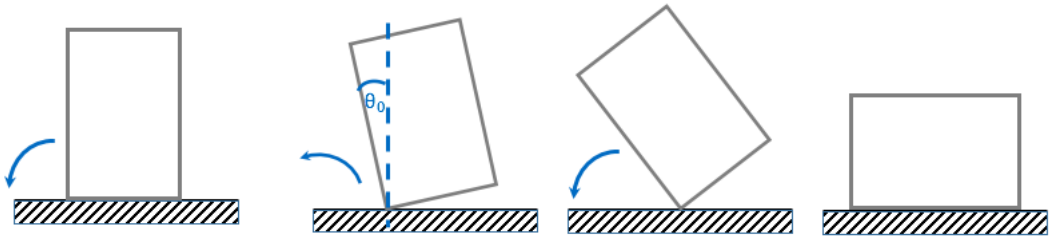

Figure 5.19: A block overturning and impacting the foundation on a different surface than the original surface that was resting on the foundation.

flexibility and the slenderness are independent characteristics of the rocking block; however, in the SFRM, the effect of slenderness can change with the deformation of the block. The stability of slender rocking blocks is attributed to their increased capacity to experience rocking motion when subjected to earthquake ground motion, compared with non-slender structures that tend to experience other nonlinear deformations. The initial drift required to cause rocking decreases for non-slender flexible blocks making them more susceptible to rocking motion. Block flexibility has the opposite effect on rocking blocks. Large initial displacements provide too much instability for the flexible non-slender structures to compensate and they are more likely to experience overturning. The amount of block vibration energy increases in non-slender blocks (see Figure 5.20) because non-slender structures have more material for developing internal vibration energy. The block vibration energy reduces the maximum deflection from the rocking response and decreases the duration of the rocking response. While slenderness in rigid structures improves the stability of the block rocking response, it has the adverse effect when considering the rocking response of flexible blocks with the SFRM. The minimum amount of block vibration energy developed within the block during the rocking response increases in non-slender flexible blocks (see Figure 5.20).

5.3.3 Effect of the Initial Drift on the Rocking Motion

The entire rocking block system is governed by the angular displacement that initiates the rocking response. The initial drift determines the rigid kinetic energy input into the system. The initial drift that will cause a block to rock is based on the rocking condition in eq. 5.3.

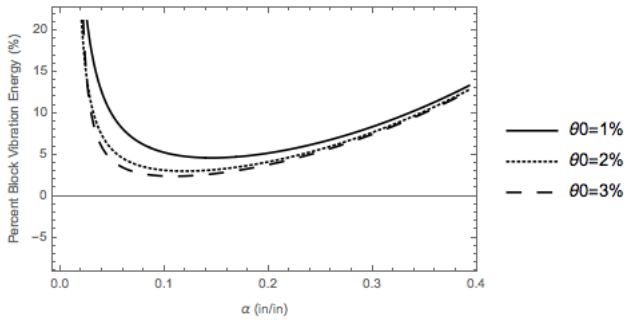

Figure 5.20: The vibration energy as a function of the slenderness $\alpha = b/h$ of the block.

The critical initial drift

$$\theta_c = \alpha + \cos^{-1}\left(\cos\alpha + \frac{I_0}{2WR}\left(\frac{4gh}{cb}\right)^2\right) \tag{5.9}$$

defines the displacement required for the block to experience rocking motion and produces the critical impact speed μ_c which promotes rocking to continue. This critical impact speed is defined by eq. 4.12 with $\theta_0 = \theta_c$ and satisfies the rocking condition. Flexible blocks have a larger capacity for developing internal vibration energy during the rocking response and the initial drift that induces rocking is larger for flexible block than rigid blocks. In the SFRM, the only energy assumed to dissipate the input energy is the internal block energy and under this assumption flexible blocks dissipate more energy at a faster rate than rigid blocks (see Figure 5.14).

The initial drift and subsequent drift angles determine the speed of the block before and after impact. The speed of the block after impact quantifies the energy dissipation as the system evolves. The COR changes after each impact because the ratio of the speed before impact and the speed after impact changes. The COR indicates the amount of rigid kinetic energy retained by the rocking system. The COR_{SFRM} is a function of the geometry of the block, the initial drift before rocking and the material of the block. The COR_{SRM} and the COR_{MSRM} are functions of the block geometry. Experimental results confirm that an accurate COR will take into account the material properties of the block and will show a decrease in the retention of rigid kinetic energy in the rocking block system when the angular speeds are small (11). The COR_{SFRM} exhibits this behavior because it incorporates the characteristics of the block that are responsible for this low energy retention when the impact speeds are small

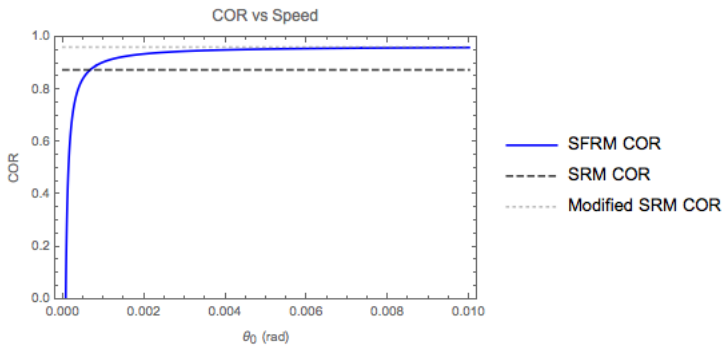

Figure 5.21: The modified, Housner and Kalliontzis CORs as a function of the initial drift.

(see Figure 5.21). This decrease occurs when the rocking response changes from the standard rocking to non-standard rocking response. The non-standard rocking response begins when the rocking condition is no longer satisfied by the impact speed. The impact speed will violate this condition when the drift angle is θ_c or smaller. The modulus of elasticity is critical to the change in the energy retention that occurs at the beginning of non-standard rocking response.

5.4 Conclusion

The flexibility of a block subjected to rocking can have a significant impact on the rocking response of that block. The SFRM incorporates this flexibility into the rocking block response and captures the effects of this flexibility on the rocking response. The significance of the block vibration energy highly dependent on the amount of flexibility within the block and is greater in more flexible blocks. The effect of flexibility is not negligible in nearly rigid blocks. The SFRM determines vibration energy exists in nearly rigid blocks and the block vibration energy contributes to the dissipation of energy in the system.

The SFRM expands the scope of rocking models to gain more information about rocking motion in flexible blocks. Incorporating the flexibility in the SFRM defines a rocking condition that indicates when rocking will occur. The geometry, initial drift and flexibility all contribute to the rocking condition for a particular rocking block system. The end of the standard rocking response is defined by this rocking condition and indicates when the non-standard rocking response begins. The non-standard rocking response is characterized by the drastic decrease

in the COR, the increase in block vibration energy and a large number of axial waves going through the block. The ability to define the rocking condition provides insight into more accurate predictions of rocking behavior in flexible blocks.

CHAPTER 6. CONCLUSION

This research project defined two mathematical representations of the rocking response of a flexible block and quantified the vibration energy within the flexible block. The vibration energy within rigid rocking blocks was shown to have a more significant effect on the rocking system than previously assumed by rigid rocking block models. The flexible model introduces an alternative view of the rocking block system that places a larger emphasis on the block flexibility and encourages including block vibration energy as a source of kinetic energy loss in addition to the kinetic energy loss at the impact interface and the kinetic energy loss to the foundation vibration energy. An itemized list of the conclusions from this study are presented below:

1. Rocking Models for Flexible Blocks

   In this thesis a rocking response for a block that develops internal deformations is defined. The internal deformations are the result of the block flexibility, defined in terms of the modulus of elasticity of the block material. A block that is able to develop internal deformations is called a flexible block and the magnitude of the internal deformations is controlled by magnitude of the block flexibility. The flexible rocking model (FRM) incorporates the internal flexural, axial, and shear deformations that are produced in a flexible block at each impact with the foundation with the external rocking motion defined by the angle between the bottom surface of the block and the foundation. The internal and external block deformations are coupled by the energy equations of the rocking block system. These coupled motions describe the deformation of the block before, during and after impact with the foundation. The simple flexible rocking model (SFRM) is the

representation of the FRM that includes only the axial deformations with the rocking motion.

2. Contribution of Internal Deformations to Rocking Motion

   The internal block deformations create vibration energy within the block. The SFRM captures the vibration energy within the block as a function of the block flexibility. The SFRM describes new characteristics of the rocking block response including the rocking condition and the block vibration energy. These two new aspects of the rocking block system change with the block flexibility. The rocking condition, which defines the beginning and ending of the rocking motion, is a function of the impact speed and the magnitude of the axial vibrations. The impact speed is influenced by the axial vibrations and the axial vibrations are the result of the flexibility within the block. The rocking response created using the SFRM assumes the energy dissipation in the rocking system is solely the result of the block vibrations. The system energy is only reduced by the block vibration energy. This energy reduction is captured with the SFRM COR. The speed of the block is gradually decreased after each impact by the SFRM COR and a response is generated with this reduced speed until the rocking condition is no longer satisfied.

3. Comparison of Flexible Models with Rigid Models

   The comparison of the SFRM and the simple rigid model (SRM) shows the contribution of the block flexibility to the rocking system. The vibration energy within the flexible block has a more significant effect on the rocking block response of blocks with more flexibility than blocks with a large modulus of elasticity (e.g. in rigid blocks). Even in blocks with a large modulus of elasticity, the block vibration energy accounts for more kinetic energy loss than what is defined by rigid rocking models. The amount of block vibration energy developed at each impact using the SFRM suggests that the FRM would produce valuable information about the rocking motion for flexible blocks and the contribution of flexural and shear vibrations.

4. Flexibility and Key Characteristics of Rocking Motion

The flexible block rocking model has different notions of stability and rocking behavior than rigid rocking block models. Flexible non-slender blocks are less likely to overturn because they develop more block vibration energy throughout the rocking response. The flexibility of the block also increases the duration of impact and reduces the chances that the block will rock about the opposite corner at the conclusion of impact compared with rigid blocks. More flexible blocks impact the foundation fewer times throughout the rocking response and require larger initial drift values to initiate rocking

6.1 Future work

This thesis presents an initial study of flexible rocking block models. The FRM and SFRM provide initial steps toward a more in-depth study of flexible block rocking models. These flexible rocking block models are complex non-linear mathematical systems associated with structural phenomena that may be experienced specifically in seismic regions. Detailed points of interest for future research regarding the investigation of flexible rocking block models are discussed below.

6.1.1 Solutions of the FRM

The FRM accounts for all modes of displacement in the block in the flexible rocking block system. The internal deformations in the FRM define the total block vibration energy of the system. A numerical solution of the nonlinear coupled partial differential equation 3.12 would be advantageous in modeling and testing experimental flexible rocking structures with elastic modulus that transfers at least 5% of the rigid kinetic energy to block vibration energy (moduli less than 1434 GPa when the initial drift is 1% the total height). The same type of analysis performed in this thesis for the SFRM could be performed to acquire this numerical solution. Comparisons with test data would yield specific information about which internal mode of displacement provides the largest contribution to the block rocking motion. The flexural deformations included in the FRM contribute to the initial drift and rocking motion and are of particular interest. It is likely that the results for semilinear and quasilinear systems

presented in this thesis will apply to the FRM; however a rigorous proof of the existence and uniqueness of solutions to eq. 3.12 and a general result for the well-posedness of quasilinear coupled partial differential equations would make a significant contribution to this area in mathematics.

6.1.2 Controlled rocking

An extension of the free rocking flexible rocking block models is the application of the FRM or SFRM to controlled rocking systems. The motion in controlled rocking systems is restricted by a cable through the center line of the block along the height. The cable is loaded causing stress in the cable and the block, called prestress, that counteracts the block rocking motion by limiting the maximum angle the block will make with the foundation during the rocking motion. In structural design, prestress is added to a member to change the initial stress distribution to a non-zero stress distribution. This initial stress distribution increases the member's ability to sustain larger displacements (1). The increased axial force of prestress may cause large stresses at the interface of the block and the foundation. The effect of the high stresses on the contribution of the block vibration energy to the controlled rocking block response is a natural continuation of investigating the effect of flexibility in rocking models.

Viscous damping is added to rigid rocking models to represent continuous dissipation in the rocking system (27). This kind of damping is inefficient for controlled rocking and unnecessary in the case of the FRM since the internal deformations are included. The prestress cable in the block can be included in the FRM as a passive control mechanism in the system. The prestress force should be included as a boundary force. This force would only occur at a single point along the boundary of the block. Defining the well-posedness and finding a numerical solution of the FRM with a single point force on the boundary is an interesting mathematics problem that broadens the application of the flexible models.

6.1.3 Flexibility at the interface

The models with block flexibility in eqs. 3.12 and 4.5 assume the foundation is rigid. Rigid rocking blocks dissipate more kinetic energy at the rocking interface with the foundation

than within the block as block vibration energy. Adding the foundation flexibility and the contribution of the impact interface to the flexible block models would define a comprehensive model of the rocking block response. Coupling the FRM (or the SFRM) to one of the rigid models that includes a flexible foundation (e.g. the Winkler foundation or the concentrated spring foundation from (1) or (3) in Figures 2.5 and 2.4) creates a rocking block model that includes these three kinds of energy dissipation mechanisms. A comprehensive model like the one described couples the effect of the block flexibility with the foundation flexibility. Adding boundary damping that corresponds with the material at the foundation is another method of including the flexibility at the interface. This boundary damping added to the FRM or the SFRM includes the effect of impact with the flexible foundation without the use of a COR. A model that considers the block flexibility and the foundation flexibility could be generalized to model two flexible blocks, with different geometric properties, stacked on top of each other.

6.2 Broader Impacts

The rocking block system is used to generalize rocking motion for structures such as building and columns. There are no perfectly rigid structures and expounding the scope of application of rocking models increases their applicability to real world structures. Properly representing the block flexibility and its effect on the rocking system will greatly increase how block rocking systems are understood. More general models will then be applicable to structures that must be designed to withstand seismic loads. A large class of models that can be used on many structures is desirable as infrastructure improvements continue to reduce the risk of loses that occur from seismic events.

BIBLIOGRAPHY

[1] Aslam, Mohammad, A.M. ASCE, William G. Godden, M. ASCE, and D. Theodore Scalise. "Earthquake Rocking Response of Rigid Bodies." Journal of the Structural Division 106.2 (1980): 377-92. Print.

[2] Baratta, Alessandro, and Ottavia Corbi. "Analysis of the Dynamics of Rigid Blocks Using the Theory of Distributions." Advances in Engineering Software 44.1 (2012): 15-25. Print.

[3] Chatzis, M. N., and A. W. Smyth. "Robust Modeling of the Rocking Problem." J. Eng. Mech. Journal of Engineering Mechanics 138.3 (2012): 247-62. Print.

[4] Christ, Michael, James Colliander, and Terence Tao. "Ill-Posedness for Nonlinear Schrodinger and Wave Equations." ArXiv:math/0311048 (2003). Preprint.

[5] "Earthquakes, Megaquakes and the Movies." Earthquakes, Megaquakes and the Movies: Lights! Cameras! Disaster! N.p., n.d. Web. 23 June 2016.

[6] "Earthquakes with 1,000 or More Deaths 1900-2014." Earthquakes with 1,000 or More Deaths 1900-2014. N.p., n.d. Web. 23 June 2016.

[7] Evans, Lawrence C. Partial Differential Equations. Providence, RI: American Mathematical Society, 2010. Print.

[8] Fountain, Henry. "A Bridge Built to Sway When the Earth Shakes." The New York Times 7 Feb. 2012: D1+. Print.

[9] Housner, George W. “The Behavior of Inverted Pendulum Structures During Earthquakes.” Bulletin of the Seismological Society of America 53.2 (1963): 403-17. Print.

[10] John, Fritz. Partial Differential Equations. 3rd ed. New York: Springer-Verlag, 1978. 111. Print.

[11] Kalliontzis, Dimitrios. Dynamic Decay of Rocking Concrete Members. Thesis. Iowa State University, Ames, IA, 2014. Print.

[12] Kalliontzis, Dimitrios, Sritharan, Sri, Schultz, Arturo. An Improved Coefficient of Restitution Estimation for Free Rocking Members. Submitted. 2016. Print.

[13] Kelly, James M. Earthquake-resistant Design with Rubber. London: Springer, 1997. page 3. Print.

[14] Koh, Aik-Siong. ”Rocking of Rigid Blocks on Randomly Shaking Foundations.” Nuclear Engineering and Design 97.2 (1986): 269-276. Print.

[15] Lagnese, J., and J.-L Lions. Modeling Analysis and Control of Thin Plates. Paris: Masson, 1988. Print.

[16] Lindblad, H., and C.D. Sogge. ”On Existence and Scattering with Minimal Regularity for Semilinear Wave Equations.” Journal of Functional Analysis 130.2 (1995): 357-426.

[17] Love, A. E. H. ”Vibrations of Rods: Problems of Dynamical Resistance.” A Treatise on the Mathematical Theory of Elasticity. New York: Dover Publications, 1944. 427-41.

[18] Milne, J. (1885). Seismic experiments. Trans. Seism. Soc. Japan, 8, 182.

[19] ”Mackay School of Mines Seismic Safety Retrofit.” Ndr-ae.com. N.p., n.d. Web. 23 June 2016.

[20] Pazy, A. "Lipschitz Perturbations of Linear Evolution Equations." Semigroups of Linear Operators and Applications to Partial Differential Equations. Vol. 44. New York: Springer-Verlag, 1983. Print.

[21] Peña, F., F. Prieto, P. B. Lourenço, A. Campos Costa, and J. V. Lemos. "On the Dynamics of Rocking Motion of Single Rigid-block Structures." Earthquake Engineering & Structural Dynamics 36.15 (2007): 2383-399. Print.

[22] Prieto, Francisco, and Paulo B. Lourenço."On the Rocking Behavior of Rigid Objects." Meccanica 40 (2005): 121-33. Print.

[23] Safavi, Bahram, and Anne S. Kiremidjian. "Seismic Energy Response or Structures." Recent Advances in Engineering Mechanics and Their Impact on Civil Engineering Practice: Proceedings of the Fourth Engineering Mechanics Division Spec (1983): 218-21. Print.

[24] Stewart, David E. "Rigid-Body Dynamics with Friction and Impact." SIAM Rev. SIAM Review 42.1 (2000): 3-39. Print.

[25] Tao, Terence. "Quasilinear well-posedness." https://terrytao.wordpress.com/2010/02/21/quasilinear-well-posedness/

[26] Tzvetkov, N. "Ill-posedness Issues for Nonlinear Dispersive Equations." GAKUTO International Series Mathematical Sciences and Applications 27 (2006): n. pag. Math/0411455. Preprint.

[27] Vassiliou, Michalis F., Kevin R. Mackie, and Bozidar Stojadinovic. "Rocking Response of Slender, Flexible Columns under Pulse Excitation." Proc. of 4th ECCOMAS Thematic Conference on Computational Methods in Structural Dynamics and Earthquake Engineering, Kos Island, Greece. Print.

[28] Wang, Feifei and Hansen, Scott. Explicit solutions for viscous wave equation with Signorini boundary conditions. University of Minnesota IMA Preprint Series 2473, 2016.

[29] (http://www-materials.eng.cam.ac.uk/mpsite/properties/non-IE/stiffness.html)

APPENDIX A. CALCULUS OF VARIATIONS FOR THE FLEXIBLE ROCKING MODEL (FRM)

The FRM is created by considering the operator L in 3.12, which defines the net energy of the flexible rocking system. Define $KE_L = \int_0^t KE\, ds$, $WE_L = \int_0^t WE\, ds$ and $SE_L = \int_0^t SE\, ds$. The minimization of $L = KE_L + WE_L - SE_L$ is equivalent to the total of the minimization of each term. Define $\mathbf{v}$ as the quadruple $\mathbf{v}$ and $\hat{\mathbf{v}}$ as the quadruple $(\hat{w}, \hat{u}, \hat{\theta}, \hat{\phi})$.

A.1 Strain Energy

The strain energy in the plate is the energy that results from the internal deformations within the plate and is defined as

$$
\begin{aligned}
SE &= \frac{1}{2}\int_{-b}^{b}\int_{\Omega}\sum_{i,j}\sigma_{ij}\epsilon_{ij}\, d\Omega\, dx \\
&= \frac{1}{2}\int_{-b}^{b}\int_{\Omega}\sigma_{22}\epsilon_{22} + 2\sigma_{12}\epsilon_{12}\, d\Omega\, dx \\
&= \frac{1}{2}\frac{E}{1-\mu^2}\int_{-b}^{b}\int_{\Omega}\epsilon_{22}^2 + 2k(1-\mu)\epsilon_{12}^2\, d\Omega\, dx \\
&= \frac{1}{2}\frac{E}{1-\mu^2}\int_{-b}^{b}\int_{0}^{2h}\int_{0}^{\tau}\left(\frac{\partial u}{\partial y} - x\frac{\partial \phi}{\partial y}\right)^2 + 2k(1-\mu)\left(\frac{1}{2}\left[\frac{\partial w}{\partial y} - \phi\right]\right)^2 dz\, dy\, dx \\
&= \frac{1}{2}\frac{E\tau}{1-\mu^2}\int_{-b}^{b}\int_{0}^{2h}\left(\frac{\partial u}{\partial y}\right)^2 - 2x\left(\frac{\partial u}{\partial y}\right)\left(\frac{\partial \phi}{\partial y}\right) + x^2\left(\frac{\partial \phi}{\partial y}\right)^2 + k\frac{(1-\mu)}{2}\left(\frac{\partial w}{\partial y} - \phi\right)^2 dy\, dx \\
&= \frac{1}{2}\frac{Eb\tau}{1-\mu^2}\int_{0}^{2h}\left(\frac{\partial u}{\partial y}\right)^2 + k\frac{(1-\mu)}{2}\left(\frac{\partial w}{\partial y} - \phi\right)^2 + \frac{b^2}{12}\left(\frac{\partial \phi}{\partial y}\right)^2 dy.
\end{aligned}
$$

This minimization of this strain energy follows:

$$\begin{aligned} SE_L\mathbf{v} &= \int_0^T SE\, dt \\ &= \int_0^T \frac{1}{2}\frac{Eb\tau}{1-\mu^2}\int_0^{2h}\left(\frac{\partial u}{\partial y}\right)^2 + k\frac{(1-\mu)}{2}\left(\frac{\partial w}{\partial y}-\phi\right)^2 + \frac{b^2}{12}\left(\frac{\partial \phi}{\partial y}\right)^2 dy\, dt \end{aligned}$$

$$\begin{aligned} SE_L(\mathbf{v}+\epsilon\hat{\mathbf{v}}) = \frac{1}{2}\frac{Eb\tau}{1-\mu^2}\int_0^T\int_0^{2h}&\left(\frac{\partial(u+\epsilon u)}{\partial y}\right)^2 + k\frac{(1-\mu)}{2}\left(\frac{\partial(w+\epsilon w)}{\partial y}-(\phi+\epsilon\hat{\phi})\right)^2 \\ &+ \frac{b^2}{12}\left(\frac{\partial(\phi+\epsilon\hat{\phi})}{\partial y}\right)^2 dy\, dt \end{aligned}$$

$$\begin{aligned} \frac{dSE_L(\mathbf{v}+\epsilon\hat{\mathbf{v}})}{d\epsilon} = \frac{Eb\tau}{1-\mu^2}\int_0^T\int_0^{2h}&\frac{\partial(u+\epsilon u)}{\partial y}\frac{\partial u}{\partial y} + k\frac{(1-\mu)}{2}\left(\frac{\partial(w+\epsilon w)}{\partial y}-(\phi+\epsilon\hat{\phi})\right)\left(\frac{\partial w}{\partial y}-\hat{\phi}\right) \\ &+ \frac{b^2}{12}\frac{\partial(\phi+\epsilon\hat{\phi})}{\partial y}\frac{\partial\hat{\phi}}{\partial y}\, dy\, dt \end{aligned}$$

$$\left.\frac{dSE_L(\mathbf{v}+\epsilon\hat{\mathbf{v}})}{d\epsilon}\right|_{\epsilon=0} = \frac{Eb\tau}{1-\mu^2}\int_0^T\int_0^{2h}\frac{\partial u}{\partial y}\frac{\partial u}{\partial y} + k\frac{(1-\mu)}{2}\left(\frac{\partial w}{\partial y}-\phi\right)\left(\frac{\partial w}{\partial y}-\hat{\phi}\right) + \frac{b^2}{12}\frac{\partial\phi}{\partial y}\frac{\partial\hat{\phi}}{\partial y}\, dy\, dt$$

$$\begin{aligned} SE_L^\epsilon = \frac{Eb\tau}{1-\mu^2}\int_0^T&\left[\frac{\partial u}{\partial y}u + k\frac{(1-\mu)}{2}\left(\frac{\partial w}{\partial y}-\phi\right)w + \frac{b^2}{12}\frac{\partial\phi}{\partial y}\hat{\phi}\right]_0^{2h} \\ &- \int_0^{2h} u\left(\frac{\partial^2 u}{\partial^2 y}\right) + w\left(k\frac{(1-\mu)}{2}\left(\frac{\partial^2 w}{\partial y^2}-\frac{\partial\phi}{\partial y}\right)\right) \\ &+ \hat{\phi}\left(k\frac{(1-\mu)}{2}\left(\frac{\partial w}{\partial y}-\phi\right)+\frac{b^2}{12}\frac{\partial^2\phi}{\partial y^2}\right) dy\, dt. \end{aligned} \tag{A.1}$$

A.2 Kinetic Energy

The displacements which will minimize the kinetic energy from (3.7) satisfy the following:

$$KE_L\mathbf{v} = \int_0^T \rho b\tau \int_0^{2h} \left(\dot\theta(y+u) - \dot w\right)^2 + \left(\dot\theta(b+w) + \dot u\right)^2 + \frac{b^2}{3}\left(\left(\dot\theta + \dot\phi\right)^2 + \left(\dot\theta\phi\right)^2\right) dy\, dt$$

$$\begin{aligned} KE_L(\mathbf{v}+\epsilon\hat{\mathbf{v}}) = \rho b\tau \int_0^T \int_0^{2h} &\left(\left(\dot\theta + \epsilon\dot{\hat\theta}\right)(y+u+\epsilon u) - \left(\dot w + \epsilon\dot{\hat w}\right)\right)^2 \\ &+ \left(\left(\dot\theta + \epsilon\dot{\hat\theta}\right)(b+w+\epsilon w) + \left(\dot u + \epsilon\dot{\hat u}\right)\right)^2 \\ &+ \frac{b^2}{3}\left(\left(\dot\theta + \epsilon\dot{\hat\theta} + \dot\phi + \epsilon\dot{\hat\phi}\right)^2 + \left(\left(\dot\theta + \epsilon\dot{\hat\theta}\right)\left(\phi + \epsilon\hat\phi\right)\right)^2\right) dy\, dt \end{aligned}$$

$$\begin{aligned} \frac{dKE_L(\mathbf{v}+\epsilon\hat{\mathbf{v}})}{d\epsilon} = 2\rho b\tau \int_0^T \int_0^{2h} &\left(\left(\dot\theta + \epsilon\dot{\hat\theta}\right)(y+u+\epsilon u) - \left(\dot w + \epsilon\dot{\hat w}\right)\right)\left(\dot{\hat\theta}(y+u+\epsilon u)\right. \\ &\left. + \left(\dot\theta + \epsilon\dot{\hat\theta}\right)u - \dot{\hat w}\right) + \left(\left(\dot\theta + \epsilon\dot{\hat\theta}\right)(b+w+\epsilon w) + \left(\dot u + \epsilon\dot{\hat u}\right)\right) \\ &\left(\dot{\hat\theta}(b+w+\epsilon w) + \left(\dot\theta + \epsilon\dot{\hat\theta}\right)w + \dot{\hat u}\right) + \frac{b^2}{3}\left(\dot\theta + \epsilon\dot{\hat\theta} + \dot\phi + \epsilon\dot{\hat\phi}\right)\left(\dot{\hat\theta} + \dot{\hat\phi}\right) \\ &+ \frac{b^2}{3}\left(\dot\theta + \epsilon\dot{\hat\theta}\right)\left(\phi + \epsilon\hat\phi\right)\left(\dot{\hat\theta}\left(\phi + \epsilon\hat\phi\right) + \left(\dot\theta + \epsilon\dot{\hat\theta}\right)\hat\phi\right) dy\, dt \end{aligned}$$

$$\begin{aligned} \left.\frac{KE_L(\mathbf{v}+\epsilon\hat{\mathbf{v}})}{d\epsilon}\right|_{\epsilon=0} = 2\rho b\tau \int_0^T \int_0^{2h} &\left(\dot\theta(y+u) - \dot w\right)\left(\dot{\hat\theta}(y+u) + \dot\theta u - \dot{\hat w}\right) \\ &+ \left(\dot\theta(b+w) + \dot u\right)\left(\dot{\hat\theta}(b+w) + \dot\theta w + \dot{\hat u}\right) \\ &+ \frac{b^2}{3}\left(\left(\dot\theta + \dot\phi\right)\left(\dot{\hat\theta} + \dot{\hat\phi}\right) + \left(\dot\theta\phi\right)\left(\dot{\hat\theta}\phi + \dot\theta\hat\phi\right)\right) dy\, dt \end{aligned}$$

$$
\begin{aligned}
KE_L^{\epsilon} = 2\rho b\tau \int_0^T \int_0^{2h} & \dot{\hat{w}} \left(\dot{w} - \dot{\theta}(y+u) \right) + w \left((\dot{\theta})^2 (b+w) + \dot{\theta}\dot{u} \right) \\
& + \dot{\hat{u}} \left(\dot{u} + \dot{\theta}(b+w) \right) + \hat{u} \left((\dot{\theta})^2 (y+u) - \dot{\theta}\dot{w} \right) + \dot{\hat{\phi}} \frac{b^2}{3} \left(\dot{\phi} + \dot{\theta} \right) + \hat{\phi} \frac{b^2}{3} \left((\dot{\theta})^2 \phi \right) \\
& + \dot{\hat{\theta}} \left[\dot{\theta} \left((y+u)^2 + (b+w)^2 + \frac{b^2}{3}(1+\phi^2) \right) - (y+u)\dot{w} + (b+w)\dot{u} - \frac{b^2}{3}\dot{\phi} \right] dy\, dt
\end{aligned}
$$

$$
\begin{aligned}
= 2\rho b\tau \int_0^T \int_0^{2h} & -w \left(\ddot{w} - \ddot{\theta}(y+u) - \dot{\theta}\dot{u} \right) + w \left((\dot{\theta})^2 (b+w) + \dot{\theta}\dot{u} \right) \\
& - u \left(\ddot{u} + \ddot{\theta}(b+w) + \dot{\theta}\dot{w} \right) + u \left((\dot{\theta})^2 (y+u) - \dot{\theta}\dot{w} \right) - \hat{\phi} \frac{b^2}{3} \left(\ddot{\phi} + \ddot{\theta} \right) + \hat{\phi} \frac{b^2}{3} \left((\dot{\theta})^2 \phi \right) \\
& - \hat{\theta} \left[\ddot{\theta} \left((y+u)^2 + (b+w)^2 + \frac{b^2}{3}(1+\phi^2) \right) + \dot{\theta} \left(2(y+u)\dot{u} + 2(b+w)\dot{w} + \frac{2b^2}{3}\phi\dot{\phi} \right) \right. \\
& \left. -\dot{u}\dot{w} - (y+u)\ddot{w} + \dot{w}\dot{u} + (b+w)\ddot{u} - \frac{b^2}{3}\ddot{\phi} \right] dy\, dt
\end{aligned}
$$

$$
\begin{aligned}
= 2\rho b\tau \int_0^T \int_0^{2h} & w \left(-\ddot{w} + \ddot{\theta}(y+u) + 2\dot{\theta}\dot{u} + (\dot{\theta})^2 (b+w) \right) \\
& + u \left(-\ddot{u} - \ddot{\theta}(b+w) - 2\dot{\theta}\dot{w} + (\dot{\theta})^2 (y+u) \right) + \hat{\phi} \frac{b^2}{3} \left(-\dddot{\phi} - \ddot{\theta} + (\dot{\theta})^2 \phi \right) \\
& + \hat{\theta} \left[-\ddot{\theta} \left((y+u)^2 + (b+w)^2 + \frac{b^2}{3}(1+\phi^2) \right) - 2\dot{\theta} \left((y+u)\dot{u} + (b+w)\dot{w} + \frac{b^2}{3}\phi\dot{\phi} \right) \right. \\
& \left. +(y+u)\ddot{w} - (b+w)\ddot{u} + \frac{b^2}{3}\dddot{\phi} \right] dy\, dt \qquad \text{(A.2)}
\end{aligned}
$$

A.3 Work Energy

The displacements which will minimize the kinetic energy from (3.8) satisfy the following:

$$\begin{aligned}
WE_L\mathbf{v} &= \int_0^T WE\,dt \\
&= \int_0^T 2\rho b\tau g \int_0^{2h} (b+w)\sin\theta + (y+u)\cos\theta\,dy\,dt \\
WE_L(\mathbf{v}+\epsilon\hat{\mathbf{v}}) &= 2\rho b\tau g \int_0^T \int_0^{2h} (b+w+\epsilon w)\sin(\theta+\epsilon\hat{\theta}) + (y+u+\epsilon u)\cos(\theta+\epsilon\hat{\theta})\,dy\,dt \\
\frac{dWE_L(\mathbf{v}+\epsilon\hat{\mathbf{v}})}{d\epsilon} &= 2\rho b\tau g \int_0^T \int_0^{2h} w\sin(\theta+\epsilon\hat{\theta}) + \hat{\theta}(b+w+\epsilon w)\cos(\theta+\epsilon\hat{\theta}) \\
&\qquad + u\cos(\theta+\epsilon\hat{\theta}) - \hat{\theta}(y+u+\epsilon u)\sin(\theta+\epsilon\hat{\theta})\,dy\,dt \\
\left.\frac{dWE_L(\mathbf{v}+\epsilon\hat{\mathbf{v}})}{d\epsilon}\right|_{\epsilon=0} &= 2\rho b\tau g \int_0^T \int_0^{2h} w\sin\theta + \hat{\theta}(b+w)\cos\theta + u\cos\theta - \hat{\theta}(y+u)\sin\theta\,dy\,dt \\
WE_L^{\epsilon} &= 2\rho b\tau g \int_0^T \int_0^{2h} w\sin\theta + \hat{\theta}(b+w)\cos\theta + u\cos\theta - \hat{\theta}(y+u)\sin\theta\,dy
\end{aligned} \tag{A.3}$$

APPENDIX B. CALCULUS OF VARIATIONS FOR THE SIMPLIFIED ROCKING MODEL (SFRM)

The SFRM is created by considering the operator L in 4.5, which defines the net energy of the flexible rocking system when only axial deformations are considered. As in Chapter A, define $KE_L = \int_0^t KE\,ds$, $WE_L = \int_0^t WE\,ds$ and $SE_L = \int_0^t SE\,ds$. The minimization of $L = KE_L + WE_L - SE_L$ is equivalent to the total of the minimization of each term. Define $\mathbf{v}$ as the couple $\mathbf{v}$ and $\hat{\mathbf{v}}$ as the couple $(\hat{u}, \hat{\theta})$.

B.1 Strain Energy

The potential energy in the plate is the strain energy within the plate and is defined as

$$\begin{aligned} SE &= \frac{1}{2}\int_{-b}^{b}\int_{\Omega}\sum_{i,j}\sigma_{ij}\epsilon_{ij}\,d\Omega\,dx \\ &= \frac{1}{2}\int_{-b}^{b}\int_{\Omega}\sigma_{22}\epsilon_{22}\,d\Omega\,dx \\ &= \frac{1}{2}\frac{E}{1-\nu^2}\int_{-b}^{b}\int_{\Omega}\epsilon_{22}^2\,d\Omega\,dx \\ &= \frac{1}{2}\frac{E}{1-\nu^2}\int_{-b}^{b}\int_{0}^{2h}\int_{0}^{\tau}(u_y)^2\;dz\,dy\,dx \\ &= \frac{1}{2}\frac{Eb\tau}{1-\nu^2}\int_{0}^{2h}(u_y)^2\;dy. \end{aligned}$$

This minimization of this potential energy follows:

$$\begin{aligned} SE_L\mathbf{v} &= \int_0^T SE\, dt \\ &= \int_0^T \frac{1}{2}\frac{Eb\tau}{1-\nu^2}\int_0^{2h} (u_y)^2\, dy\, dt \end{aligned}$$

$$SE_L(\mathbf{v}+\epsilon\hat{\mathbf{v}}) = \frac{1}{2}\frac{Eb\tau}{1-\nu^2}\int_0^T\int_0^{2h} ((u_y+\epsilon\hat{u}_y))^2\, dy\, dt$$

$$\frac{\partial SE_L(\mathbf{v}+\epsilon\hat{\mathbf{v}})}{\partial\epsilon} = \frac{Eb\tau}{1-\nu^2}\int_0^T\int_0^{2h} (u_y+\epsilon\hat{u}_y)\hat{u}_y\, dy\, dt$$

$$\left.\frac{\partial SE_L(\mathbf{v}+\epsilon\hat{\mathbf{v}})}{\partial\epsilon}\right|_{\epsilon=0} = \frac{Eb\tau}{1-\nu^2}\int_0^T\int_0^{2h} u_y\hat{u}_y\, dy\, dt$$

$$SE_L^\epsilon = \frac{Eb\tau}{1-\nu^2}\int_0^T [u_y\hat{u}]_0^{2h} - \int_0^{2h}\hat{u}\,(u_{yy})\, dy\, dt. \tag{B.1}$$

B.2 Kinetic Energy

The displacements which will minimize the kinetic energy from (4.3) satisfy the following:

$$KE_L\mathbf{v} = \int_0^T \rho b\tau \int_0^{2h} \left(\dot{\theta}(y+u)\right)^2 + \left(\dot{\theta}b + \dot{u}\right)^2 + \frac{b^2}{3}\left(\dot{\theta}\right)^2 \, dy\, dt$$

$$KE_L(\mathbf{v}+\epsilon\hat{\mathbf{v}}) = \rho b\tau \int_0^T \int_0^{2h} \left(\left(\dot{\theta}+\epsilon\dot{\hat{\theta}}\right)(y+u+\epsilon\hat{u})\right)^2 + \left(\left(\dot{\theta}+\epsilon\dot{\hat{\theta}}\right)b + \left(\dot{u}+\epsilon\dot{\hat{u}}\right)\right)^2 + \frac{b^2}{3}\left(\left(\dot{\theta}+\epsilon\dot{\hat{\theta}}\right)^2\right) d$$

$$\begin{aligned}\frac{\partial KE_L(\mathbf{v}+\epsilon\hat{\mathbf{v}})}{\partial\epsilon} &= 2\rho b\tau \int_0^T \int_0^{2h} \left[\left(\dot{\theta}+\epsilon\dot{\hat{\theta}}\right)(y+u+\epsilon\hat{u})\right]\left(\dot{\hat{\theta}}(y+u+\epsilon\hat{u}) + \left(\dot{\theta}+\epsilon\dot{\hat{\theta}}\right)\hat{u}\right) \\ &\quad + \left[\left(\dot{\theta}+\epsilon\dot{\hat{\theta}}\right)b + \left(\dot{u}+\epsilon\dot{\hat{u}}\right)\right]\left(\dot{\hat{\theta}}b + \dot{\hat{u}}\right) + \frac{b^2}{3}\left(\dot{\theta}+\epsilon\dot{\hat{\theta}}\right)\left(\dot{\hat{\theta}}\right) \, dy\, dt\end{aligned}$$

$$\left.\frac{\partial KE_L(\mathbf{v}+\epsilon\hat{\mathbf{v}})}{\partial\epsilon}\right|_{\epsilon=0} = 2\rho b\tau \int_0^T \int_0^{2h} \left(\dot{\theta}(y+u)\right)\left(\dot{\hat{\theta}}(y+u) + \dot{\theta}\hat{u}\right) + \left(\dot{\theta}b + \dot{u}\right)\left(\dot{\hat{\theta}}b + \dot{\hat{u}}\right) + \frac{b^2}{3}\left(\dot{\theta}\dot{\hat{\theta}}\right) \, dy\, dt$$

$$\begin{aligned}KE_L^{\epsilon} &= 2\rho b\tau \int_0^T \int_0^{2h} \dot{\hat{u}}\left(\dot{u}+\dot{\theta}b\right) + \hat{u}\left((\dot{\theta})^2(y+u)\right) + \dot{\hat{\theta}}\left[\dot{\theta}\left((y+u)^2 + \frac{4b^2}{3}\right) + b\dot{u}\right] \, dy\, dt \\ &= 2\rho b\tau \int_0^T \int_0^{2h} -\hat{u}\left(\ddot{u}+\ddot{\theta}b\right) + u\left((\dot{\theta})^2(y+u)\right) - \hat{\theta}\left[\ddot{\theta}\left((y+u)^2 + \frac{4b^2}{3}\right) + 2\dot{\theta}\,(y+u)\,\dot{u} + b\right. \\ &= 2\rho b\tau \int_0^T \int_0^{2h} \hat{u}\left(-\ddot{u} - \ddot{\theta}b + \dot{\theta}^2(y+u)\right) + \hat{\theta}\left[-\ddot{\theta}\left((y+u)^2 + \frac{4b^2}{3}\right) - 2\dot{\theta}(y+u)\dot{u} - b\ddot{u}\right] \, d\end{aligned} \tag{B.2}$$

B.3 Work Energy

The displacements which will minimize the kinetic energy from (4.4) satisfy the following:

$$\begin{aligned}
WE_L\mathbf{v} &= \int_0^T WE\,dt \\
&= \int_0^T 2\rho b\tau g \int_0^{2h} b\sin\theta + (y+u)\cos\theta\,dy\,dt \\
WE_L(\mathbf{v}+\epsilon\hat{\mathbf{v}}) &= 2\rho b\tau g \int_0^T \int_0^{2h} b\sin(\theta+\epsilon\hat{\theta}) + (y+u+\epsilon\hat{u})\cos(\theta+\epsilon\hat{\theta})\,dy\,dt \\
\frac{\partial WE_L(\mathbf{v}+\epsilon\hat{\mathbf{v}})}{\partial\epsilon} &= 2\rho b\tau g \int_0^T \int_0^{2h} \hat{\theta}b\cos(\theta+\epsilon\hat{\theta}) \\
&\qquad + \hat{u}\cos(\theta+\epsilon\hat{\theta}) - \hat{\theta}(y+u+\epsilon\hat{u})\sin(\theta+\epsilon\hat{\theta})\,dy\,dt \\
\left.\frac{\partial WE_L(\mathbf{v}+\epsilon\hat{\mathbf{v}})}{\partial\epsilon}\right|_{\epsilon=0} &= 2\rho b\tau g \int_0^T \int_0^{2h} \hat{\theta}b\cos\theta + \hat{u}\cos\theta - \hat{\theta}(y+u)\sin\theta\,dy\,dt \\
WE_L^\epsilon &= 2\rho b\tau g \int_0^T \int_0^{2h} \hat{\theta}b\cos\theta + \hat{u}\cos\theta - \hat{\theta}(y+u)\sin\theta\,dy
\end{aligned} \tag{B.3}$$

B.4 Conservation of Energy

The conservation of energy law tells us that if the only forms of energy in this system are kinetic, strain energy and the work energy due to gravity, then their should be no change in energy in the system. In other words

$$0 = \left.\frac{\partial L(\mathbf{v}+\epsilon\hat{\mathbf{v}})}{\partial\epsilon}\right|_{\epsilon=0} = KE_L^\epsilon + WE_L^\epsilon - SE_L^\epsilon \tag{B.4}$$

Choose the element of $\hat{\mathbf{v}}$ from the space of functions $\mathbf{V} = \{V \times \Theta\}$ where

$$V = \left\{L^2(0,2h)\times L^2(0,T)\,|\,\hat{v}(0,t) = \hat{v}(2h,t) = \hat{v}(y,0) = \hat{v}(y,T) = 0\right\} \tag{B.5}$$

$$\Theta = \left\{L^2(0,T)\,|\,\hat{\theta}(0) = \hat{\theta}(T) = 0\right\} \tag{B.6}$$

B.4.1 Change of Variables

The change of variables in Section 4.3.1 considers the total vertical distance that any point on the block experiences. This total vertical displacement is a combination fo the axial deformation and the vertical component of the rocking motion. In this case eq. B.2, B.3 and B.1

are replaced with the following equations in the conservation of energy eq. B.4 in the previous section:

$$KE_L^{\sim\epsilon} = -2\rho b\tau \int_0^T \left[\hat{\theta}\ddot{\theta} \left(\frac{8h^3}{3} + \frac{2b^2 h}{3} \right) + \int_0^{2h} \hat{v}\ddot{v}\, dy \right] dt \tag{B.7}$$

$$WE_L^{\epsilon} = \rho\tau g \int_0^T \hat{\theta} \left[\left(4b^2 h\theta - 4bh^2 - 2b \int_0^{2h} v\, dy \right) \sin\theta \right] + 2b \int_0^{2h} \hat{v} \cos\theta\, dy\, dt \tag{B.8}$$

$$SE_L^{\epsilon} = \frac{Eb\tau}{1-\nu^2} \int_0^T \left[v_y \hat{v} \right]_0^{2h} - \int_0^{2h} \hat{v}\, (v_{yy})\ dy\, dt. \tag{B.9}$$

The conservation of energy tells us that if the only forms of energy in this system are kinetic, strain energy and the work energy due to gravity, then their should be no change in energy in the system, that is

$$0 = \left. \frac{\partial L(\mathbf{v} + \epsilon\hat{\mathbf{v}})}{\partial \epsilon} \right|_{\epsilon=0} = KE_L^{\epsilon} + WE_L^{\epsilon} - SE_L^{\epsilon} \approx KE_L^{\sim\epsilon} + WE_L^{\epsilon} - SE_L^{\epsilon}. \tag{B.10}$$

APPENDIX C. LIPSCHITZ CONDITION

This section 4.6.1, the Lipschitz coefficient for the semilinear PDE is presented. The complete calculation of this coefficient is defined in this section. Consider $\mathbf{u}_1 = \left(\theta,\, \dot{\theta},\, u,\, \dot{u}\right)$ and $\mathbf{u}_2 = \left(\psi,\, \dot{\psi},\, w,\, \dot{w}\right)$ both in V. The constant C that satisfies the condition $||\tilde{f}(\mathbf{u}_1, y) - \tilde{f}(\mathbf{u}_2, y)||_V \leq C||\mathbf{u}_1 - \mathbf{u}_2||_V$ is the Lipschitz coefficient that guarantees the Lipschitz continuity of the semilinear equation $\tilde{A}(y)\dot{\mathbf{v}} = \tilde{L}\mathbf{v} + \tilde{f}(\mathbf{v}, y)$ using eq. 4.35 - 4.37. The only non-zero components of $f = (f_1, f_2, f_3, f_4)$ are the only components that needs to be bounded. Hence the focus of this section is proving the Lipschitz continuity of f_2 and f_4. From equation eq. 4.37,

$$f(\mathbf{u}, y) = \begin{pmatrix} 0 \\ \int_0^{2h} (\dot{\theta})(y+u)\left[\dot{\theta}\left((y+u)^2 + \frac{4b^2}{3}\right) + 2b\dot{u}\right] - g\left[\left((y+u)^2 + \frac{b^2}{3}\right)\cos\theta + b(y+u)\sin\theta\right]\, dy \\ 0 \\ (\dot{\theta})^2(y+u) - g\cos\theta \end{pmatrix} \tag{C.1}$$

$$= \begin{pmatrix} 0 \\ \int_0^{2h} (\dot{\theta})^2(y+u)\left((y+u)^2 + \frac{4b^2}{3}\right) + 2b\dot{\theta}\dot{u}(y+u) - g\left[\left((y+u)^2 + \frac{b^2}{3}\right)\cos\theta + b(y+u)\sin\theta\right]\, dy \\ 0 \\ (\dot{\theta})^2(y+u) - g\cos\theta \end{pmatrix} \tag{C.2}$$

$$f(\mathbf{u}_1, y) - f(\mathbf{u}_2, y) = \begin{pmatrix} 0 \\ \dot{\theta}^2(y+u)\left((y+u)^2 + \frac{4b^2}{3}\right) + 2b\dot{\theta}\dot{u}(y+u) - g\left[\left((y+u)^2 + \frac{b^2}{3}\right)\cos\theta + b(y+u)\sin\theta\right. \\ -\dot{\psi}^2(y+w)\left((y+w)^2 + \frac{4b^2}{3}\right) + 2b\dot{\psi}\dot{w}(y+w) + g\left[\left((y+w)^2 + \frac{b^2}{3}\right)\cos\psi + b(y+w)\sin\right. \\ 0 \\ (\dot{\theta})^2(y+u) - g\cos\theta - (\dot{\psi})^2(y+w) - g\cos\psi \end{pmatrix}$$

$$= \begin{pmatrix} 0 \\ \int_0^{2h} \dot{\theta}^2\left((y+u)^3 - (y+w)^3 + \frac{4b^2}{3}(u-w)\right) + \left((y+w)^3 + \frac{4b^2}{3}(y+w)\right)\left(\dot{\theta}^2 - \dot{\psi}^2\right) \\ +2b\dot{\theta}\left((\dot{u}-\dot{w})(y+u) + \dot{w}(u-w)\right) + 2b\left(\dot{\theta} - \dot{\psi}\right)(y+w)\dot{w} \\ -g\left[\left((y+u)^2 + \frac{b^2}{3}\right)(\cos\theta - \cos\psi) + \left((y+u)^2 - (y+w)^2\right)\cos\psi\right. \\ \left. +b(y+u)(\sin\theta - \sin\psi) + b(u-w)\sin\psi\right]\, dy \\ 0 \\ (\dot{\theta})^2(u-w) + \left(\dot{\theta}^2 - \psi^2\right)(y+u) - g(\cos\theta - \cos\psi) \end{pmatrix}$$

$$
\begin{aligned}
|f_2(\mathbf{u}_1, y) - f_2(\mathbf{u}_2, y)| \leq \int_0^{2h} \Big| & \dot{\theta}^2 \left((y+u)^3 - (y+w)^3 \right) - g \left((y+u)^2 - (y+w)^2 \right) \cos\psi \\
& + (u-w) \left[\frac{4b^2}{3} \dot{\theta}^2 + 2b\dot{\theta}\dot{w} - gb \sin\psi \right] + 2b\dot{\theta} \left(y+u \right) \left(\dot{u} - \dot{w} \right) \\
& + (y+w) \left[\left((y+w)^2 + \frac{4b^2}{3} \right) \left(\dot{\theta} + \dot{\psi} \right) + 2b\dot{w} \right] \left(\dot{\theta} - \dot{\psi} \right) \\
& - g \left[\left((y+u)^2 + \frac{b^2}{3} \right) (\cos\theta - \cos\psi) + b(y+u) \left(\sin\theta - \sin\psi \right) \right] \Big| \, dy
\end{aligned}
$$

$$
\begin{aligned}
\leq \int_0^{2h} & \left| \dot{\theta}^2 \right| \left| (y+u)^3 - (y+w)^3 \right| - g \left| (y+u)^2 - (y+w)^2 \right| |\cos\psi| \\
& + |u-w| \left| \frac{4b^2}{3} \dot{\theta}^2 + 2b\dot{\theta}\dot{w} - gb \sin\psi \right| + 2b \left| \dot{\theta} \right| |y+u| \, |\dot{u} - \dot{w}| \\
& + |y+w| \left| \left((y+w)^2 + \frac{4b^2}{3} \right) \left(\dot{\theta} + \dot{\psi} \right) + 2b\dot{w} \right| \left| \dot{\theta} - \dot{\psi} \right| \\
& + g \left[\left| (y+u)^2 + \frac{b^2}{3} \right| |\cos\theta - \cos\psi| + b \, |y+u| \, |\sin\theta - \sin\psi| \right] \, dy
\end{aligned}
$$

$$
\begin{aligned}
\leq & \left| \dot{\theta}^2 \right| \int_0^{2h} \left| (y+u)^3 - (y+w)^3 \right| \, dy - g \int_0^{2h} \left| (y+u)^2 - (y+w)^2 \right| \, dy \, |\cos\psi| \\
& + \int_0^{2h} |u-w| \left| \frac{4b^2}{3} \dot{\theta}^2 + 2b\dot{\theta}\dot{w} - gb \sin\psi \right| \, dy + 2b \left| \dot{\theta} \right| \int_0^{2h} |y+u| \, |\dot{u} - \dot{w}| \, dy \\
& + \int_0^{2h} |y+w| \left| \left((y+w)^2 + \frac{4b^2}{3} \right) \left(\dot{\theta} + \dot{\psi} \right) + 2b\dot{w} \right| \, dy \left| \dot{\theta} - \dot{\psi} \right| \\
& + g \left[\int_0^{2h} \left| (y+u)^2 + \frac{b^2}{3} \right| \, dy \, |\cos\theta - \cos\psi| + b \int_0^{2h} |y+u| \, dy \, |\sin\theta - \sin\psi| \right]
\end{aligned}
$$

$$
\begin{aligned}
|f_2(\mathbf{u}_1,y)-f_2(\mathbf{u}_2,y)| \le{}& \left|\dot\theta^2\right| \int_0^{2h} c_3\,|u-w|\;dy - g\int_0^{2h} c_2\,|u-w|\;dy \\
&+ \int_0^{2h} |u-w|\;dy \left(\int_0^{2h} \frac{4b^2}{3}\left|\dot\theta^2\right| + 2b\left|\dot\theta\dot w\right| + gb\,|\sin\psi|\;dy\right) + 2b\left|\dot\theta\right| \int_0^{2h} |y+u|\,|\dot u-\dot w| \\
&+ \left(\int_0^{2h} |y+w|\;dy\right)\left|\left((y+w)^2+\frac{4b^2}{3}\right)\left(\dot\theta+\dot\psi\right)+2b\dot w\right|\;dy\left|\dot\theta-\dot\psi\right| \\
&+ g\left[\int_0^{2h}\left|(y+u)^2+\frac{b^2}{3}\right|\;dy\,|\cos\theta-\cos\psi| + b\int_0^{2h}|y+u|\;dy\,|\sin\theta-\sin\psi|\right]
\end{aligned}
$$

$$
\begin{aligned}
\le{}& \left[\left(c_3+\frac{8b^2h}{3}\right)\left|\dot\theta\right|^2 - gc_2 + 2b\left|\dot\theta\right|\int_0^{2h}|\dot w|\;dy + 2gbh\right]\int_0^{2h}|u-w|\;dy \\
&+ 4bh\left|\dot\theta\right|\int_0^{2h}|y+w|\;dy\int_0^{2h}|\dot u-\dot w|\;dy \\
&+ \left(\int_0^{2h}|y+w|\;dy\right)\left(\int_0^{2h}\left|(y+w)^2+\frac{4b^2}{3}\right|\left|\dot\theta+\dot\psi\right|+2b\,|\dot w|\;dy\right)\left|\dot\theta-\dot\psi\right| \\
&+ g\left[\int_0^{2h}\left|(y+u)^2+\frac{b^2}{3}\right|\;dy + b\int_0^{2h}|y+u|\;dy\right]|\theta-\psi|
\end{aligned}
$$

where c_k is the local Lipschitz constant of the function $f(p)=p^k$ for $f: H^2_{\Gamma_0}(\Omega)\to\mathbb{R}$. The initial energy in the system, $E_0 = WR\cos(\theta_0-\alpha)$ is constant, therefore at any given time the energy in the system is the sum of the kinetic, strain and work energy. Then for

$$
\begin{aligned}
E(t) = {}& \left(\frac{1}{2}I_0+\rho\tau b\int_0^{2h}2yu+u^2\,dy\right)\dot\theta^2 + \rho b\tau\int_0^{2h}2\dot\theta\dot u+\dot u^2\,dy + \frac{Eb\tau}{(1-\nu^2)}\int_0^{2h}u_y^2\,dy \\
&+ WR\left[cos\left(\theta_0-\alpha\right)-\cos\left(\theta-\alpha\right)\right] + 2\omega\tau R\sin\alpha\cos\theta\int_0^{2h}u\,dy,
\end{aligned}
$$

where ω is the weight per unit volume, the angular speed is always bounded by E_0. Similarly, $\dot u^2$, u, $y+u$, $(y+u)^2$ and u^2 are also bounded by the initial energy. The vibrations, u, are an order of magnitude 10^{-3} smaller than the height y so we approximate the quantity $y+u\approx y$ then $y+u\le y+c_0$.

$$
\int_0^{2h}|y+u|\;dy \le \int_0^{2h}|y|+c_0\,dy = 2h^2+2hc_0
$$

$$
\begin{aligned}
\int_0^{2h}\left|(y+u)^2+\frac{b^2}{3}\right|\;dy &\le \int_0^{2h}\left|(y+u)^2\right|+\frac{b^2}{3}\,dy \le ||y+u||^2_{L^2(0,2h)}+\frac{2b^2h}{3} \le ||y||^2_{L^2(0,2h)}+||c_0||^2_{L^2(0,2h)}+\frac{2b^2h}{3} \\
&= \frac{8h^3}{3}+\frac{2b^2h}{3}+2h\,|c_0|^2
\end{aligned}
$$

and hence,

$$
\begin{aligned}
|f_2(\mathbf{u}_1, y) - f_2(\mathbf{u}_2, y)| \leq & \left[\left(c_3 + \frac{8b^2h}{3}\right)\left|\dot{\theta}\right|^2 + gc_2 + 2b\left|\dot{\theta}\right|\int_0^{2h}|\dot{w}|\ dy + 2gbh\right]\int_0^{2h}|u-w|\ dy \\
& + 4bh\left|\dot{\theta}\right|\left(2h^2 + 2hc_0\right)\int_0^{2h}|\dot{u}-\dot{w}|\ dy \\
& + \left(2h^2 + 2hc_0\right)\left(\left(\frac{8h^3}{3} + \frac{2b^2h}{3} + 2h\,|c_0|\right)\int_0^{2h}\left|\dot{\theta}+\dot{\psi}\right|\ dy + 2b\int_0^{2h}|\dot{w}|\ dy\right)\left|\dot{\theta}-\dot{\psi}\right| \\
& + g\left[\left(\frac{8h^3}{3} + \frac{2b^2h}{3} + 2h\,|c_0|\right) + b\left(2h^2 + 2hc_0\right)\right]|\theta - \psi| \\
\\
\leq & \left[\left(c_3 + \frac{8b^2h}{3}\right)E_0 + gc_2 + 2bE_0^2 + 2gbh\right]\int_0^{2h}|u-w|\ dy \\
& + 4bhE_0\left(2h^2 + 2hc_0\right)\int_0^{2h}|\dot{u}-\dot{w}|\ dy \\
& + \left(2h^2 + 2hc_0\right)\left(\left(\frac{8h^3}{3} + \frac{2b^2h}{3} + 2h\,|c_0|\right)E_0 + 2bE_0\right)\left|\dot{\theta}-\dot{\psi}\right| \\
& + g\left[\left(\frac{8h^3}{3} + \frac{2b^2h}{3} + 2h\,|c_0|\right) + b\left(2h^2 + 2hc_0\right)\right]|\theta - \psi| \\
\\
\leq & \ 4c_{\max}\left(||u-w||_{L^1(0,2h)} + ||\dot{u}-\dot{w}||_{L^1(0,2h)} + \left|\dot{\theta}-\dot{\psi}\right| + |\theta-\psi|\right) \\
\leq & \ 4c_{\max}\left(2h\,||u-w||_{\infty} + 2h\,||\dot{u}-\dot{w}||_{\infty} + \left|\dot{\theta}-\dot{\psi}\right| + |\theta-\psi|\right) \\
\leq & \ C_1\,||\mathbf{u}_1 - \mathbf{u}_2||_V\,.
\end{aligned}
$$

The terms in f_4 are bounded by the totally energy of the system as follows:

$$
\begin{aligned}
\left|(\dot{\theta})^2(u-w)\right| &\leq \left|\dot{\theta}\right|^2|u-w| \leq E_0\,|u-w| \\
\left|\left(\dot{\theta}^2 - \psi^2\right)(y+u)\right| &\leq \left|\dot{\theta}-\psi\right|\left|\dot{\theta}+\psi\right||y+u| \leq 2E_0\left|\dot{\theta}-\psi\right|
\end{aligned}
$$

then for f,

$$
\begin{aligned}
||f_4(\mathbf{u}_1, y) - f_4(\mathbf{u}_2, y)||^2_{L^2(\Omega)} &= \left|\left|(\dot{\theta})^2(u-w) + \left(\dot{\theta}^2 - \dot{\psi}^2\right)(y+u) - g\left(\cos\theta - \cos\psi\right)\right|\right|^2_{L^2(\Omega)} \\
&\leq \left|\left|(\dot{\theta})^2(u-w)\right|\right|^2_{L^2(\Omega)} + \left|\left|\left(\dot{\theta}^2 - \dot{\psi}^2\right)(y+u)\right|\right|^2_{L^2(\Omega)} + g\,||\cos\theta - \cos\psi||^2_{L^2(\Omega)} \\
&\leq \left|\dot{\theta}\right|^2||u-w||^2_{L^2(\Omega)} + \left|\dot{\theta}^2 - \dot{\psi}^2\right|^2||y+u||^2_{L^2(\Omega)} + 2gh\,|\cos\theta - \cos\psi|^2 \\
&\leq E_0\,||u-w||^2_{L^2(\Omega)} + 4E_0^2\left|\dot{\theta}-\dot{\psi}\right|^2 + 2gh\,|\theta-\psi|^2 \\
&\leq C_2\,||\mathbf{u}_1 - \mathbf{u}_2||_V\,,
\end{aligned}
$$

where $C_2 = \max(E_0, E_0^2, 2gh)$. Then we have $||f(\mathbf{u}_1, y) - f(\mathbf{u}_2, y)||_V \leq C||\mathbf{u}_1 - \mathbf{u}_2||_V$ with $C = \max(C_1, C_2)$.

APPENDIX D. IMPACT SPEED

The equation for the impact speed $\dot{\theta}_1^2$ in eq. 4.12 in Section 4.2.1 is a result of the change in energy at the instant impact begins. At this moment, there is no strain energy and the change in the work energy from t_0 to t_1 is equivalent to the change in kinetic energy. The detailed calculation using the equivalent forms of energy is shown below:

$$
\begin{aligned}
\Delta WE &= \Delta KE \\
WE_0 - WE_1 &= KE_0 - KE_1 \\
4\rho\tau g\left(bh^2 - \left[b^2 h\sin\theta_0 + bh^2\cos\theta_0\right]\right) &= \rho\tau\dot{\theta}_1^2\left(\frac{16bh^3}{3} + \frac{16b^3h}{3}\right) \\
4\rho bh\tau g\left(h[1-\cos\theta_0] - b\sin\theta_0\right) &= \rho bh\tau\dot{\theta}_1^2\left(\frac{16h^2}{3} + \frac{16b^2}{3}\right) \\
\dot{\theta}_1^2 &= \frac{4g}{\left(\frac{16h^2}{3} + \frac{16b^2}{3}\right)}\left(h[1-\cos\theta_0] - b\sin\theta_0\right) \\
&= \frac{3g}{4\left(b^2+h^2\right)}\left(h[1-\cos\theta_0] - b\sin\theta_0\right) \\
&= \frac{3g}{4\sqrt{b^2+h^2}}\left(\cos\alpha - \cos(\alpha-\theta_0)\right) \\
&= \frac{3g}{4R}\left(\cos\alpha - \cos(\alpha-\theta_0)\right) \\
\dot{\theta}_1^2 &= \frac{WR}{I_0}\left(\cos\alpha - \cos(\alpha-\theta_0)\right) \qquad \text{(D.1)}
\end{aligned}
$$

where the geometric constants W, R, and I_0 are defined in Section 2.2.1 for eq. 2.1. The alternative approach for calculating $\dot{\theta}^2$ described in Remark 4.2.1 is shown in the steps below for non-zero initial speed, $\dot{\theta}_0$:

$$
\begin{aligned}
I_0 \dot{\theta} \ddot{\theta} &= WR\,\dot{\theta} \sin(\alpha - \theta) \\
\frac{d}{dt}\left(\frac{I_0 \dot{\theta}^2}{2}\right) &= WR\,\frac{d\left(\cos(\alpha - \theta)\right)}{dt} \\
\int_{\dot{\theta}_0}^{\dot{\theta}_1} d\left(\frac{I_0 \dot{\theta}^2}{2}\right) &= WR \int_{\theta_0}^{0} d\left(\cos(\alpha - \theta)\right) \\
I_0\left(\frac{\dot{\theta}_1^2 - \dot{\theta}_0^2}{2}\right) &= WR\left(\cos\alpha - \cos(\alpha - \theta_0)\right) \\
\dot{\theta}_1^2 &= \dot{\theta}_0^2 + \frac{WR}{I_0}\left(\cos\alpha - \cos(\alpha - \theta_0)\right).
\end{aligned}
$$

APPENDIX E. SPEED AFTER IMPACT

Immediately after impact, the strain energy is not zero and contributes to the rotational speed of the block. The speed after impact relies on the amount of vibration energy generated during impact. The SE, KE and WE in the SFRM are defined by eq. 4.2, 4.3, and 4.4 for any time, t as

$$SE = \frac{Eb\tau}{1-\mu^2}\int_0^{2h} (u_y)^2 \, dy \tag{4.2}$$

$$KE = \rho b\tau \int_0^{2h} \left(\dot{\theta}(y+u)\right)^2 + \left(\dot{\theta}b + \dot{u}\right)^2 + \frac{b^2}{3}\left(\dot{\theta}\right)^2 dy \tag{4.3}$$

$$WE = \rho\tau g\left[4b^2h\sin\theta + 4bh^2\cos\theta + 2b\int_0^{2h} u\cos\theta\, dy\right]. \tag{4.4}$$

After changing the energy equations to reflect the total displacement, $v \approx u + b\theta$, described in Section 4.3.1 for any point on the rocking block, the SE, KE and WE in the are defined by eq. 4.14, 4.15, and 4.16, assuming u is small, as

$$SE = \frac{Eb\tau}{1-\mu^2}\int_0^{2h} (v_y)^2 \, dy \tag{4.14}$$

$$\begin{aligned} KE &\approx \rho b\tau \int_0^{2h} \left(\dot{\theta}y\right)^2 + (\dot{v})^2 + \frac{b^2}{3}\dot{\theta}^2\, dy \\ &= \rho b\tau\left[\dot{\theta}^2\left(\frac{8h^3}{3} + \frac{2b^2h}{3}\right) + \int_0^{2h} (\dot{v})^2 \, dy\right] \end{aligned} \tag{4.15}$$

$$WE = \rho\tau g\left[4b^2h\sin\theta + (4bh^2 - 4b^2h\theta)\cos\theta + 2b\int_0^{2h} v\cos\theta\, dy\right]. \tag{4.16}$$

At the instant before impact, $\theta = 0$, $\dot{\theta} = \dot{\theta}_1$ and there are no longitudinal waves. Therefore $SE = 0$ and the kinetic energy is

$$KE = \rho b\tau \int_0^{2h} \left(\dot{\theta}y\right)^2 + \left(\dot{\theta}_1 b\right)^2 + \frac{b^2}{3}\dot{\theta}^2\, dy = \rho\tau\dot{\theta}_1^2\left(\frac{8bh^3}{3} + \frac{8b^2h}{3}\right). \tag{E.1}$$

The kinetic energy immediately before impact is a function of the block speed at impact. The rotational impact speed, the block speed and the kinetic energy are shown below in Table E.2

for initial drift values $\theta_0 = 1\% - 3\%$:

$\theta_0\%$	$\dot{\theta}_1$ (rad/s)	μ (in/s)	KE (kip-in)
0.01	0.186577	1.30604	0.091464
0.02	0.260649	1.82454	0.178503
0.03	0.315242	2.20669	0.261108.

(E.2)

The work energy due to gravity at the instant before impact is the constant

$$W = \rho\tau g\left[4bh^2 + 2b\int_0^{2h} b\theta\, dy\right] = 4\rho bh^2\tau g = 40.26 \text{ k-in.}$$

Immediately after impact, the speed of the block is combination of the rotational speed, $\dot{\theta}_2$, of the block and the speed of the internal deformations within the block. These speeds are represent in the energy equations in eq. 4.14 - 4.16 :

$$\begin{aligned}
SE &= \frac{Eb\tau}{1-\mu^2}\int_0^{2h}\left(v_y(y,t_{\text{sep}})\right)^2\, dy \\
KE &\approx \rho b\tau\int_0^{2h}\left(\dot{\theta}_2 y\right)^2 + \left(\dot{v}(y,t_{\text{sep}})\right)^2 + \frac{b^2}{3}\dot{\theta}_2^2\, dy \\
&= \rho\tau\left[\dot{\theta}_2^2\left(\frac{8bh^3}{3}+\frac{2b^3h}{3}\right) + b\int_0^{2h}\left(\dot{v}(y,t_{\text{sep}})\right)^2\, dy\right] \\
WE &= \rho\tau g\left[4bh^2 + 2b\int_0^{2h} v(y,t_{\text{sep}})\, dy\right].
\end{aligned}$$

The total energy before and the total energy after impact must be equivalent and hence

$$0 = \Delta SE + \Delta KE + \Delta WE \tag{E.3}$$

where

$$\Delta SE = \frac{Eb\tau}{1-\mu^2}\int_0^{2h}\left(v_y(y,t_{\text{sep}})\right)^2\, dy \tag{E.4}$$

$$\begin{aligned}
\Delta KE &= \rho\tau\left[\dot{\theta}_2^2\left(\frac{8bh^3}{3}+\frac{2b^3h}{3}\right) + b\int_0^{2h}\left(\dot{v}(y,t_{\text{sep}})\right)^2\, dy\right] - \rho\tau\dot{\theta}_1^2\left(\frac{8bh^3}{3}+\frac{8b^2h}{3}\right) \\
&= \rho\tau\left[\left(\dot{\theta}_2^2-\dot{\theta}_1^2\right)\left(\frac{8bh^3}{3}+\frac{8b^2h}{3}\right) - \dot{\theta}_2^2\frac{6b^2h}{3} + b\int_0^{2h}\left(\dot{v}(y,t_{\text{sep}})\right)^2\, dy\right]
\end{aligned} \tag{E.5}$$

$$\Delta WE = 2\rho b\tau g\int_0^{2h} v(y,t_{\text{sep}})\, dy. \tag{E.6}$$

Substituting eq. E.4 - E.6 into eq. E.3,

$$0 = \frac{Eb\tau}{1-\mu^2}\int_0^{2h}(v_y)^2\, dy + \rho\tau\left[\dot{\theta}_2^2\left(\frac{8bh^3}{3}+\frac{2b^3h}{3}\right) + b\int_0^{2h}(\dot{v})^2\, dy\right] - \rho\tau\dot{\theta}_1^2\left(\frac{8bh^3}{3}+\frac{8b^2h}{3}\right) + 2\rho b\tau g\int_0^{2h} v\, dy \tag{E.7}$$

and solving eq. E.7 for $\dot{\theta}_2^2$,

$$\dot{\theta}_2^2 = -\left(\frac{\frac{Eb}{\rho(1-\nu^2)} \int_0^{2h} (v_y)^2 \, dy + b \int_0^{2h} (\dot{v})^2 \, dy - \dot{\theta}_1^2 \left(\frac{8bh^3}{3} + \frac{8b^2h}{3} \right) + 2bg \int_0^{2h} v \, dy}{\left(\frac{8bh^3}{3} + \frac{2b^3h}{3} \right)} \right). \tag{E.8}$$

The explicit definition of $\dot{\theta}_2^2$ requires information from the total displacement v is defined by eq. 4.23 in Section 4.3.2. At the separation time, eq. 4.23 is

$$v = \begin{cases} \text{Region 1}: & \dot{\theta}_1 bt - \frac{gt^2}{2} \\ \text{Region 2}: & \frac{\dot{\theta}_1 by}{c} + g\left(\frac{y^2}{2c^2} - \frac{ty}{c} \right) \\ \text{Region 3}: & \dot{\theta}_1 bt - \frac{gt^2}{2} \\ \text{Region 4}: & \frac{\dot{\theta}_1 by}{c} + g\left(\frac{y^2}{2c^2} - \frac{ty}{c} \right) \\ \text{Region 5}: & \frac{\dot{\theta}_1 by}{c} + g\left(\frac{y^2}{2c^2} - \frac{ty}{c} \right) \\ \text{Region 6}: & \frac{4\dot{\theta}_1 bh}{c} - \dot{\theta}_1 bt + g\left(\frac{8h^2}{c^2} - \frac{4hy}{c^2} + \frac{y^2}{c^2} - \frac{4ht}{c} + \frac{t^2}{2} \right) \\ \text{Region 7}: & \frac{4\dot{\theta}_1 bh}{c} - \dot{\theta}_1 bt + g\left(\frac{8h^2}{c^2} - \frac{4hy}{c^2} + \frac{y^2}{c^2} - \frac{4ht}{c} + \frac{t^2}{2} \right) \\ \text{Region 8}: & g\left(\frac{16h^2}{c^2} - \frac{4hy}{c^2} + \frac{y^2}{2c^2} + t\left(\frac{y}{c} - \frac{4h}{c} \right) \right) - \frac{\dot{\theta}_1 by}{c}. \end{cases} \tag{E.9}$$

The total displacement, speed, and curvature for any point along the block are

$$v(y, t_{\text{sep}}) = -\frac{g}{2c} \left(2y \left(\frac{4h - y}{c} - \frac{y}{c} \right) + \frac{2y^2}{c} \right) \tag{E.10}$$

$$\dot{v}(y, t_{\text{sep}}) = -\dot{\theta}_1 b \tag{E.11}$$

$$v_y(y, t_{\text{sep}}) = \frac{g}{c} \left(\frac{4h - y}{c} - \frac{y}{c} \right). \tag{E.12}$$

and their respective integrals over the entire height of the block are

$$\int_0^{2h} v(y, t_{\text{sep}}) \, dy = -\frac{16gh^3}{3c^2} \tag{E.13}$$

$$\int_0^{2h} \dot{v}(y, t_{\text{sep}})^2 \, dy = 4b^2 h \dot{\theta}_1^2 \tag{E.14}$$

$$\int_0^{2h} v_y(y, t_{\text{sep}})^2 \, dy = \frac{32g^2h^3}{3c^4}. \tag{E.15}$$

The speed after impact in eq. E.8 with eq. E.10 - E.15 is

$$\dot{\theta}_2^2 = \left(\frac{4gh}{c} \right)^2 \left(\frac{hg}{b} \right) \left(\frac{\rho\tau - 1}{W} \right) + \dot{\theta}_1^2 \left(\left(\frac{1}{2} \right)^2 + \left(\frac{h}{b} \right)^2 \right) \tag{E.16}$$

E.1 Coefficient of Restitution

The energy of the block immediately after impact with the foundation is the sum of the vibration energy and the residual rigid energy.

$$E_{\text{Before}} = E_{\text{After}} = E_{\text{vibration}} + E_{\text{rigid after}}. \tag{E.17}$$

The internal block deformation is the only contributor to the vibration energy in the SFRM. This vibration energy, E_{vib} defined in eq. 4.28, is the only portion of the energy after impact that is not considered rigid energy. The rigid energy in the block after impact is assumed to be any energy that does not have a component from the block deformations. The internal displacement defined by eq. E.9, initial drift values between $1 \sim 3\%$, and the properties of the block 5.1 and 5.2 used in (11), define the vibration energy of the system immediately after impact. The following table lists the amount of vibration energy and the percentage of the total energy that is accounted for by the vibration energy:

$\theta_0\%$	E_{Before}	E^b_{vib}	$E^b_{\text{vib}}\%$
1.	40.3434	2.87008	7.11413
2.	40.4227	2.84907	7.04818
3.	40.498	2.82919	6.986.

(E.18)

The coefficient of restitution that is defined by the portion of kinetic energy retained by the system is a useful measure for comparing the SRM, SFRM and the modified SRM. The COR_{SFRM} is defined by the square of the ratio of the speed immediately after impact with the speed immediately before impact defined in eq. 4.29. This COR is assumed to represent the amount of energy that is retained in the system after the internal deformations resulting from impact. An entire rocking response for the SFRM is created using the iterative approach described in Section 5.1 (see Figure 5.8).

APPENDIX F. D'ALEMBERT'S FORMULA INTEGRATION CALCULATIONS

The second equation in (4.5) in Section 4.1 can be rewritten so that the wave operator in eq. 4.6 is on the left hand side of the equation and all the other nonlinear terms are on the right hand side of the equation:

$$\begin{cases} \ddot{u} - \tilde{E}u_{yy} = f(u,y,t) & \text{in } (0,2h)\times(0,\infty) \\ u = u_0,\ u_t = -2\mu & \text{in } (0,2h)\times\{t=0\}, \\ u(0) = 0,\ u_y(2h) = 0 & \text{in } (0,\infty) \end{cases} \tag{F.1}$$

where

$$\tilde{E} = \frac{E}{\rho(1-\nu^2)}, \tag{F.2}$$

$$f(u,y,t) = \gamma(y+u) - \beta, \tag{F.3}$$

$$\gamma = \dot{\theta}^2 \tag{F.4}$$

$$\beta = \ddot{\theta}b + g\cos\theta. \tag{F.5}$$

This equation represents the axial deformations within the block in the SFRM system with known constants $\dot{\theta}(t_0) =: \dot{\theta}_1$ and $\ddot{\theta}(t_0) =: \ddot{\theta}_1$ from eq. 2.1. The integrations that are required to use D'Alembert's formula to solve the nonlinear wave equation

$$\begin{cases} \ddot{u} - \tilde{E}u_{yy} = f(u,y,t) & \text{in } (0,2h)\times(0,\infty) \\ u = 0,\ u_t = -2\mu & \text{in } (0,2h)\times\{t=0\}, \\ u(0) = 0,\ u_y(2h) = 0 & \text{in } (0,\infty) \end{cases} \tag{F.6}$$

where

$$\tilde{E} = \frac{E}{\rho(1-\nu^2)}, \tag{F.7}$$

$$f(u,y,t) = \gamma(y+u) - \beta, \tag{F.8}$$

$$\gamma = \dot{\theta}_1^2 \tag{F.9}$$

$$\beta = \ddot{\theta}_1 b + g. \tag{F.10}$$

is outlined in this appendix.

F.1 Integrating 1^e

In order to solve eq. F.6, the datum for the problem–the nonlinear right hand side, the initial conditions, and the boundary conditions—must be extended as described in Section 4.3.2. The extension of the unit function is

$$1^e = \begin{cases} \vdots & \\ -1 & 2L \le y \le 4L \\ 1 & 0 \le y \le 2L \\ -1 & -2L \le y \le 0 \\ \vdots & \end{cases} \tag{F.11}$$

and the regions in Figure 4.3 that share the same integrand are regions 1 & 3, bounded above by $t = \frac{y}{c}$ and $t = \frac{4h-y}{c}$ for $0 \le y \le 4h$, regions 2, 4, & 5, bounded below by $t = \frac{y}{c}$ and above by $t = \frac{4h-y}{c}$ for $-4h \le y \le 2h$, and regions 6 & 7, bounded below by $t = \frac{y}{c}$ and $t = \frac{4h-y}{c}$ and above by $t = \frac{4h+y}{c}$ and $t = \frac{8h-y}{c}$ for $-4h \le y \le 6h$. For the unit function,

$$1^e = \begin{cases} \vdots & \\ -1 & 2L \le y \le 4L \\ 1 & 0 \le y \le 2L \\ -1 & -2L \le y \le 0 \\ \vdots & \end{cases} \tag{F.12}$$

the regions that share the same integrand are regions 1 & 3, bounded above by $t = \frac{y}{c}$ and $t = \frac{4h-y}{c}$ for $0 \le y \le 4h$, regions 2, 4, & 5, bounded below by $t = \frac{y}{c}$ and above by $t = \frac{4h-y}{c}$

for $-4h \leq y \leq 2h$, and regions 6 & 7, bounded below by $t = \frac{y}{c}$ and $t = \frac{4h-y}{c}$ and above by $t = \frac{4h+y}{c}$ and $t = \frac{8h-y}{c}$ for $-4h \leq y \leq 6h$.

1. Regions 1 & 3:

$$\int_0^t \int_{y-c(t-s)}^{y+c(t-s)} 1^e \, dx \, ds = \int_0^t 2c(t-s) \, ds = -c(t-s)^2 \Big|_0^t = ct^2$$

2. Regions 2,4, & 5:

   Define $t_0 = t - \frac{y}{c}$ as the time where the line $s = \frac{x-(y-ct)}{c}$, from the point (y,t) in the region to the point $y - ct$ on the x-axis, crosses the s-axis from a point (y, t) in the region.

$$\begin{aligned}
\int_0^t \int_{y-c(t-s)}^{y+c(t-s)} 1^e \, dx \, ds &= \int_0^{t_0} \int_{y-c(t-s)}^{y+c(t-s)} 1^e \, dx \, ds + \int_{t_0}^t \int_{y-c(t-s)}^{y+c(t-s)} 1^e \, dx \, ds \\
&= \int_0^{t_0} \int_{y-c(t-s)}^{c(t-s)-y} 1^e \, dx + \int_{c(t-s)-y}^{y+c(t-s)} 1^e \, dx \, ds + \int_{t_0}^t \int_{y-c(t-s)}^{y+c(t-s)} 1^e \, dx \, ds \\
&= ct^2 - \frac{(y-ct)^2}{c}
\end{aligned}$$

3. Regions 6 & 7:

   Define $t_1 = t + \frac{y-2L}{c}$ as the time on the line $s = \frac{(y+ct)-x}{c}$, from the point (y, t) to the point $y + ct$ on the x-axis, when $x = 2L$.

$$\begin{aligned}
\int_0^t \int_{y-c(t-s)}^{y+c(t-s)} 1^e \, dx \, ds &= \int_0^{t_1} \int_{y-c(t-s)}^{y+c(t-s)} 1^e \, dx \, ds + \int_{t_1}^{t_0} \int_{y-c(t-s)}^{y+c(t-s)} 1^e \, dx \, ds + \int_{t_0}^t \int_{y-c(t-s)}^{y+c(t-s)} 1^e \, dx \, ds \\
&= \int_0^{t_1} \int_{y-c(t-s)}^{2L-(y+c(t-s)-2L)} 1^e \, dx + \int_{2L-(y+c(t-s)-2L)}^{y+c(t-s)} 1^e \, dx \, ds \\
&\quad + \int_{t_1}^{t_0} \int_{y-c(t-s)}^{c(t-s)-y} 1^e \, dx + \int_{c(t-s)-y}^{y+c(t-s)} 1^e \, dx \, ds + \int_{t_0}^t \int_{y-c(t-s)}^{y+c(t-s)} 1^e \, dx \, ds \\
&= \frac{4L(2L-(y+ct))}{c} - \frac{(2L-y)^2}{c} + \frac{(ct)^2}{c} + \frac{4y(L-y)}{c} + \frac{y^2}{c}
\end{aligned}$$

F.2 Integrating y^e

The integration of the identity function over the different regions follows the same procedure as the unity function over with different regions. In this case, regions 1 & 2, bounded above by $t = \frac{2h-y}{c}$ and $t = \frac{2h+y}{c}$ for $-2h \leq y \leq 2h$, regions 3, 4, & 6, bounded below by $t = \frac{2h-y}{c}$ and above by $t = \frac{2h+y}{c}$ for $-2h \leq y \leq 6h$, and regions 5 & 7, bounded below by $t = \frac{2h+y}{c}$ and above by $t = \frac{6h-y}{c}$ for $-4h \leq y \leq 6h$.

1. Regions 1 & 2:

$$\int_0^t \int_{y-c(t-s)}^{y+c(t-s)} x^e \, dx \, ds = \int_0^t \frac{(y+c(t-s))^2}{2} - \frac{(y-c(t-s))^2}{2} \, ds = \int_0^t 2yc(t-s) \, ds = -yc(t-s)^2\Big|_0^t = yct$$

2. Regions 3,4, & 6:

   Define $t_0 = t + \frac{y-L}{c}$ as the time on the line $s = -\frac{x-(y+ct)}{c}$, emanating from a point (y,t) in the region, when $x = L$.

$$\begin{aligned}
\int_0^t \int_{y-c(t-s)}^{y+c(t-s)} x^e \, dx \, ds &= \int_0^{t_0} \int_{y-c(t-s)}^{y+c(t-s)} x^e \, dx \, ds + \int_{t_0}^t \int_{y-c(t-s)}^{y+c(t-s)} x^e \, dx \, ds \\
&= \int_0^{t_0} \int_{y-c(t-s)}^{L} x \, dx + \int_L^{y+c(t-s)} 2L - x \, dx \, ds + \int_{t_0}^t \int_{y-c(t-s)}^{y+c(t-s)} x \, dx \, ds \\
&= \frac{(L-(y+ct))^3}{3c} + yct^2
\end{aligned}$$

3. Regions 5 & 7:

   Define $t_1 = t - \frac{y+L}{c}$ as the time on the line $s = \frac{x-(y-ct)}{c}$, emanating from a point (y,t) in the region, when $x = -L$.

$$\begin{aligned}
\int_0^t \int_{y-c(t-s)}^{y+c(t-s)} x^e \, dx \, ds &= \int_0^{t_1} \int_{y-c(t-s)}^{y+c(t-s)} x^e \, dx \, ds + \int_{t_1}^{t_0} \int_{y-c(t-s)}^{y+c(t-s)} x^e \, dx \, ds + \int_{t_0}^{t} \int_{y-c(t-s)}^{y+c(t-s)} x^e \, dx \, ds \\
&= \int_0^{t_1} \int_{y-c(t-s)}^{-L} -2L - x \, dx + \int_L^{-L} x \, dx + \int_L^{y+c(t-s)} 2L - x \, dx \, ds \\
&\quad + \int_{t_1}^{t_0} \int_{y-c(t-s)}^{L} x \, dx + \int_L^{y+c(t-s)} 2L - x \, dx \, ds + \int_{t_0}^{t} \int_{y-c(t-s)}^{y+c(t-s)} x \, dx \, ds \\
&= \frac{(L-(y+ct))^3}{6c} - \frac{(L+(y-ct))^3}{6c} - \frac{(2y)^3}{6c} + 2Lytcy(L+y)(L-y)c.
\end{aligned}$$

APPENDIX G. MODEL COMPARISON

This section details the calculations that determine the rocking response from the experimental data in (11) discussed in 5.2.1. Each pictured captured by the LED camera recorded the (x,y,z) position of each of the eight sensors on the block (see Figure 5.9). The rocking response in (11) is measured by the angle between the block and the foundation. The angle between the foundation and the rocking block, shown in the rocking response in Figure 5.10, was determined by comparing the change in position of Sensors 5 and 8. Figure G.1 shows how the difference in the measured x and y coordinates, respectively, are related to the angular rotation, ϕ. The angle ϕ_0 is the angle of the line through the two sensors with the vertical side of the block. The angle ϕ is the angle between the line through the two sensors and the vertical axis. The angular displacement θ is the difference between ϕ and ϕ_0. These angles are labeled in figure G.2. θ is shown in figure 5.10 for all six tests.

Remark G.0.1. *Any two sensors could have been used to create this response. The two sensors at the bottom of the block were arbitrarily chosen*

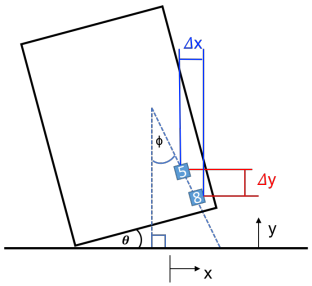

Figure G.1: Schematic diagram of angles to find ϕ

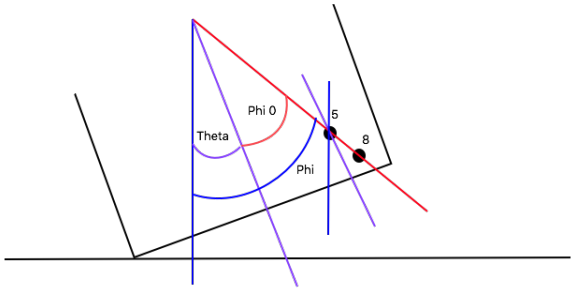

Figure G.2: Schematic diagram of angles to find θ

Table G.1: Comparison of speed before and after the first impact of the rocking response.

$\theta_0\%$	$\dot{\theta}_{1_{\text{SRM}}}$	$\dot{\theta}_{1_{\text{Mod SRM}}}$	$\dot{\theta}_{1_{\text{SFRM}}}$	$\dot{\theta}_{2_{\text{SRM}}}$	$\dot{\theta}_{2_{\text{Mod SRM}}}$	$\dot{\theta}_{2_{\text{SFRM}}}$
1.	0.187227	0.187227	0.186577	0.175134	0.180859	0.177036
2.	0.261514	0.261514	0.260649	0.244624	0.25262	0.247711
3.	0.316239	0.316239	0.315242	0.295814	0.305484	0.299751
4.	0.360426	0.360426	0.359341	0.337147	0.348167	0.341772
5.	0.397603	0.397603	0.396461	0.371923	0.38408	0.377135

G.1 Speed at First Impact

The speed at the first impact, $\dot{\theta}_1$ and the speed directly after the first impact (equivalent to the speed at the second impact), $\dot{\theta}_2$ for initial drift values from $\%1 - \%5$ are shown below in Table G.1 for the SRM, SFRM, and modified SRM.

G.2 Rocking Responses for the SRM, SFRM and Modified SRM

The six experimental tests conducted in (11) consisted of one test with a 1 % initial drift; two tests with 2% initial drift; and three tests with 3% initial drift. The comparisons of these three sets of experimental tests with the SRM, SFRM and modified SRM are shown below in Figures G.3 and G.4 for $\theta_0 = 2\%$ and 3% respectively.

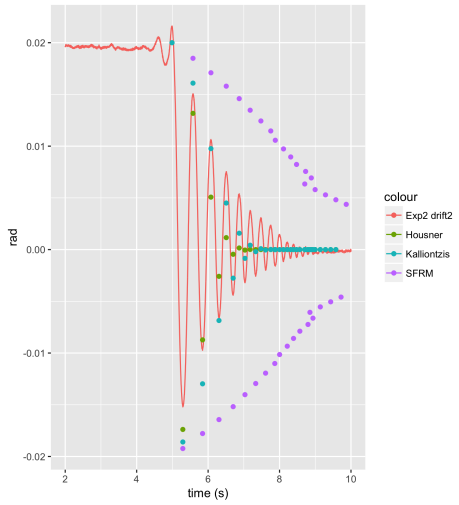

Figure G.3: Response of the flexible system compared with Housner COR and Kalliontzis COR with the test data from (11) for $\theta_0 = 2\%$.

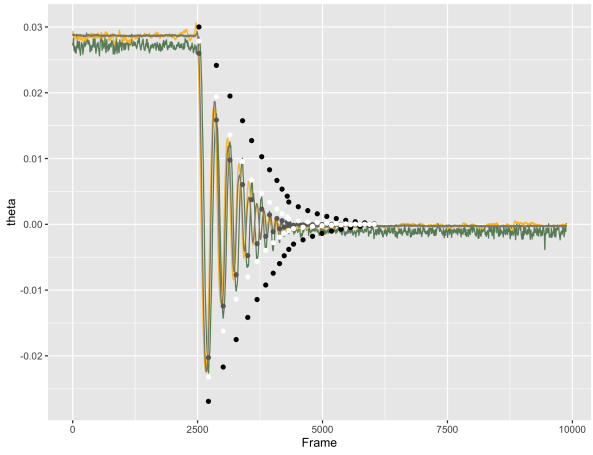

Figure G.4: Response of the flexible system compared with Housner COR and Kalliontzis COR with the test data from (11) for $\theta_0 = 3\%$.

Table G.2: List of materials with their modulus of elasticity, E

Material	**E (MPa)**
Rubber, small strain	$10 \sim 100$
ABS plastics	$1400 \sim 3100$
Chlorinated PVC (CPVC)	2900
Acrylic	3200
Epoxy resins	3200
Fiberboard, Medium density	4000
Pine wood (along grain)	9000
Ice (H_20)	9100
Mild Steel 1020	210000

The SFRM defines the axial deformation of the block. The evidence of this axial deformation of the block from the experiments in (11) is a result of the relative displacement between locations on the block. In particular, the sensor locations are used to determine the axial deformation that occurs within the block during the experimental rocking response given the three different initial drift values. Figures G.5 - G.10 show the relative displacement between sensors for all six of the experimental tests from (11).

G.3 Young's Moduli

The moduli of elasticity for various materials are shown in Table G.2. This table provides an additional reference to Figure 5.17 for materials that will experience deformations according to Figures 5.14 and 5.16.

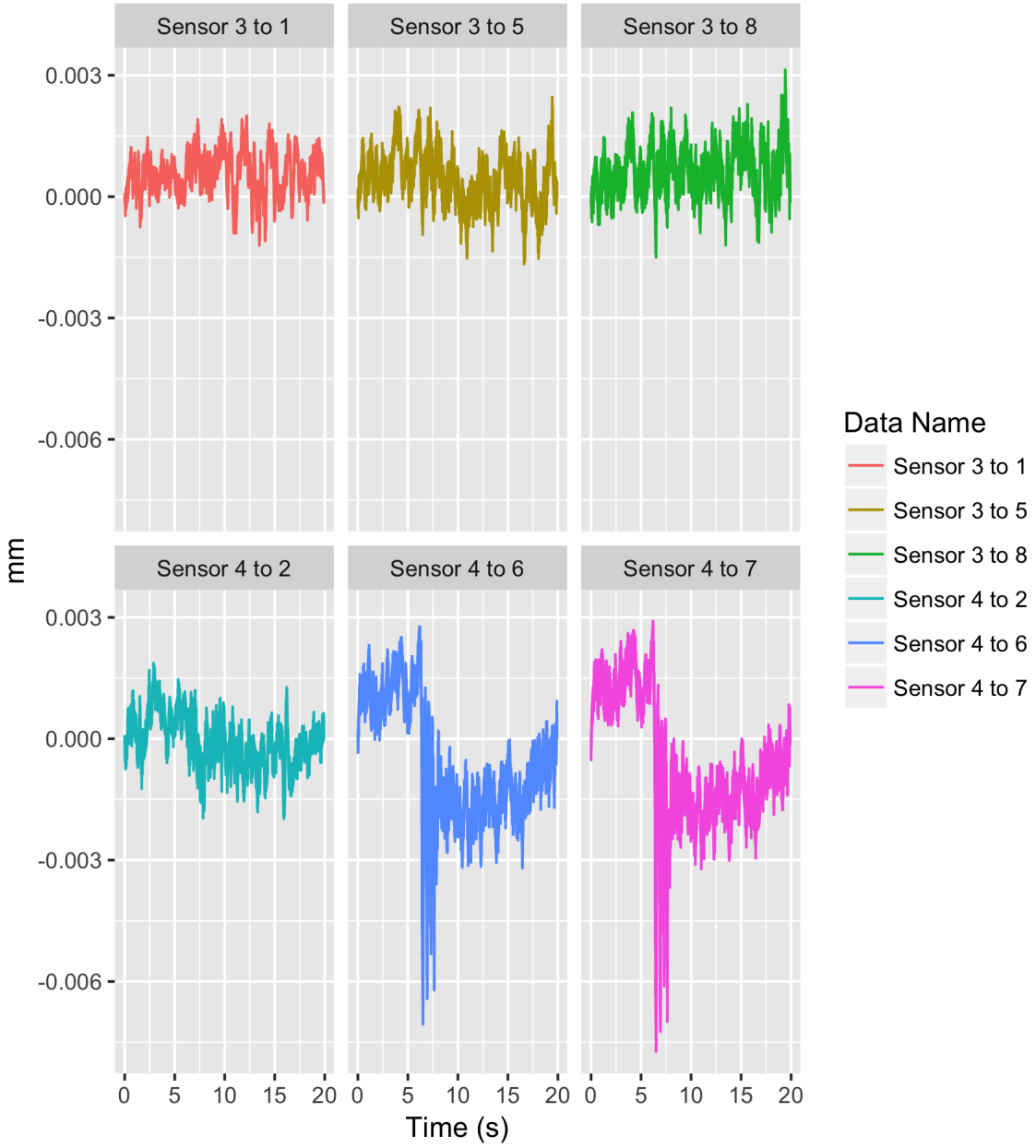

Figure G.5: Relative displacement between sensors as labeled in Figure 5.9 for experimental Test 1 with $\theta_0 = 1\%$

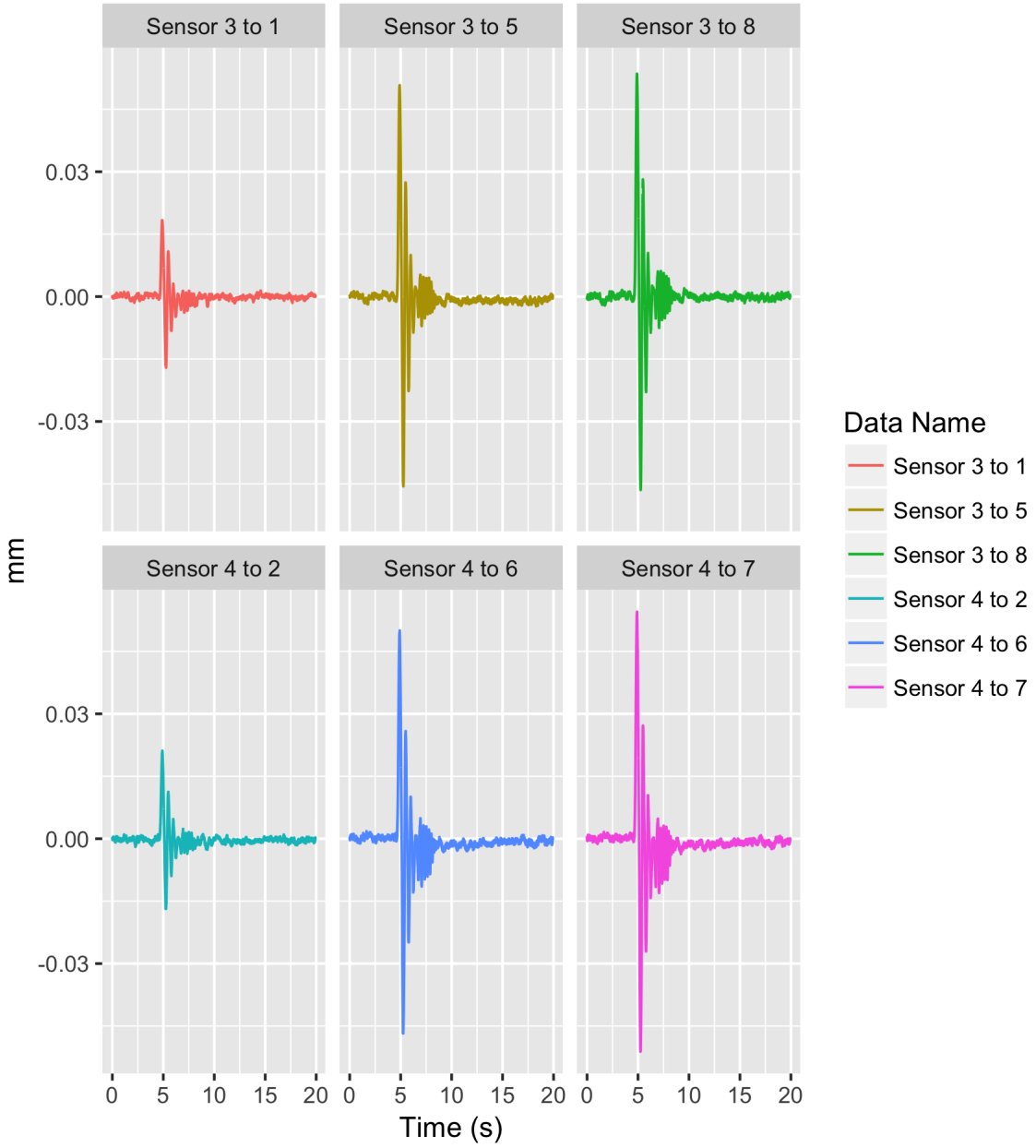

Figure G.6: Relative displacement between sensors as labeled in Figure 5.9 for experimental Test 2 with $\theta_0 = 2\%$

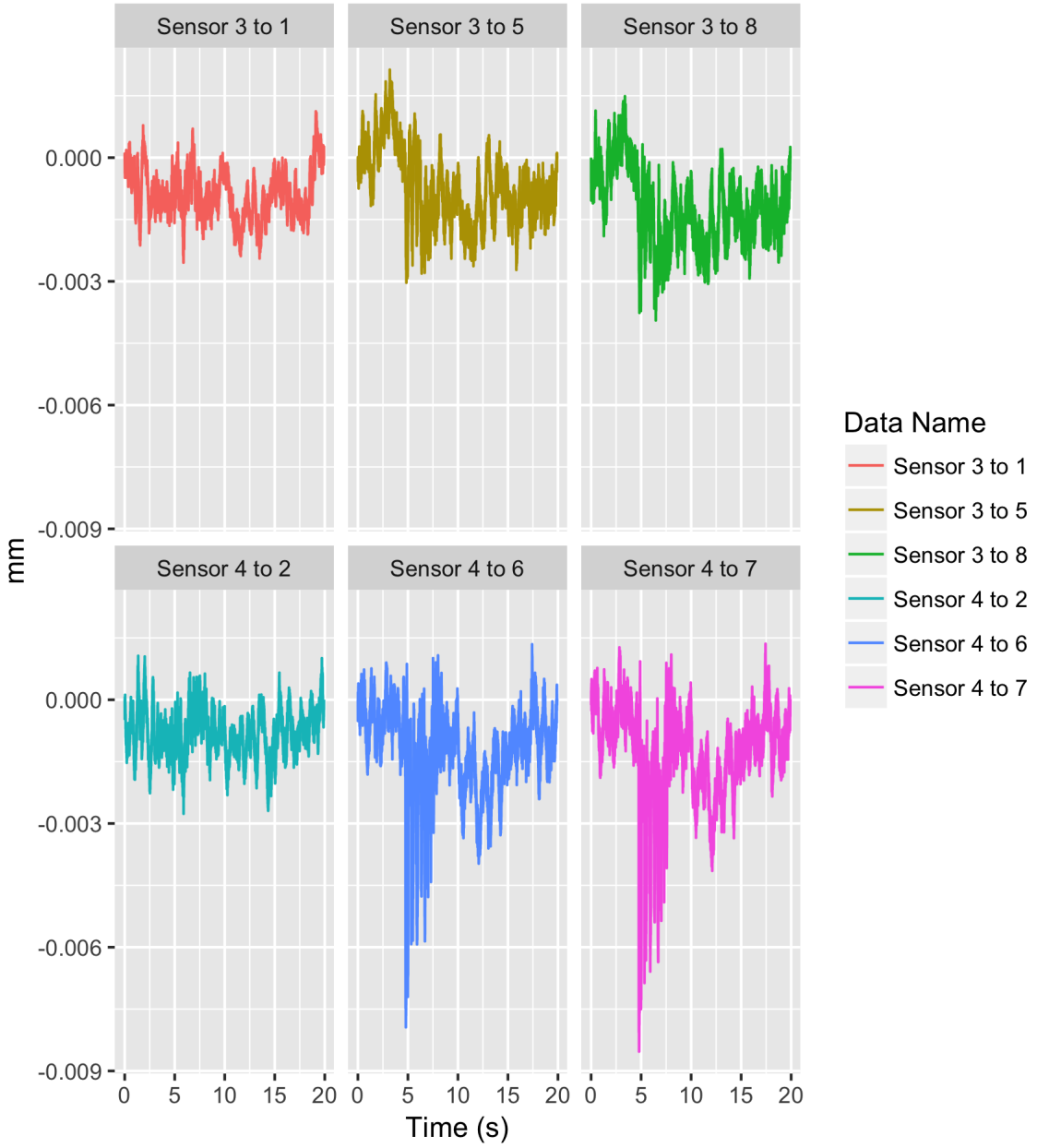

Figure G.7: Relative displacement between sensors as labeled in Figure 5.9 for experimental Test 3 with $\theta_0 = 2\%$

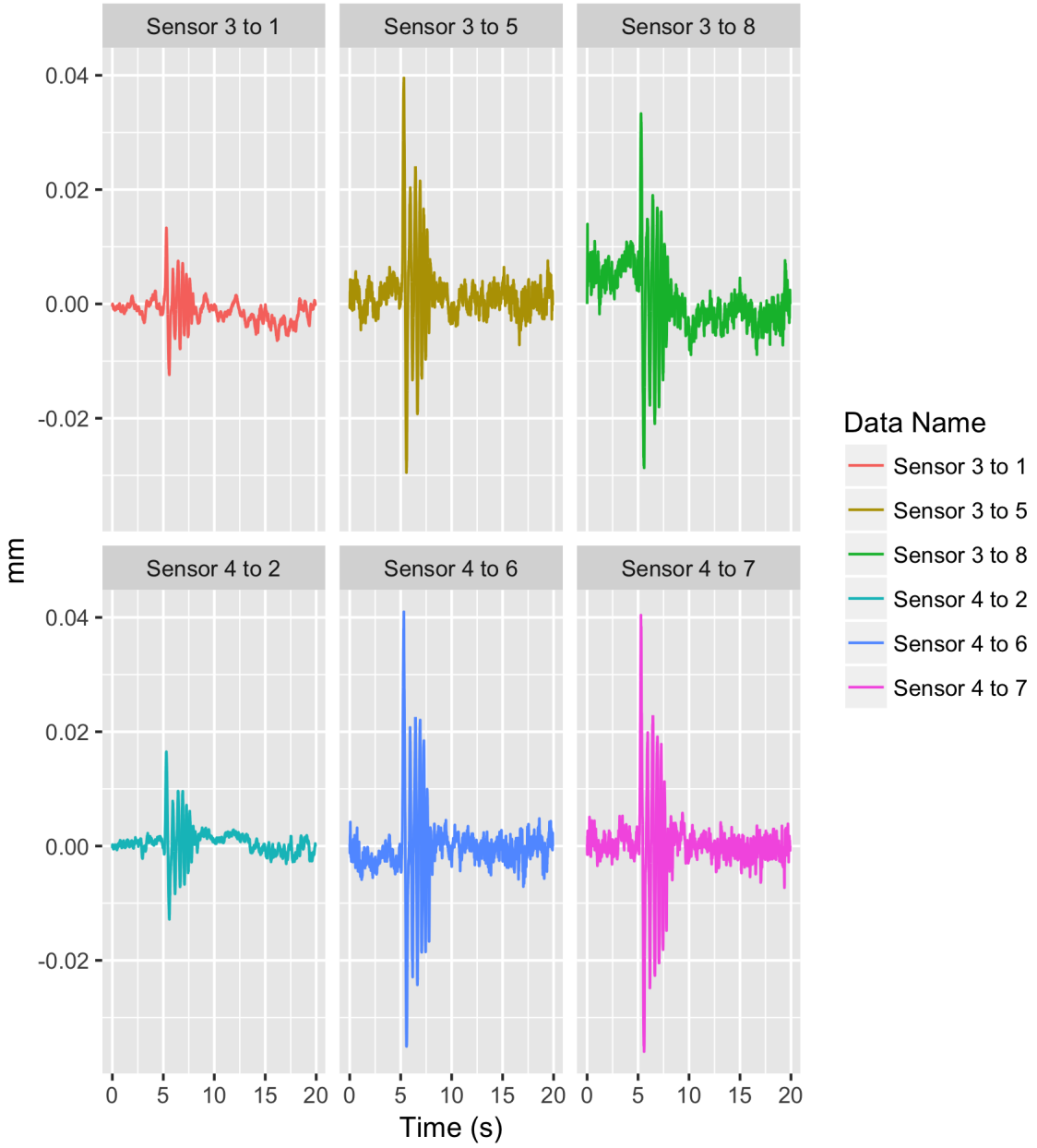

Figure G.8: Relative displacement between sensors as labeled in Figure 5.9 for experimental Test 4 with $\theta_0 = 3\%$

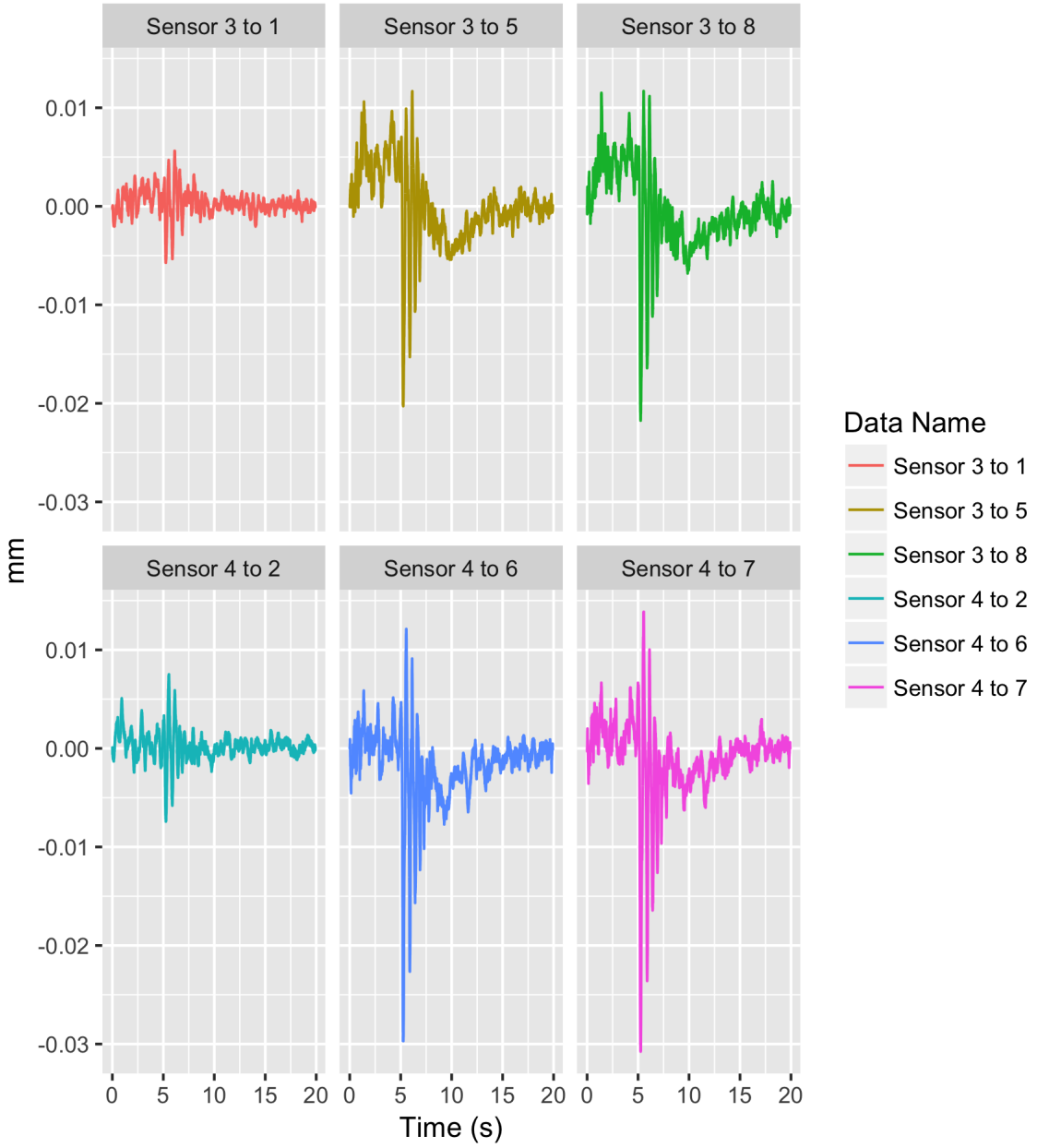

Figure G.9: Relative displacement between sensors as labeled in Figure 5.9 for experimental Test 5 with $\theta_0 = 3\%$

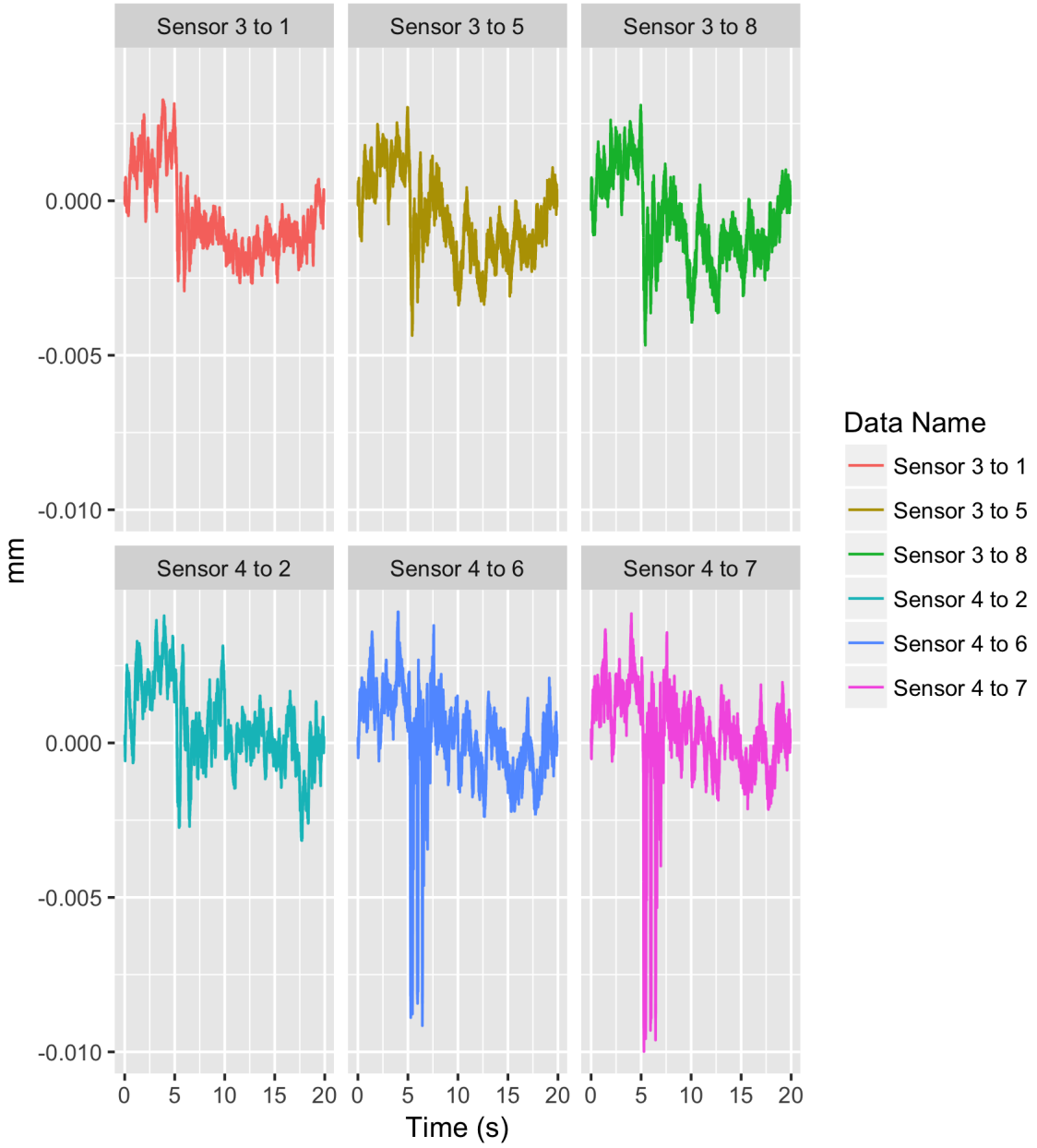

Figure G.10: Relative displacement between sensors as labeled in Figure 5.9 for experimental Test 6 with $\theta_0 = 3\%$